Regulation of heat-induced cell death by the pro-apoptotic Bcl-2 family protein PUMA

by

Rebecca Lee-Anne Rumney

A Thesis
Presented to
The University of Guelph

In partial fulfillment of requirements
for the degree of
Master of Science
in
Molecular and Cellular Biology

Guelph, Ontario, Canada

ABSTRACT

REGULATION OF HEAT-INDUCED CELL DEATH BY THE PRO-APOPTOTIC BCL-2 FAMILY PROTEIN PUMA

Rebecca Lee-Anne Rumney
University of Guelph, 2014

Advisor:
Dr. Richard D. Mosser

Apoptosis is often deregulated in a number of human diseases. Hyperthermia induced apoptosis is a model system for studying the consequences of protein misfolding and is mediated by the Bcl-2 family of proteins. This family consists of both pro-apoptotic and anti-apoptotic members that control mitochondrial integrity. The BH3-only pro-apoptotic members are strong inducers of apoptosis. Our examination of the effect of hyperthermia on the BH3-only protein PUMA, found that although protein levels were rapidly depleted following exposure to heat shock, levels of PUMA mRNA increased. This suggests that post-transcriptional mechanisms control the translation of PUMA mRNA in heat-shocked cells. We therefore examined whether miRNA-mediated inhibition of PUMA translation was responsible for the loss of PUMA protein. We provide evidence for the role of miR-24-2 and miR-29a as mediators of this repression and that strategies directed at the inhibition of these miRNAs could be effective in sensitizing cells to heat-induced apoptosis.

ACKNOWLEDGEMENTS

I am very appreciative to a lot of people for the successful completion of this thesis. I am particularly thankful to Dr. Dick Mosser for not only mentoring me but also for his continuing support and dedication as my supervisor. His guidance and steadiness in research along with his peaceful atmosphere provides inspiration beyond the lab. Through his supervision, I have been kept up to date on cutting edge research in cellular response to heat shock and miRNA regulation. I would also like to thank my advisory committee members for their ongoing support and valued advice throughout my research. I am very grateful for the opportunity to work with such a well-rounded and knowledgeable team of experts.

I thank all my colleagues from the Mosser lab and surrounding labs, all of whom I met at the University of Guelph and have been not only great friends but also great co-workers. The atmosphere they created in the lab made for an enjoyable experience over the years. Coming into the lab was truly a pleasure surrounded by peers who were always available for advice and a good laugh.

Last, but not least, I'd like to give a big thank you to friends and family who encouraged and believed in me through all obstacles and continue to support me to strive for greatness. Without their love and inspiration, I could not have finalized this project.

TABLE OF CONTENTS

LIST OF FIGURES

LIST OF TABLES

LIST OF ABBREVIATIONS

AGO	Argonaute
AMP	Ampicillin
APAF1	Apoptotic protease-activating factor-1
ASP	Aspartic acid
BBC3	Bcl-2 binding component-3
BCA	Bicinchoninic acid
Bcl-2	B Cell lymphoma-2
BH	Binding homology
BH3-only	Binding homology-3 only
$CaPO_4$	Calcium phosphate
CARD	Caspase activation and recruitment domain
cDNA	Complementary DNA
CED	*Caenorhabditis elegans* gene
DDH_2O	Double distilled H_2O
DGCR8	DiGeorge critical region-8
DNA	Deoxyribonucleic acid
dNTP	Deoxynucleotide triphosphate
dsDNA	Double stranded DNA
EBV	Epstein-Barr virus
GTP	Guanosine triphosphate
HSC70	Heat shock cognate protein-70
HSP	Heat shock protein

HSP70	Heat shock protein-70
HSF1	Heat shock transcription factor-1
miRNA	Micro RNA
MOMP	Mitochondrial outer membrane permeabilization
mRNA	Messenger RNA
NT	Nucleotide
OD	Optical density
OMM	Outer mitochondrial membrane
PCR	Polymerase chain reaction
PUMA	p53 up-regulated modulator of apoptosis
qPCR	Quantitative PCR
RISC	RNA-induced silencing complex
RNA	Ribonucleic acid
RNAi	RNA interference
RPM	Rotations per minute
RT	Room temperature
RT-PCR	Reverse transcription PCR
shRNA	Short hairpin RNA
ssDNA	Single stranded DNA
Tm	Melting temperature
UV	Ultra violet
XPO-5	Exportin-5
3'UTR	3' untranslated region

CHAPTER 1: INTRODUCTION

1.1 General features of apoptosis

Apoptosis, the major form of genetically programmed cell death, is an evolutionarily conserved process designed to eliminate unwanted, damaged, aged and misplaced cells during embryonic development and tissue homeostasis (Meier et al., 2000; Borner, 2003). Regulated cell death was first discovered in 1842, described as the process of shrinkage necrosis (Meier and Vousden, 2007; Cotter, 2009). It was not until 1972 that the term apoptosis was proposed based on the common morphological features of dying cells (Kerr et al., 1972). In contrast to necrosis, Kerr et al proposed that apoptosis does not rupture the plasma membrane (Figure 1). Instead, they observed that this programmed cell death is characterized by chromosome condensation, and shrinkage of the nucleus and cytoplasm followed by cell fragmentation into plasma membrane bound "apoptotic bodies" (Kerr et al., 1972; Golstein, 1998). These apoptotic bodies are rapidly engulfed by phagocytes and digested in their lysosomes, a system so effective that little cell death is apparent in the tidy removal of unwanted cells (Kerr et al., 1972; Kanduc et al., 2002; Nagata et al., 2010).

Apoptosis refers to physiological cell death caused by a variety of stimuli or conditions (Kerr et al., 1972). This physiological form of cell death plays many essential roles in multicellular organisms (Golstein, 1998). In the vertebrate epiblast for example, cell death eliminates the less fit cells and shapes the embryo by removing superfluous cells such as interdigital cells during limb formation (Claveria et al., 2013). Altruistic cell suicide also eliminates excess neurons, male germ cells to match target cell number and hollows out ducts such as acini driving formation of the mammary gland (Czabotar et al., 2014). Throughout life, apoptosis is essential for the proper balance of rapidly renewing cells such as those of the hematopoietic system and intestinal epithelium, and for the eradication of irreparably damaged or potentially dangerous cells (Fadeel et al., 1999; Strasser et al., 2011). For example, in the immune system, cells that are superfluous after fighting infection or are dangerous because their antigen receptors recognize self-tissue must be removed (Czabotar et al., 2014). Programmed cell death also drives the suicide of infected cells to limit pathogen spread (Czabotar et al.,

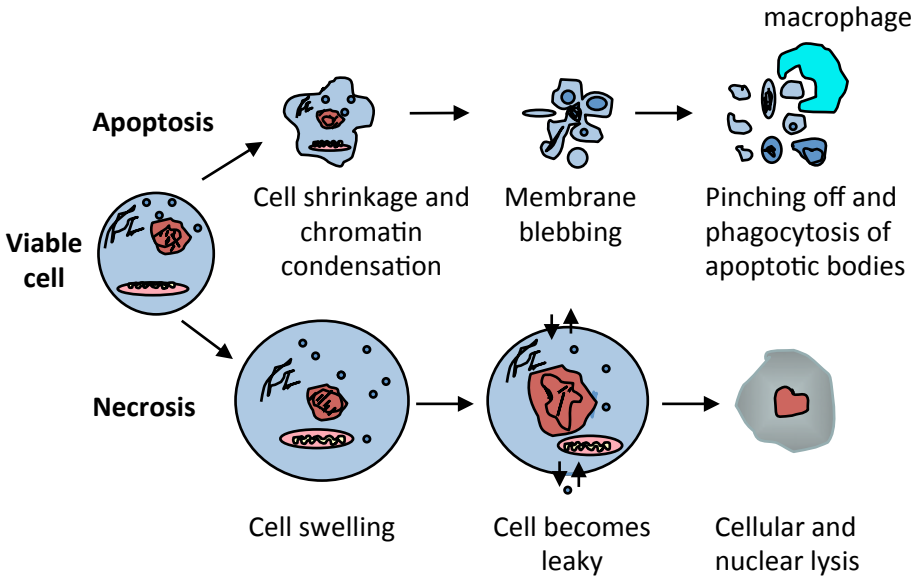

Figure 1: Apoptosis vs. necrosis. Apoptosis (top) is an active and inherently controlled means of cell death. The physiological features of programmed cell death include: cell shrinking, chromatin condensation, membrane blebbing and pinching off into apoptotic bodies that can be phagocytized by macrophages. Necrosis (bottom) is invariably caused by noxious stimuli as a result of an irreversible disturbance of cellular homeostatic mechanisms. Not involved in the control of cell populations, this form of cell death differs in that in comprises of cell swelling, loss of membrane integrity and organelles, degradation of DNA and eventual cell lysis into the extracellular environment.

2014). In adult humans it is understood that apoptosis is responsible for the orderly removal of over 60 billion cells per day counter-balancing cell proliferation to maintain homeostasis (Fadeel et al., 1999). Aberrant apoptotic signaling contributes to numerous human disorders and diseases and abnormal resistance to apoptosis contributes to a wide range of acute diseases including infection, ischemia and chronic pathologies such as neurodegenerative diseases, neuromuscular diseases, and AIDS (Thompson, 1995; Mattson, 2000; Zornig et al., 2001; Rathmell and Thompson, 2002; Green and Evan, 2002; Cory and Adams, 2002; Hotchkiss et al., 2009). It is accepted that diseases such as cancer, immunodeficiency syndromes and neurological disorders not only contribute to alterations in susceptibility to apoptosis, but can also enhance resistance to their conventional therapies (Plati et al., 2011; Hikisz and Kilianska, 2012).

1.2 Caspases and cellular demolition

All of the morphological changes that take place during apoptosis are controlled by a biochemical cascade of events that results in cell shrinking, nuclear fragmentation, chromatin digestion and membrane blebbing (Taylor et al., 2008). The demolition process of apoptosis relies on the activation of a family of aspartate-specific cysteine proteases of the caspase family (Vaux and Strasser, 1996; Wolf and Green, 1999). Caspases are the key players of the apoptotic process that cleave vital cellular substrates after aspartate residues and trigger the activation of enzymes responsible for chromatin digestion (Earnshaw et al., 1999; Borner, 2003). Although present in healthy cells, these enzymes require activation via induced dimerization or catalytic cleavage in response to apoptotic stimuli (Shi, 2002; Borner, 2003). Based on structure and function, caspases are divided into two groups: initiator caspases and effector caspases (Nicholson, 1999; Timmer and Salvesen, 2007). The initiator caspases (ex: caspases-8, -9 and -10) are characterized by a long N-terminal pro-domain of over 90 amino acids (Borner, 2003). In the case of pro-caspase-9, following an apoptotic signal, the pro-domain of caspase-9 interacts with a specific scaffold protein called apoptotic protease-activating factor 1 (Apaf1) creating the apoptosome, which acts to cluster the initiator caspases (Kumar and Colussi, 1999; Riedl and Salvesen, 2007). This proximity then allows the caspases to form an active dimeric complex (Earnshaw et al., 1999; Nicholson, 1999; Borner, 2003). Active initiator caspases then activate effector caspases (caspase-3, -6 and -7) through the proteolytic cleavage at specific internal Asp residues, which amplifies the apoptotic signal (Riedl and Salvesen, 2007). The cleavage by the

initiator caspases then allows the formation of the active site within the effector caspases. Active effector caspases then cleave intracellular substrates ultimately leading to the dismantling of the cell into membrane-enclosed vesicles known as apoptotic bodies (Utz and Anderson, 2000; Borner, 2003; Taylor et al., 2008). These packages are phagocytized by neighboring macrophages resulting in the orderly removal of cellular contents of the dying cell (Vaux and Strasser, 1996; Strasser et al., 2011).

1.3 Regulation of apoptosis

Activation of an initiator caspase triggers a cascade of downstream caspase activation making apoptosis a highly regulated process. In mammals, apoptosis can be triggered by at least two distinct caspase-dependent apoptosis signaling pathways initiated from either signals at the cell surface or by sensing damage within the cell (Borner, 2003; Strasser et al., 2011). Activation of the extrinsic pathway, also known as the death receptor pathway, is triggered by ligation of extracellular death-inducing ligands of the tumor necrosis factor receptor (TNFR) family with their cell surface associated death receptors on the plasma membrane, which leads to the activation of caspase-8 and subsequently the effector caspases (Krammer, 2000; Screaton and Xu, 2000; Locksley et al., 2001; Strasser et al., 2009) (Figure 2). In the extrinsic pathway the signal, death receptor-ligand interaction, leads directly to caspase activation (Huang et al., 1999). By contrast the intrinsic pathway involves the transmission of intracellular signals that act upon the Bcl-2 family of apoptotic regulatory proteins, which control the integrity of the outer mitochondrial membrane (OMM) (Figure 2). The release of mitochondrial death effector proteins leads to apoptosome formation and caspase activation. Both pathways lead to cell death by caspase activation but are largely independent from one another. The focus of this thesis is the intrinsic death pathway.

1.3.1 The intrinsic apoptotic pathway

The apoptotic threshold of the intrinsic pathway to caspase activation is controlled by interactions on the mitochondrial outer membrane between three functionally and structurally distinct subgroups of the Bcl-2 family of apoptotic proteins that act as a tripartite apoptotic switch. Activators of the intrinsic pathway include protein-damaging stress, UV- and γ-irradiation DNA damage, chemotherapeutic drugs, bacterial or viral infection and the deprivation

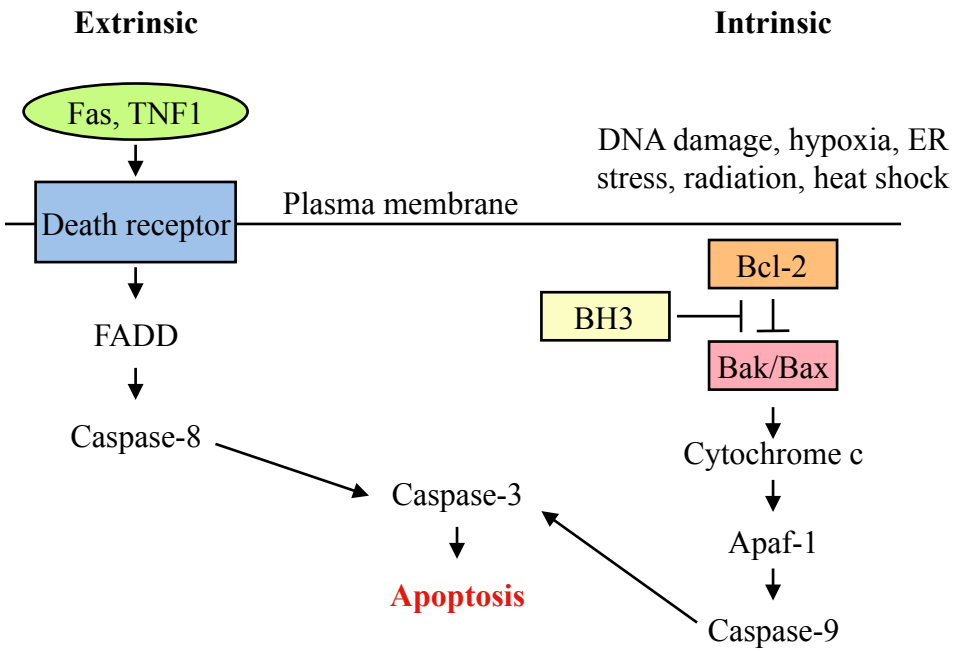

Figure 2: Extrinsic and intrinsic apoptotic pathways. Activation of the extrinsic pathway (death receptor pathway) is triggered by the binding of extracellular death ligands such as tumor necrosis factor 1 (TNF1) or FAS ligand to associated death receptors located on the cell surface. Death receptors attract procaspase-8 through interactions with an adaptor protein, FADD (Fas-associated death domain). Recruitment of procaspase-8 results in its activation to the initiator caspase-8 allowing it to process effector caspases, such as caspase-3 resulting in its activation. Active caspase-3 cleaves a large number of cellular substrates, which results in cellular destruction. This pathway does not require Bcl-2 proteins to trigger cell death. However active caspase-8 can cross-talk with the intrinsic pathway by cleaving the Bcl-2 protein family member Bid to the active tBid, activating Bak/Bax on the mitochondria and triggering the release of cytochrome c. The intrinsic apoptotic pathway is triggered by signals from inside the cell. These signals can originate from cytotoxic insults that damage cellular molecules such as proteins or DNA. The BH3-only members of the Bcl-2 family sense and convey these signals to the other members and affect their ability to regulate the release of cytochrome c from the mitochondria. Pro-apoptotic proteins induce cytochrome c release while anti-apoptotic Bcl-2 members suppress this release. The release of cytochrome c from mitochondria is necessary for apoptosome formation the major component of which is Apaf-1, which acts as an adaptor for procaspase-9 recruitment. Apaf1 can then associate with the initiator procaspase-9 facilitating its auto-activation. This complex can now process procaspase-3 to produce the active executioner, caspase-3, which cleaves various proteins and cellular substrates leading to cell death.

of growth factors (Borner, 2003; Chipuk et al., 2010). These stress-inducing apoptotic stimuli activate the pro-apoptotic members of the Bcl-2 family including Bak, which is embedded in the OMM in an inactive state, and Bax, which acquires the ability to translocate from the cytosol and become embedded in the OMM through conformational changes in its structure (Lithgow et al., 1994; Suzuki et al., 2000).

During apoptosis, stress-induced Bak and Bax change their structure from monomers resembling the anti-apoptotic members to the active homo-oligomers that can permeabilize the OMM. This activation on the OMM allows the formation of channels through which not only cytochrome c but also other death-inducing factors, such as SMAC/DIABLO as well as caspases can translocate from the inter-membrane space of the mitochondria to the cytoplasm (Du et al., 2000; Desagher and Martinou, 2000; Zamzami and Kroemer, 2001). Once in the cytosol, cytochrome c released from mitochondria triggers apoptosome formation and caspase activation (Li et al., 1998; Chipuk et al., 2010). Cytochrome c elicits its effect by binding to the adapter Apaf1 in the cytosol causing its conformational change that, in turn, triggers its oligomerization into the caspase activation platform, the apoptosome (Cain et al., 2002; Tait and Green, 2010; Hikisz and Kilianska, 2012) (Figure 3). Apaf1 consists of a caspase recruitment domain (CARD) that allows the interaction with procaspase-9, a linker region (WD-40) that binds to cytochrome c, and a CED-4 homologous domain, which contains two binding sites involved in protein-protein interactions. Once the apoptosome is complete, the binding of procaspase-9 activates the caspase cascade leading to active caspase-3, ultimately resulting in cellular destruction (Zou et al., 1999; Riedl and Salvessen, 2007; Hikisz and Kilianska, 2012). Once mitochondrial outer membrane permeabilization (MOMP) is achieved, cell death is unavoidable, regardless of caspase activity, due to a steady decline in mitochondrial function. Although cells can survive MOMP under certain circumstances, this may have pathophysiological consequences to the cell (Tait and Green, 2010). In healthy cells, anti-apoptotic members of the Bcl-2 family prevent the formation of the apoptosome.

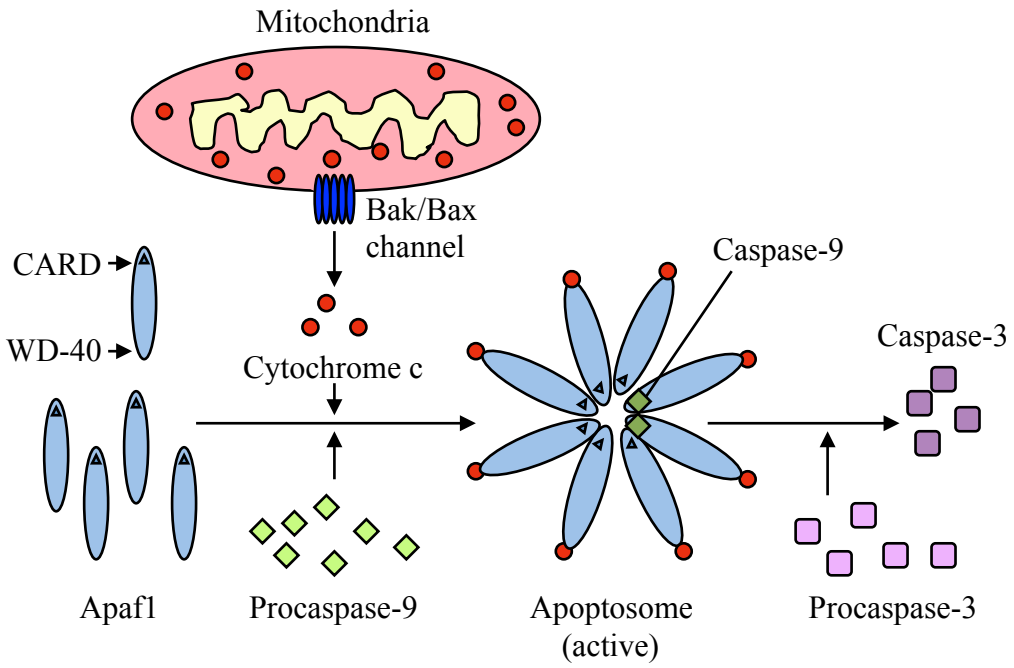

Figure 3: Apoptosome formation. The apoptosome is a large protein complex that forms during the execution of apoptosis. The major component of the apoptosome is the apoptotic protease-activating factor 1 (Apaf1), which acts as an adaptor for procaspase-9 recruitment. The N terminus contains a caspase recruitment domain (CARD) that allows Apaf1 to interact with procaspase-9. Next is a linker region that connects to a stretch of multiple peptide binding motives (WD-40), which are responsible for binding cytochrome c. Formation of the apoptosome occurs in the cytosol and is initiated by the binding of cytochrome c to the WD-40 region on Apaf1, resulting in a conformational change that, in turn, triggers its oligomerization into the caspase activation platform. Once the apoptosome has formed from the oligomerization of 8 Apaf1 molecules, the CARD domain of Apaf1 can then associate with the initiator procaspase-9 facilitating caspase-9 to adopt a catalytically active conformation. Active caspase-9 then cleaves the executioner procaspase-3 and active caspase-3 goes on to cleave a large number of cellular substrates, which ultimately results in cellular destruction.

1.4 Bcl-2 protein family "regulators of apoptosis"

Molecular insights into apoptosis first emerged during the 1980s and 1990s from a convergence of mammalian cancer cytogenetics and genetic studies on developmentally programmed cell death in *Caenorhabditis elegans* (Czabotar et al., 2014). The previously unknown gene Bcl-2 was identified from the breakpoint region of a recurrent chromosomal translocation (18q21) in human follicular lymphoma (Tsujimoto et al., 1985; Vaux et al., 1988). The B-cell lymphoma (Bcl-2) family of proteins are central regulators of stress-induced apoptosis as they control diverse survival and death signals that are generated inside and outside the cell (Strasser et al., 2000; Adams and Cory, 2001). Bcl-2 proteins are found in all cells and consist of 12 distinct members, many of which are expressed as alternate isoforms. Structurally, they all contain at least one of the conserved sequence motifs called Bcl-2 homology (BH) domains. This family is functionally subdivided into two classes based on their activity and number of BH domains: anti-apoptotic and pro-apoptotic proteins including the BH3-only members (Adams and Cory, 2007) (Table 1 and Figure 4). Mutual interactions between the pro-apoptotic and anti-apoptotic members set the threshold that determines whether a cell should survive or die (Borner, 2003). In a sense they act as checkpoints through which survival and death signals must pass to elicit the cell's fate as they control stress-induced cell death (Chipuk et al., 2010).

Table 1: Bcl-2 protein family members

Pro-apoptotic	Anti-apoptotic	BH3-only
Bak	A1/BFL-1	Bad
Bax	Bcl-2	Bid
Bok	Bcl-w	Bik
	Bcl-xL	Bim
	Mcl-1	Bmf
		BNIP 1, 2 and 3
		Hrk
		Noxa
		PUMA

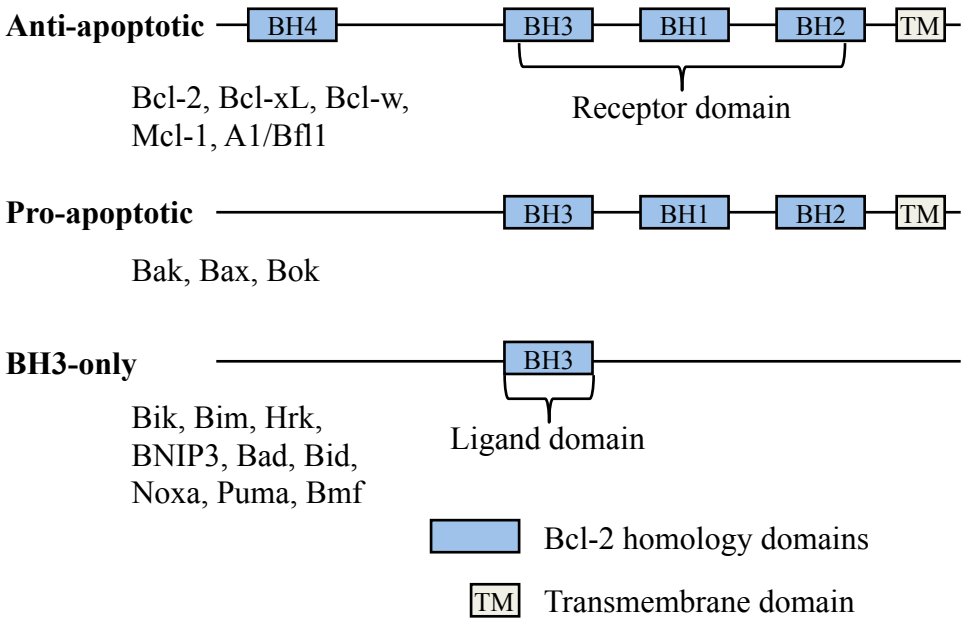

Figure 4: Classification of the Bcl-2 family of proteins. The Bcl-2 family of apoptotic regulators is divided into 3 groups based on their activity and number of Bcl-2 homology (BH) domains. The anti-apoptotic Bcl-2 members, including Bcl-2, Bcl-xL, Bcl-W, Mcl-1 and A1 share all four conserved BH domains of structural homology. These proteins work together to inhibit the release of cytochrome c from the mitochondria by means of preventing the activation of the pro-apoptotic members Bak/Bax in the OMM. The pro-apoptotic Bcl-2 members are divided into multi-domain effector proteins, such as Bak, Bax and Bok, as well as the large subgroup of BH3-only proteins, all of which trigger or sensitize the cell to apoptosis. The pro-apoptotic proteins Bak, Bax and Bok possess only three BH domains. Unlike the anti-apoptotic members, the active conformation of Bak/Bax damage rather than protect the OMM of stressed cells forming channels that result in cell death. The pro-apoptotic and anti-apoptotic proteins have very similar sequence homology and structure. Both groups posses a transmembrane domain at their C terminus, which plays a role in anchoring the protein into intracellular membranes. The BH3-only proteins form the largest subgroup of Bcl-2 proteins and include: Bik, Bim, Hrk, BNIP3, Bad, Bid, Noxa, PUMA and Bmf, all of which retain only the BH3 domain. The pro-apoptotic BH3-only proteins are sensors of diverse apoptotic signals that act upstream of the anti-apoptotic members, inhibiting their ability to block Bak/Bax activation.

1.4.1 Anti-apoptotic Bcl-2 proteins

The anti-apoptotic Bcl-2 members, including Bcl-2 itself, Bcl-xL, Mcl-1, Bcl-W and A1/BFL-1 share 4 conserved BH domains of structural homology. These proteins prevent cell death against diverse cytotoxic signals, both physiological and imposed, maintaining the integrity of the endoplasmic reticulum, mitochondrial and nuclear membranes thus protecting cells from apoptosis (Er et al., 2006; Youle and Strasser, 2008). The close proximity of BH 1, 2 and 3 form a hydrophobic pocket that operates as a receptor for the BH3 domain of the pro-apoptotic BH3-only members. The anti-apoptotic Bcl-2 proteins work together to inhibit the release of cytochrome c from the mitochondria by means of preventing the activation of the pro-apoptotic members Bak and Bax in the OMM (Chipuk et al., 2010). The anti-apoptotic proteins' normal function is to prevent inappropriate cell death and therefore requires the neutralization of the pro-apoptotic proteins by the anti-apoptotic members (Adams and Cory, 2007).

1.4.2 Pro-apoptotic Bcl-2 effector proteins

Just as the anti-apoptotic Bcl-2 proteins promote tumourigenesis when deregulated, the pro-apoptotic members function as tumor suppressors. The pro-apoptotic Bcl-2 members are divided into multi-domain effector proteins, such as Bak, Bax and the less well known Bok, as well as the large subgroup of BH3-only proteins, all of which trigger or sensitize the cell to apoptosis (Huang and Strasser, 2000; Antonsson, 2001). The pro-apoptotic effector proteins Bak, Bax and Bok possess three BH domains and adopt similar globular structures: a helical bundle surrounding a central hydrophobic core helix (Muchmore et al., 1996; Chipuk et al., 2010; Hikisz and Kilianska, 2012). This groove constitutes a crucial surface for interactions with the BH3 domain of pro-apoptotic members of the Bcl-2 family (Czabotar et al., 2014). These interactions primarily occur on intracellular membranes, such as that of the OMM where many of the Bcl-2 family members are directed by their carboxy-terminal hydrophobic transmembrane domain (Kvansakul et al., 2008). Unlike the anti-apoptotic members, the active conformation of Bak/Bax damage rather than protect the OMM of stressed cells, forming pores that result in membrane dysfunction (Strasser et al., 2011). The most studied pro-apoptotic proteins Bak and Bax exist in an inactive monomeric state in healthy cells, while in stressed cells they are major inducers of MOMP (Antignani and Youle, 2006).

1.4.3 Pro-apoptotic BH3-only initiator proteins

The BH3-only proteins form the largest subgroup of Bcl-2 proteins and include: Bid, Bad, Bim, Bik, Noxa, PUMA, Hrk, BNIP1/2/3 and Bmf, all of which have only the BH3 domain in common (Lomonosova and Chinnadurai, 2008; Hikisz and Kilianska, 2012). The pro-apoptotic BH3-only proteins act as sensors of diverse cytotoxic stress signals that act upstream of the anti-apoptotic members, inhibiting their ability to block Bak/Bax activation (Adams and Cory, 2007, Czabotar et al., 2014). This occurs through interactions between the pro-apoptotic and anti-apoptotic proteins on the outer mitochondrial membrane.

1.5 Role of Bak and Bax in MOMP

Recent studies have focused on the effects of the Bcl-2 family members on MOMP. Although over a decade has passed since the discovery of the BH3-only protein PUMA, the question of how this protein activates Bak/Bax, consequently leading to MOMP, remains unresolved. At present, two hypotheses have been proposed concerning the relationship of the Bcl-2 protein family members by means of direct or indirect activation of the mitochondrial apoptotic pathway, shown in Figure 5 (Adams and Cory, 2007; Chipuk et al., 2010; Strasser et al., 2011).

1.5.1 The indirect model of activation

In the indirect model Bak/Bax activation occurs only when the BH3-only proteins bind to and inhibit all anti-apoptotic Bcl-2 proteins (Willis et al., 2007). This occurs through interactions between the amphipathic α-helix of the BH3 domain on the pro-apoptotic BH3-only members and the hydrophobic pocket of the BH1, 2 and 3 domains present on the target anti-apoptotic members, inactivating them and liberating the pro-apoptotic Bak/Bax (Sattler et al., 1997; Borner, 2003; Chipuk et al., 2010). Some of the BH3-only members have varying affinities for different anti-apoptotic proteins, whereas others have the ability to interact with all members (Kuwana et al., 2005; Lomonosova and Chinnadurai, 2008). Recent structural studies have shown a certain level of plasticity among the BH3 binding groove of the anti-apoptotic members, which probably contributes to their ability to associate with multiple BH3 domains (Lee et al., 2009). Bim, Bid, and PUMA bind all anti-apoptotic members with high affinity and thus are potent inducers of apoptosis, while Bad and Noxa which target only a few of the anti-apoptotic

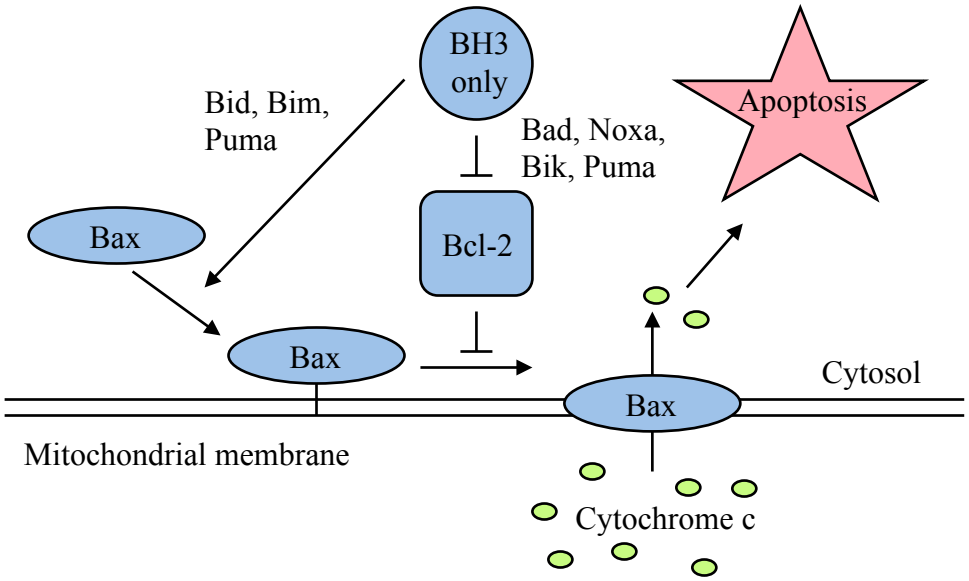

Figure 5: Direct and indirect activation of the intrinsic apoptotic pathway. Apoptosis is initiated by the release of cytochrome c from the mitochondria inter-membrane space to the cytosol via channels formed by the oligomerization of Bak or Bax in the OMM. There are two models explaining Bak/Bax activation through interaction of the Bcl-2 protein family members: the direct activation model and the indirect activation model. In the indirect model, Bak/Bax activation occurs only when the BH3-only proteins bind to and inhibits all anti-apoptotic Bcl-2 proteins, displacing and liberating the pro-apoptotic Bak/Bax for subsequent activation. Conversely, in the direct model, BH3-only proteins can directly activate Bak/Bax in the absence of the anti-apoptotic members. It is suggested that certain BH3-only members (Bid, Bim and PUMA) are known as activators, capable of interacting directly with Bak/Bax to induce conformational changes that lead to their activation and oligomerization. Other BH3-only protein members (Bad, Noxa, Bik, and PUMA) are classified as sensitizers. These sensitizers act to sequester the anti-apoptotic members and thereby inhibit their ability to suppress Bak/Bax activation. By freeing up Bak/Bax the sensitizers allow their activator relatives to bind and activate Bak/Bax.

relatives are weak inducers (Chen et al., 2005; Kim et al., 2006). The differential ability of certain BH3-only proteins to induce apoptosis when overexpressed can be explained by this differential specificity for anti-apoptotic members (Chipuk and Green, 2008). It is proposed that efficient apoptosis requires the neutralization of all anti-apoptotic members within a given cell (Kim et al., 2006; Kim et al., 2009). In spite of this, co-expression of certain members such as Bad and Noxa, with opposite specificity, target all the anti-apoptotic members allowing the activation and oligomerization of Bak/Bax in the OMM. The BH3-only proteins however are latent killers that require activation by distinct cytotoxic stimuli. This shift in Bak/Bax into their active conformation leads to MOMP and ultimately apoptosis of the cell (Chipuk and Green, 2008).

1.5.2 The direct model of activation

Conversely, in the direct model, BH3-only proteins can directly activate the pro-apoptotic effectors Bak/Bax in the absence of the anti-apoptotic members. It is suggested that certain BH3-only members (Bid, Bim and PUMA) are known as activators, capable of interacting directly with Bak/Bax to induce conformational changes that lead to their activation and oligomerization (Gavathiotis et al., 2008). Other BH3-only members (Bad, Noxa, Bik, and PUMA) are classified as sensitizers (Hikisz and Kilianska, 2012). These sensitizers act to sequester the anti-apoptotic members (Bcl-2, Bcl-xL and Mcl-1) and thereby inhibit their ability to suppress Bak/Bax activation (Figure 6). By freeing up Bak/Bax the sensitizers allow their activator relatives to bind and activate Bak/Bax (Adams and Cory, 2007; Chipuk and Green, 2008). In this model, Bid, Bim and PUMA are strong inducers of apoptosis both because of high affinities to all the anti-apoptotic Bcl-2 members and due to their ability to bypass the anti-apoptotic inhibition step and directly activate Bak/Bax. Although two alternate models exist to describe the activation of Bak/Bax in the OMM leading to MOMP, genetic and biochemical evidence supports the idea that both the direct and indirect models apply in many circumstances. Thus, a unified model that operates within a tripartite network of interactions between the three subgroups of the Bcl-2 family of proteins (Czabotar et al., 2014). The dominant pathway in this model varies depending on the biological state of the cells, such as non-transformed cells versus tumor cells or according to cytotoxic and cell death stimuli and ultimately determines the fate of the cell (Czabotar et al., 2014).

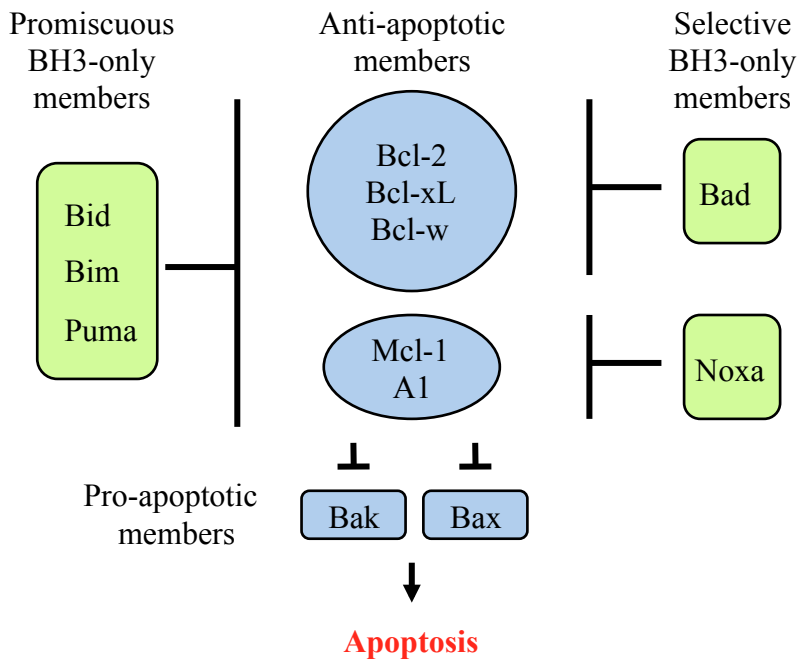

Figure 6: Differential binding specificity of BH3-only proteins. Neutralization of multiple anti-apoptotic proteins by either a combination of selective BH3-only proteins or singly by promiscuous BH3-only proteins is necessary for Bak/Bax activation. Some of the BH3-only proteins have selective affinities for different anti-apoptotic members, whereas others have the ability to interact with all members. Bim, Bid, and PUMA bind all anti-apoptotic members with high affinity and thus are potent inducers of apoptosis, while Bad and Noxa, which target only a few of the anti-apoptotic members, are weak inducers. The differential ability of certain BH3-only proteins to induce apoptosis when overexpressed can be explained by this differential specificity for anti-apoptotic members. It is proposed that efficient apoptosis requires the neutralization of all anti-apoptotic members within a given cell. In spite of this, co-expression of certain members such as Bad and Noxa, with opposite specificity, targets all the anti-apoptotic members and therefore can effectively trigger cell death.

1.6 BH3-only protein PUMA (bbc3)

Thirteen years ago, two independent laboratories first discovered and cloned the PUMA (p53 Up-regulated Modulator of Apoptosis) protein as a transcriptional target of p53 (Nakano and Vousden, 2001; Yu et al, 2001). In the same year, Han and colleagues identified the bbc3 (Bcl-2 binding component 3) gene that corresponds to the PUMA cDNA (Han et al., 2001). PUMA is a highly efficient pro-apoptotic protein, thought to be one of the most powerful and effective "killers" among the BH3-only proteins. The bbc3 gene has been reported to encode 4 different forms (α, β, γ and δ) of which only the α and β forms contain the BH3 domain and thus display the pro-apoptotic activity. The length of the α PUMA transcript is 1.6-1.9 kb encoding a 193 amino acid protein (Yu et al., 2001). This protein is highly conserved among vertebrate species, yet shows no significant homologies to any other known proteins aside from those with the BH3 domain (Hikisz and Kilianska, 2012). It has been demonstrated in a localization study that PUMA is mainly restricted to the OMM in humans (Yu et al., 2003). The PUMA gene is mapped to chromosome 19q13.3, a region that is frequently deleted in a large number of human cancers including B-cell malignancies, as well as neural, colorectal and ovarian cancers (Yu et al., 2001). When present however, PUMA is able to effectively trigger apoptosis and eliminate cancer cells in the span of only a few hours (Jeffers et al., 2003; Yu et al., 2003).

1.7 Regulation of the BH3-only protein PUMA

Regulation of the Bcl-2 family occurs through distinct cytotoxic stimuli in a variety of ways, including enhanced transcription and post-translational modifications (Fricker et al., 2010). Importantly, PUMA mRNA is induced by p53-dependent and p53-independent apoptotic stimuli in several cancer cell lines (Yu and Zhang, 2008). These results support the idea that the regulation of PUMA mRNA levels and thus the pro-apoptotic activity of the protein represent a common target in different cell death pathways (Han et al., 2001; Hikisz and Kilianska, 2012). The complexity of PUMA function results from this protein's involvement with a vast number of physiological and pathological processes, including the immune response, cancer, and neurodegenerative diseases as well as bacterial and viral infections (Jeffers et al., 2003). Regulation of PUMA expression during programmed cell death is coordinated by different transcription factors, most notably p53 but also through the activity of several other transcription

factors including p73, sp1, Fox03a, E2f1, CHOP, TRB3, AP-1 and c-Myc (Nakano and Vousden, 2001; Jeffers et al., 2003; Hikisz and Kilianska, 2012).

1.7.1 p53-dependent apoptosis

The PUMA gene is a direct transcriptional target of the tumor suppressor p53 (Strasser et al., 2011). The mutual interaction between p53 and PUMA is an efficient mechanism for preventing the growth and division of abnormal cells, thereby protecting against the development of cancer (Happo et al., 2010). It is known that p53 is required for the induction of PUMA in response to DNA damage, but can also act on PUMA in response to oxidative stress, deficiency of growth factors, or viral infection (Wang et al., 2007; Hikisz and Kilianska, 2012). More so, a lack of PUMA expression is often associated with the mutation or deletion of p53 function, which contributes to over 50% of human cancers (Muller and Vousden, 2013). Furthermore, p53 acts as a sensor of cell stress, responsible for tumor growth inhibition by either cell cycle arrest followed by DNA repair or by causing apoptosis through activating the transcription of several pro-apoptotic genes, including PUMA. p53-dependent regulation of pro-apoptotic PUMA expression and subsequent apoptosis relies on the functioning of GSK-3 (Glycogen synthase kinase-3) and acetyltransferase Tip60, which control the choice between cell cycle arrest and apoptosis (Charvet et al., 2011).

1.7.2 p53-independent apoptosis

Stimuli from stressed or damaged cells can up-regulate PUMA expression either by p53-mediated activation or by other transcription factors (Yu et al., 2008). PUMA plays a very important role in p53-independent apoptosis involved in the removal of damaged cells during hypoxia, infection and cytokine or growth factor depletion. These conditions are strong signals for apoptosis, which can lead to irreversible damage in cells and tissues (Wu et al., 2007; Hikisz and Kilianska, 2012). During such pathological conditions, induction of PUMA mRNA expression and activity level is due to the activity of other transcription factors, such as p73, Sp1 or Fox03a depending on the cell types (Michalak et al., 2008; Yu et al., 2008; Hikisz and Kilianska, 2012). Although the mechanism remains unknown, the regulation of PUMA occurs mainly without the participation of p53 in compromised cells.

Both p53-dependent and p53-independent inductions of apoptosis via PUMA are involved in the immune response after bacterial and viral infections (Wei et al., 2008). The immune response starts with increased T cell proliferation but once the pathogen has been eliminated, the number of T cells needs to be controlled through apoptosis to decrease the immune response. PUMA plays a role in T cell apoptosis and is driven both by p53 and Fox03a (Fischer et al., 2008; Hikisz and Kilianska, 2012). This ensures the proper functioning of the immune system to prevent pathological conditions, such as autoimmunity (Fischer et al., 2008).

1.8 Heat shock proteins and the heat shock response

During the progression of cancer, transformed cells are subjected to a vast number of apoptotic stimuli that are the consequences of cell stress (Evan and Vousden, 2001). Proteotoxic stressors, for example, cause protein misfolding or malfunction in cells, which then require the induction of heat shock protein (HSP) synthesis to achieve proper proteostasis (Buchberger et al., 2010; Richter et al., 2010). HSPs were first discovered in 1962 by experiments in *Drosophila*, as proteins synthesized in response to various stresses such as hyperthermia (Ritossa, 1962; Mirault, 1978). Heat shock proteins are molecular chaperones that are required for the translocation of proteins across intracellular membranes (Chicoro et al., 1988). These proteins participate in the folding and assembly of newly synthesized proteins into larger complexes, prevent aggregation and target irreversibly misfolded or unfolded proteins for proteasomal degradation (Pelham, 1988; Hartl, 2011). Exposure to hyperthermic conditions induces the expression of this group of proteins, an evolutionarily conserved response to proteotoxic stress (Tissieres et al., 1974). In mammals, HSPs are divided into families according to their molecular size and consist of both constitutively expressed proteins such as HSC70, which is expressed in healthy cells to assist in folding and intracellular translocation of proteins, and the stress-inducible form HSP70. HSP70 is only highly induced in stressed cells where it assists HSC70 in the prevention and removal of heat-damaged proteins. Activation of the heat shock response is under the control of the heat shock transcription factor 1 (HSF1) (Morimoto, 1998; Vabulas et al., 2010). HSF1 exists in an inactive monomeric state in non-stressed cells. Accumulation of misfolded proteins in cells experiencing proteotoxic stress diverts the molecular chaperones from HSF1, allowing it to attain the trimeric DNA-binding competent state. Once in the nucleus, activated HSF1 binds to heat shock elements (nnTTCnnGAAnnTTC) found in the promoter region of all heat-inducible genes,

up-regulating the synthesis of HSPs (Powers and Workman, 2007). As new heat shock protein synthesis eventually leads to the refolding or removal of heat-damaged proteins, the excess HSPs are then free to repress HSF1, returning it to its inactive monomeric state as the proteotoxic response dissipates (Powers and Workman, 2007; Vabulas et al., 2010).

1.9 Inhibition of apoptosis in thermotolerant cells by molecular chaperones

The cellular response to heat shock is adaptive, thereby allowing organisms to cope with potentially lethal proteotoxic conditions. Interestingly, exposure to mild hyperthermia induces a state of heat resistance or thermotolerance within cells during their recovery. This state of thermotolerance is dependent on HSPs, particularly HSP70 (Li et al., 1995). From hours to days after exposure to mild hyperthermia, cells express increased levels of HSPs that protect them during successive exposures to elevated temperature, temporarily conferring resistance to normally lethal temperatures or other proteotoxic stresses (Gerner and Schnider, 1975). The elevated thermotolerance of HSP expressing cells is caused by the inhibition of stress-induced apoptosis (Mosser and Morimoto, 2004). The degree of resistance to apoptosis correlates with the expression levels of HSP70 (Mosser and Martin, 1992). Thus overexpression of HSP70 protects cells from heat stress induced apoptosis and this protective effect extends to other stressful stimuli as well, which may be a contributing factor in tumor development (Mosser and Morimoto, 2004). Overexpression of HSPs found in many tumor types is often associated with increased resistance to anticancer therapeutic agents. Sustained HSP70 overexpression is associated with increased metastasis, resistance to chemotherapy and radiotherapy and poor prognosis (Isomoto et al., 2003). Interestingly, tumor cells rely on HSP70s continuous synthesis and when down-regulated cells undergo apoptosis (Rohde et al., 2005).

HSP70 has been shown to act at multiple levels to suppress the heat-induced apoptotic signal. HSP70 overexpression prevents Bax activation thereby inhibiting cytochrome c release and caspase activation (Mosser et al., 1997; Mosser et al., 2000). Possible mechanisms by which HSP70 blocks heat-induced Bax activation are by direct interactions with Bax or by preventing the activation of the stress-activated JNK (c-jun N-terminal kinase) or by preventing apoptosome formation and caspase activation (Jaattela et al., 1998; Beere et al., 2000; Mosser et al., 2000). JNK is normally activated in heat-stressed cells but inhibited by HSP70 overexpression (Mosser

et al., 1997; Gabai et al., 1998). Hyperthermia might also cause changes in the expression or activity of the Bcl-2 family of apoptotic proteins whose function is regulated by stress-induced changes in conformation and protein-protein interaction. Specific BH3-only proteins are sensitive to distinct forms of cellular stress. Exposure to hyperthermic conditions has been shown to increase PUMA mRNA levels but decrease the levels of PUMA protein (Figure 7; Stankiewicz, unpublished; Stephanie Hallows, 2005 unpublished). This anti-apoptotic effect is consistent with the efforts of malignant cells to maintain homeostasis in hostile environments.

Preliminary unpublished studies on PUMA demonstrate its important role in heat-induced apoptosis, however the exact mechanisms that control the decreased expression of this protein and increased expression of mRNA in heat-stressed cells are currently unknown but suggest some form of post-transcriptional control perhaps involving microRNAs.

1.10 microRNAs

Developmental studies in the 1990s revealed the first endogenous ~22 nucleotide (nt) regulatory ribonucleic acids (RNAs) in *C. elegans* and demonstrated that diverse 3' untranslated region (UTR) motifs mediated crucial modes of post-transcriptional repression of gene expression in *Drosophila melanogaster* (Lai et al., 1998, Reinhart et al., 2000). This post-transcriptional modification of gene expression is carried out by the action of a group of single stranded RNAs known as microRNAs (miRNAs).

1.10.1 miRNA biogenesis

miRNAs are defined as small, non-coding RNAs that repress the translation of target messenger RNAs (mRNAs) (Hammond, 2006; Fabian et al., 2010). Mature miRNAs function by the formation of hairpin transcripts that are processed into short RNAs that associate with Argonaute (Ago) proteins and form the RNA-induced silencing complex (RISC), a ribonucleoprotein complex mediating post-transcriptional gene silencing (Hammond, 2006). The RISC complex also guides complementary miRNAs to target mRNAs for degradation, destabilization, or translational inhibition by the Ago protein (Lagos-Quintana et al., 2001; Hammond, 2006; Fabian et al., 2010).

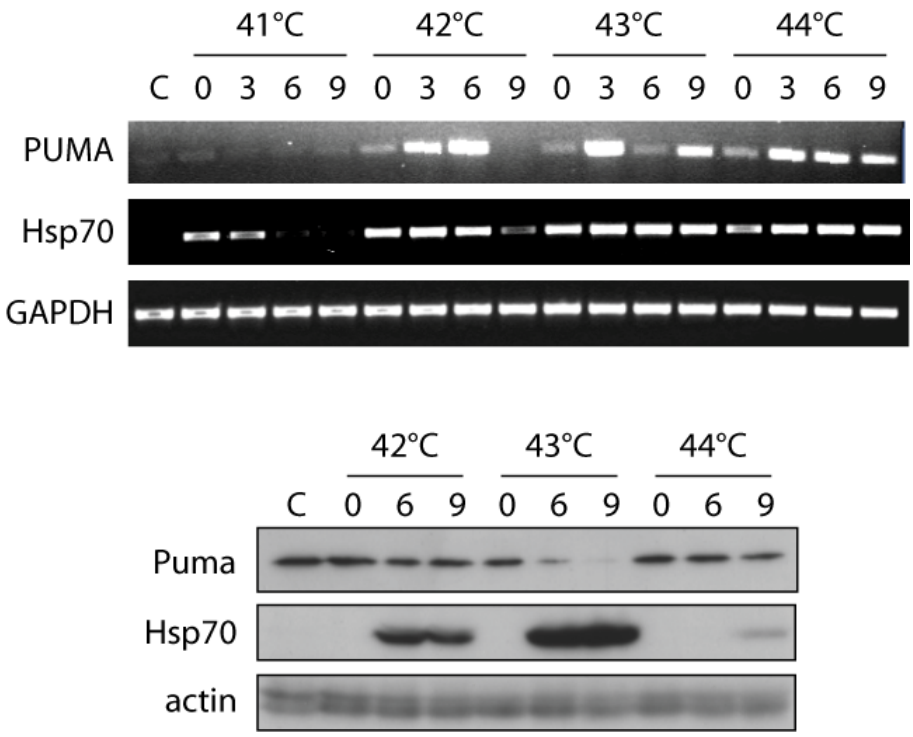

Figure 7: Preliminary characterization of PUMA protein and mRNA expression. PUMA mRNA and protein expression in PErTA70 cells under control and heat shock conditions at various temperatures. **A)** Preliminary results from RT-PCR show an increase in PUMA mRNA expression following heat shock at 42°C, 43°C and 44°C for 1 h (Hallows, 2005 unpublished; n = 1). **B)** Meanwhile, western blot analysis reveals a decrease in PUMA protein expression following exposure to 42°C or 43°C for 1 h (Stephanie Hallows, 2005 unpublished; n = 1).

miRNA biogenesis starts with the transcription of miRNA genes by either RNA polymerase II/III into primary miRNA (pri-miRNA) transcripts (Lee et al., 2004; Borchert et al., 2006). The long primary miRNA transcript is synthesized in the nucleus from non-coding DNA and processed by an RNAse enzyme named Drosha and the DGCR8 (DiGeorge critical region 8) protein, also known as Pasha, to a ~70 nt precursor miRNA (pre-miRNA). After nuclear processing, the pre-miRNA is exported to the cytoplasm by Exportin-5 (XPO5) in a complex with Ran-GTP (Yi et al., 2003). It is in the cytoplasm where the miRNA is further processed by the RNAse enzyme Dicer to give rise to the mature ~22 nt miRNA. RISC, with its core Argonaute (Ago2) protein component, is the cytoplasmic effector of the miRNA pathway and binds a single-stranded miRNA, guiding it to its target mRNAs (MacRae et al., 2008). Mature miRNA is able to regulate gene expression by either binding to the 3'UTR of its target mRNA (Figure 8) causing translational inhibition or even its targeted destruction (Hammond, 2006; Fabian et al., 2010). Yet, the consequences for mRNA targets are very different: mRNA degradation results in irreversible removal from the transcriptome, whereas the level of mRNA targets can remain constant or even increase upon inhibition of translation.

1.10.2 miRNA regulation of the stress response

miRNAs are widely expressed and regulate essentially all signaling pathways playing an important role in gene silencing and controlling a number of essential processes including cell proliferation, development, differentiation and apoptosis (Cimmino et al., 2005; Garzon, 2009; Wang et al., 2010). There are over 1000 human microRNAs currently identified in the miRNA database released October 10, 2010 (http://www.mirbase.org), even outnumbering kinases and phosphatases, indicating their extensive role in the regulation of cellular processes. Each miRNA is predicted to bind hundreds of target mRNAs, therefore a large portion of human genes are subject to miRNA regulation (Hammond, 2006; Friedman et al., 2009; Fabian et al., 2010). This binding morphology implies that expression of the mRNA target is likely to be under the control of multiple miRNAs (Krek et al., 2005). Consequently, nearly all developmental, physiological and disease-related processes appear to be regulated by miRNAs, at least to some degree (Flynt and Lai, 2008). Notably, miRNA processing defects may also enhance tumourigenesis (Kumar et al., 2007). Aberrant miRNA processing leads to altered expression of mature miRNAs, often

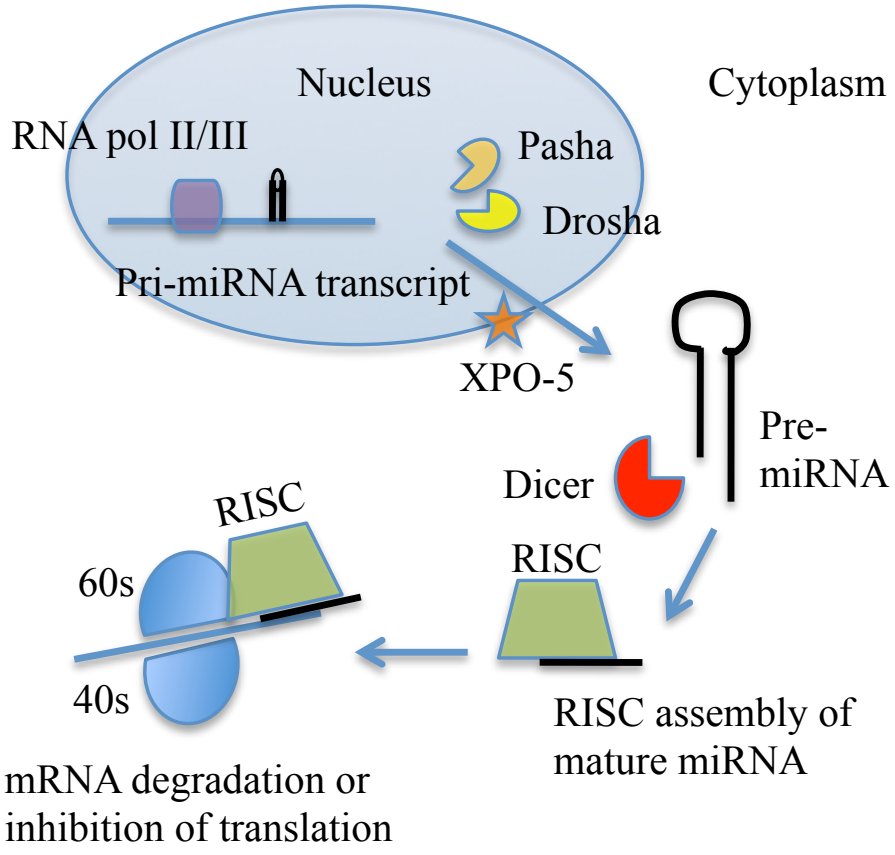

Figure 8: miRNA regulation of gene expression. miRNAs are generated as primary (pri-miRNA) transcripts by RNA polymerase II/III in the nucleus. After being processed by the endonucleases Drosha and Pasha, the stem-loop structure of the precursor miRNA (pre-miRNA) is exported out of the nucleus by Exportin-5 (XPO-5). The endonuclease Dicer releases the mature miRNA, which is then assembled into the RNA-induced silencing complex (RISC). The RISC directs its bound miRNA to partially complementary mRNA 3' untranslated regions, resulting in inhibition of translation or targeted destruction of the mRNA.

contributing to disease. Over 120 miRNA transcripts demonstrate differential expression in response to hyperthermia (Wilmink et al., 2010) and interestingly HSP70 has also been shown to influence miRNA processing (Iwasaki et al., 2010). At present, this mechanism is, however, not well understood.

1.10.3 miRNA modulation by p53

Recent reports show that misexpression of miRNAs, whether elevated or reduced, are seen in all types of cancer (Hammond, 2006; Wang et al., 2010). As a protein that senses environmental stress and modulates the level of miRNAs, p53 regulates the expression of specific miRNAs at two different levels: transcription and processing. Upon DNA damage, p53 induces the transcription of some miRNAs that together promote tumourigenesis by blocking p53, thus preventing cell cycle arrest or apoptosis (Hermeking, 1997). These miRNAs can be classified as oncogenic miRNAs. In addition, p53 enhances the processing of certain pri-miRNAs in cancer cells by associating with DDX5, a cofactor of Drosha (Suzuki et al., 2009). Overexpression of these miRNAs can act as tumor suppressors, not necessarily by inhibiting cell growth, but by preventing the progression of cancer (Hammond, 2006). Interestingly, most p53 mutations found in cancers are located in a domain that is required for both the miRNA processing function and transcriptional activity (Suzuki et al., 2009). Therefore, loss of p53 function in transcription and miRNA processing might contribute to tumor progression.

1.10.4 miRNA regulation of apoptotic proteins

Numerous studies have uncovered highly specific miRNA profiles during development and tumourigenesis. It is currently undisputed that miRNAs function as important regulators of apoptosis. Recent studies show that miRNAs can regulate the expression of key apoptotic regulators including the Bcl-2 family proteins. Zhang and colleagues found that miRNA (miR) -221 and miR-222 directly target PUMA mRNA translation in various types of cancer cells (Zhang et al., 2010). Additionally, RNA interference (RNAi) mechanisms have been shown to regulate apoptosis directly by targeting these miRNAs and ultimately altering the expression of PUMA in glioblastoma, A549 lung and MCF-7 breast cancer cell lines (Zhang et al., 2010). A knockout of miR-221/miR-222 results in restoration of the pro-apoptotic PUMA protein and its activity inducing cancer cell apoptosis and inhibition of tumor growth in these cells. miR-221

and miR-222 are only a few of the miRNAs shown to target and alter the expression of PUMA and may therefore be potential therapeutic targets in the treatment of certain types of cancers (Zhang et al., 2010). Alternatively, Ouyang and colleagues found miR-29a to target PUMA mRNA when studying forebrain ischemia (Ouyang et al., 2013). Another very recent study on the liver carcinoma cell line, HepG2, has raised the possibility that miR-483-3p modulates PUMA and that it's induced expression can protect cells from apoptosis (Veronese et al., 2010). miR-BART5, an Epstein-Barr Virus (EBV) encoded miRNA is another miRNA that has been shown to have anti-apoptotic activity targeting PUMA expression in nasopharyngeal carcinoma (NPC) and in EBV-associated gastric carcinoma latently infected with EBV to protect these cells from apoptosis. Interestingly, this was the first evidence that some viruses are able to modulate cellular apoptosis through miRNAs (Choy et al., 2008). Because a large number of miRNAs contribute to the development of cancer and other disease, the discovery of miRNA pathways has opened up a novel therapeutic approach for treatment.

1.10.5 Therapeutic roles of miRNAs

Evasion of apoptosis is both a hallmark of cancer and is involved in tumourigenesis and drug resistance. Overcoming chemotherapeutic drug resistance remains a key challenge in the fight against cancer (Johnstone et al., 2002). This drug resistance may be in large part due to resistance to apoptosis. Where apoptosis can be effectively induced, dramatic clinical responses are often seen (Lynch et al., 2004). This reinforces the basic concept that achieving efficient apoptosis is essential for optimizing therapeutic responses and therefore clinical outcome.

Recently miRNAs have been shown to be important in regulating apoptotic proteins and therefore cell death. The field of miRNAs based pharmacogenomics is still relatively new but given their involvement in the regulation of apoptosis and the understanding that most chemotherapeutic drugs kill cells by this mechanism, core apoptosis pathway-targeting miRNAs have good potential as predictors of anti-cancer drug efficacy (Lima et al., 2011). This, along with the abundance and wide range of activity of miRNAs, makes them attractive candidates as biomarkers for cancer. In addition, modulation of miRNA expression with miRNA mimetics or antagomirs may be a possible therapeutic avenue (Garzon et al., 2010). One advantage of using miRNAs as therapeutic targets is that they often regulate multiple mRNA targets that belong to

the same signaling pathway or protein complexes at the same time (Ebert and Sharp, 2010; Tsang et al., 2010). The key is to identify which miRNAs and which targets are involved in each particular disease. There are ongoing efforts to deliver miRNA mimics or perfectly complementary antagomir inhibitors to increase or decrease, respectively, the levels of specific miRNAs *in vivo*. In cases where a specific miRNA-mRNA target interaction should be modulated, short oligonucleotides termed "target protectors" have been successfully applied in mammalian cells (Choi et al., 2007). The idea of a target protector is that a single-strand oligonucleotide could specifically interfere with a single target while leaving the regulation of the other targets of the same miRNA unaffected. Ultimately, this avenue of research will lead to better understanding and treatment of diseases in which miRNAs mediate the modulation of mRNA expression. Once better understood, the expression of the miRNAs can be altered effectively to restore the expression of the target mRNA and protein.

1.11 Research proposal

Because PUMA expression is a strong inducer of apoptosis in stressed cells, it is important to examine how stressful conditions such as heat-induced stress may affect protein and mRNA levels. Preliminary studies have shown an increase in PUMA mRNA and a decrease in PUMA protein expression in heat-shocked cells. Changes in PUMA expression following heat shock may be attributed to a number of things including a change in the rate of PUMA transcription or translation or a change in protein/mRNA stability. In this project, we investigate changes in mRNA translation. Altered expression and therefore function of PUMA brings up the question of what other mechanisms besides HSPs are controlling the expression of PUMA protein and mRNA levels in heat-stressed cells. The effect of miRNAs, which are key regulators of stress-induced apoptotic pathways will be assessed. There are only a few reports on the effects of hyperthermia on heat-induced miRNA expression (Wilmink et al., 2010). Heat-induced altered expression of a miRNA that targets the PUMA 3'UTR may explain the translational suppression of PUMA mRNA resulting in the eventual turnover of the existing pools of PUMA protein. Ultimately, I will test whether the overexpression of candidate miRNAs that target the PUMA 3'UTR influence the abundance of PUMA mRNA and protein and whether heat shock affects the abundance of these miRNAs. Once the expression of PUMA is better characterized,

we can then further investigate what mechanisms are responsible for the altered expression seen in so many disorders and diseases.

CHAPTER 2: MATERIALS AND METHODS

2.1 Bacterial transformation

Escherichia coli (K12 – DH5α) were transformed with plasmid DNA by heat shock treatment of chemically competent cells. *E. coli* were made competent by incubation in a solution containing 100 mM $CaCl_2$. A frozen aliquot of competent *E. coli*, from -80°C, was thawed on ice for 30 min. 100 µl of the thawed *E. coli* was transferred to a labeled 1.5 ml microcentrifuge tube along with approximately 25 ng of plasmid DNA. The bacterial solution was then placed on ice for another 30 min. The contents of the tube were later heat-pulsed at 42°C in a circulating water bath for 1 min before being returned to ice for another 2 min. Over the flame of a Bunsen burner, 900 µl of LB broth (Appendix A) was added to each tube and pipetted gently to mix. Tubes were then set to incubate on a shaker (220 rpm) at 37°C for 1 h. Aliquots of 50 and 200 µl of transformation were plated on LB agar plates with 50 mg/ml Ampicillin (Appendix A). Transformed cells were gently spread across the surface of the plate in a circular motion under a Bunsen burner flame using a sterile bent glass rod. Plates were left to incubate upside down in a 37°C incubator overnight to allow colony formation of *E. coli* that contained the Ampicillin resistance gene (Amp^r) from the plasmid (Rosman and Miller, 1990). Mini/midi-preps could then be used to extract the desired DNA from the *E. coli.*

2.2 Alkaline lysis mini-prep

Under the flame of a Bunsen burner, 3.5 ml of LB broth with Ampicillin (Amp) were added to a labeled 13 ml bacterial culture tube (Fisher Scientific). Single colonies were selected from the transformation plate with the use of a micropipette tip by pinching and transferred to the bacterial culture tube by ejecting the tip into the LB/Amp broth. Bacteria culture tubes were placed on a shaker (220 rpm) at 37°C overnight (16 h). The following day, all tips were removed from the bacteria culture tubes under the flame of a Bunsen burner and 1 ml of the culture was transferred to a labeled 1.5 ml microcentrifuge tube. Samples were centrifuged to pellet the overnight culture of transformed bacteria. After the supernatant was removed, the pellet was resuspended in 100 µl GTE with RNAse (Appendix A). The cells were lysed with the addition of 100 µl SDS/NaOH Buffer (Appendix A) by inverting the tubes 5 times before incubating them at

room temperature for no more than 5 min. This step allowed for the lysis of the cell wall and membrane, denaturation of chromosomal DNA and proteins and the pH 12.0 caused DNA to denature from dsDNA to ssDNA. The lysis buffer was then neutralized with the addition of 200 µl of 5 M potassium acetate Buffer (pH 4.8; Appendix A) and inverted 3 times to mix. The lysed cell solution was then centrifuged at 10,000 x g for 5 min in a centrifuge (Eppendorf 5417C) allowing the plasmid DNA to be recovered in the supernatant. The supernatant was transferred to a new 1.5 ml microcentrifuge tube before being washed with 1 ml of 95% ethanol and pelleted once again at the bottom of the tube by centrifugation at 10,000 x g for 20 min. The supernatant was removed and the precipitated DNA was washed a second time with 70% ethanol before being centrifuged a final time at 10,000 x g for 10 min to remove any remaining salts. All remaining supernatant was discarded and the pellet was left to air dry in a flow hood for approximately 20 min. The pellet was resuspended in 50 µl of 1/10 TE Buffer (Appendix A) and stored at -20°C until use.

2.3 Midi/Maxi-prep

The PureLink™HiPure Plasmid DNA purification kit (Invitrogen™) was used to collect and isolate high yields of highly pure plasmid DNA. This protocol is very similar to that of the mini-prep amplification above, differing only in the volume of starting *E. coli* culture and the use of an anion exchange column to purify the DNA once it has been amplified. In this protocol, an input of 200 ml of *E. coli* cells transformed with DNA and grown overnight were harvested and passed through a pre-packed midi-prep anion exchange column (Invitrogen™). The eluted midi-prep DNA was resuspended in 100 – 200 µl of 1/10 TE Buffer, quantified by nano-drop (ND8000, Thermo Scientific) photospectrometry and stored at -20°C until use.

2.4 Nano-drop 8000 spectrophotometer

The nano-drop spectrophotometer (ND8000, Thermo Scientific) in the genomics facility at the University of Guelph was used to measure the quality and quantity of nucleic acids within the range of 2.5 – 3700 ng/µl. The absorbance pedestals were blanked and cleaned with ddH_2O and Kim Wipes® prior to use. Once samples were thawed and mixed well, 0.5 – 2 µl samples were pipetted onto the optical pedestals of the reader and measured using full-spectrum UV – Vis absorbance measurements.

2.5 Examining DNA by gel electrophoresis

Ultrapure agarose powder was melted in 200 ml of 1X TAE Buffer (Appendix A) for 3 min in a microwave. The percentage of the gel was made based on the range of resolution of linear DNA required (ex: 1% gel effective for 10 – 0.5 kb DNA fragments and 1.5% gel for 3 – 0.2 kb fragments). 10 μl of RedSafe™ (Intron Technology) DNA staining solution was added to the boiled agarose gel components and swirled to mix before being poured into the gel-casting tray with the appropriate sized combs. RedSafe allowed DNA staining proportional to the amount of DNA in the wells. Once polymerized, the porous gel permits negatively charged DNA to migrate towards the positively charged electrodes in the electric field. The addition of 10X loading dye to the DNA samples (Appendix A) facilitated loading samples into the wells and sizing the bands. A GeneRuler™ 1kb Plus DNA Ladder was also used to help estimate size as well as concentration of the observed fragments of DNA (Fermentas). Gels were run at 120 Volts for 45 min – 1h 45 min depending on the percentage of the gel and the size of the desired product.

2.6 Isolation of DNA from agarose gel

DNA bands were visualized in an agarose gel on a Foto/PrepI UV transilluminator (Fotodyne) wearing the necessary protective equipment. A sterile razor blade was used to cut the gel slice containing the desired DNA fragment. The isolated portion of the gel was then transferred to a 1.5 ml microcentrifuge tube and weighed. 3 volumes of 6 M NaCl solution from the Qiaex®II gel extraction kit (Qiagen) was added to the tube and vortexed to mix. Next, silica beads were added at a ratio of 1 μl/μg DNA and heated to 55°C for 10 min, vortexing every 2 min to dissolve the agarose. The DNA was bound to the silica beads in high salt concentrations and centrifuged at max speed for 2 min to pellet the beads/DNA and discard the supernatant. The beads were washed with 70% Ethanol, centrifuged and the supernatant was removed to allow the beads to air dry. DNA was then eluded with 1/10 TE Buffer as the silica beads released the DNA in low salt. The DNA was then stored at -20°C until further use.

2.7 DNA purification

Up to 40 μg of 100 bp – 2 kb dsDNA PCR products were rapidly and efficiently purified using the PureLink™ PCR Purification kit from Invitrogen. The kit was designed to remove

primers, dNTPs, enzymes and residual salts leaving a purified PCR product suitable for restriction enzyme digestion and cloning. The PCR product was mixed with the Binding Buffer to adjust conditions for subsequent dsDNA binding to the PureLink™ Spin Column. Once the dsDNA was bound to the silica-based membrane in the column, impurities were removed by thorough washing with the Wash Buffer. The dsDNA was then eluted in low salt Elution Buffer or ddH_2O (Invitrogen). The final purified DNA products were stored at -20°C until further use.

2.8 DNA cloning and restriction enzyme digest

All restriction enzymes and their buffers were purchased from New England BioLabs. 1 unit of restriction enzyme was used to completely digest 1 μg of substrate DNA in a 50 μl reaction volume in 1 h using the appropriate buffer and optimal temperature for the enzyme. The optimal temperature, salt concentration and requirement for BSA to maintain activity varies for each enzyme and determines which NEB Buffer to use. When performing multiple digests, some enzymes required heat inactivation after the first digestion, before subjecting the DNA to further digests with other restriction enzymes or ligation. Not all enzymes could be heat inactivated and digested DNA sometimes required purification using a spin column. Reactions were set up as follows: 5 μl 10X NEB Buffer, 5 μl 10X BSA (if necessary), 1 U enzyme per 1 μg DNA and the reaction was brought up to 50 μl with ddH_2O.

2.8.1 psiCHECK-2 plasmid digest

The psiCHECK-2 plasmid (Promega) was transformed into competent *E. coli* and mini-prep DNA was screened by gel electrophoresis (Figure 9). Once confirmed as the proper DNA plasmid, further amplification of the DNA was done with the use of a midi-prep (Invitrogen kit) and column purified (Invitrogen Kit). The psiCHECK-2 plasmid was digested with Xho1 (cutting at 1643 bp) in CutSmart Buffer for 2 h at 37°C in a circulating water bath. A portion of the digest was verified by running the product on an analytical 1% agarose gel to ensure complete digestion of the plasmid. XhoI was then heat inactivated at 65°C for 20 min before digesting the now linearized psiCHECK-2 with a second restriction enzyme. The second digest was completed with NotI (cutting at 1674 bp) in NEB Buffer 3.1 for 3 h at 37°C and heat inactivated at 65°C for 20 min (New England BioLabs). Both enzymes used were unique to the

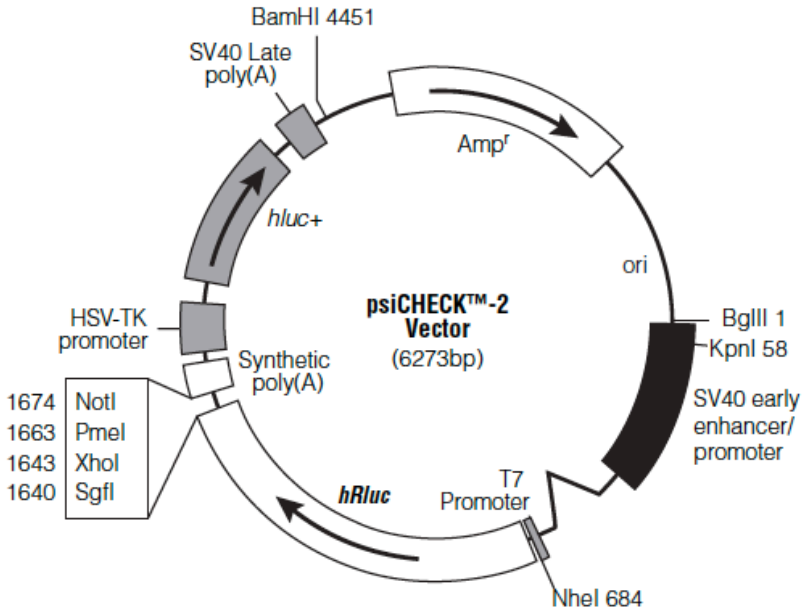

Figure 9: psiCHECK-2 vector (Promega). This luciferase expression plasmid was used to examine the effect of the miR-24-2, miR-27a and miR-29a binding sites in the PUMA 3'UTR on reporter gene expression. The PUMA 3'UTR was cloned into the XhoI and NotI restriction sites downstream of the renilla luciferase gene (*hRluc*). Mutations in each of the miRNA binding sites were created by site directed mutagenesis to create PUMA 3'UTR mut-miR-24-2, PUMA 3'UTR mut-miR-27a and PUMA 3'UTR mut-miR-29a reporter plasmids. The plasmid also contains a firefly luciferase gene (*hluc*+) that can be used to normalize each transfection for transfection efficiency.

plasmid and located downstream of the renilla luciferase gene. A preparative gel was then run with the entire digest to separate the desired fragment from the cut fragment of the plasmid using the QiaexII gel extraction kit (Qiagen). After the desired portion of linearized plasmid was successfully isolated, the DNA was run on an analytical gel to quantitate the DNA for ligation with the PUMA 3'UTR insert.

2.8.2 Phusion PCR of the PUMA 3'UTR insert

The PUMA 3'UTR DNA insert (Figure 10) was created by PCR using human genomic DNA and primers (Table 2: DDM273 and DDM274) containing a restriction site for Xho1 at the 5' end and a Not1 restriction site at the 3' end. These primers were used to perform PCR using Phusion® high fidelity DNA polymerase (New England BioLabs). The Phusion PCR reaction was as follows: 10 ng human genomic DNA, 100 μM of each primer, 1X Phusion HF Buffer, 200 μM dNTPs, 0.5 μl of Phusion© Taq polymerase and the reaction was brought up to 50 μl with ddH_2O. Using a BioRad automatic thermocycler, the Phusion PCR conditions were set as follows; 98°C for 30 s, followed by 30 cycles of; 98°C for 10 s, 70°C for 30 s, 72°C for 30 s followed by a final extension cycle at 72°C for 5 min. The PCR product was purified using a spin column and digested with the same enzymes as the psiCHECK-2 plasmid (Xho1 and Not1). This allowed the ends of the PUMA 3'UTR DNA insert to correspond with the ends of the cut psiCHECK-2 plasmid. Once the double digest was complete, the insert was purified and run on an analytical agarose gel to quantitate the DNA for ligation.

2.8.3 psiCHECK-2 + PUMA 3'UTR ligation

The ligation was performed using a molar ratio of 3:1 (insert to vector) with a total of <50 ng DNA and a control ligation of vector without insert. The ligation mixture contained 20 ng of the cut psiCHECK-2 vector (5903 bp) and 5 ng of the PUMA 3'UTR insert (981 bp), 1 μl 10X T4 Ligase Buffer and 1 μl T4 DNA Ligase enzyme (BioLabs) in a total volume of 10 μl. The ligation mixture was incubated overnight (16 h) in a 16°C water bath overnight. The following day, the ligation mixture was transformed into competent *E. coli* bacteria and spread onto an LB/Amp agar plate. After 16 h incubation at 37°C, several colonies were transferred to 3 ml LB/Amp broth in a bacterial culture tube and grown overnight in a 37°C shaker. Mini-preps

Figure 10: PUMA 3'UTR sequence. Shown are the 981 nucleotides that follow the stop codon. The location of the three miRNA binding sites (miR-29a, miR24-2, miR-27a) are shown in red boxes.

were performed from the liquid bacterial cultures, screened by restriction enzyme digest with Not1 and Xho1 and run by analytical agarose gel electrophoresis to confirm the presence of the expected bands at 981bp and 6242bp.

2.9 Cell lines

Various cell lines were used in multiple different experiments depending on their expression of the target gene and transfection efficiency. In all cell lines used, the respective media was supplemented with 1% penicillin/streptomycin antimicrobial cocktail, 1% l-glutamine and 10% Fetal Bovine Serum (FBS) (Invitrogen Inc. Burlington, ON). All cell lines were grown at their optimal conditions of 37°C with 5% CO_2 in a humidified incubator.

2.9.1 PEER cells

PEER cells are a human acute lymphoblastic T cell line isolated from a seven-year-old girl with lymphoma (Ravid et al., 1980). These lymphoid cells were grown in suspension in sterile vented flasks in Roswell Park Memorial Institute (RPMI) media (Life Technologies) supplemented as described above. These cells were used for transient and stable transfections with plasmid DNA.

2.9.3 PErTA12 cells

PErTA12 cells are PEER cells genetically engineered to express reverse tetracycline-controlled transactivator (rtTA) and were grown as described for PEER cells except that G418 was added at a final concentration of 200 µg/ml.

2.9.2 PErTA70 cells

PErTA70 cells are an engineered human acute lymphoblastic T cell line, PEER, inducible to overexpress HSP70 using tetracycline-regulated expression (Mosser et al., 2000). PErTA70 cells were grown in suspension in vented tissue culture flasks with RPMI media with the addition of 200 µg/ml Hygromycin B and Geneticin (G418) selective antibiotics (Life Technologies) for drug selection of cells stably expressing plasmids encoding the reverse tetracycline regulated transactivator (rtTA) and a rtTA regulated HSP70 gene.

2.9.4 HEK293T cells

The human embryonic epithelial kidney cell line (HEK293) was used for transfections as these cells showed the highest transfection efficiency across an array of transfection reagents (Pear et al., 1993). The large T antigen is the immortalizing agent allowing for these cells to be passaged indefinitely throughout experimentation. HEK293T cells are adherent cells that required trypsinization using 1X Trypsin Buffer (Appendix A). These cells grow optimally in high glucose Dulbecco's Modified Eagle Medium (DMEM, Life Technologies) supplemented as above, in sterile tissue culture plates.

2.9.5 HeLa cells

The HeLa cell line is one of the most commonly used immortal cell lines derived from a woman with human cervical carcinoma. These cells were used in transfection as they seem to have higher transfection efficiency and elevated endogenous expression of the target microRNAs. Specifically, HeLa cells showed the best response to transient co-transfections. HeLa PC cells are an adherent cell line requiring trypsinization with 1X Trypsin for splitting and passaging cells. These cells were plated in sterile tissue culture plates in high glucose DMEM media supplemented as above.

2.10 Cell maintenance

Cell culture was used in all experiments and was therefore a crucial part of this thesis. In order to maintain health, proliferating cells and prevent contamination, proper cell culture technique was vital.

2.10.1 Freezing cells

Back-up stocks of all cells used in experimentation were kept frozen both at -80°C and in liquid nitrogen tanks. These stocks were created from back-up cultures of cells in log phase of growth. Cells were spun down at 1,100 x g and ~ 5 x 10^6 cells were resuspended in 1 ml of the appropriate media with 10% Dimethyl Sulfoxide (DMSO). DMSO is used as a cryoprotectant to reduce ice formation when freezing cells. The cells were then transferred to a cryotube and frozen at -80°C in a Styrofoam casing before transferring them to a liquid nitrogen tank.

2.10.2 Thawing cells

A circulating water bath was set to 37°C and the appropriate media was warmed to that same temperature. Cells from liquid nitrogen or -80°C were thawed in the 37°C water bath until there was no more ice left in the cryotube (1 – 2 min). The cells were then transferred to a new labeled sterile tissue flask or plate with the appropriate amount of fresh media and left to recuperate at 37°C overnight. If drug selection was necessary, the drugs were only added 16 h after being thawed.

2.10.3 Hemocytometer cell counts

Cells were counted before being passaged, plated for transfection or heat shock experiments with the use of a hemocytometer grid. One drop of a cell suspension (~ 20 μl) was added to the pedestal between the cover slip and the plate of one of the two grids. Any excess cell suspension flowed into the margins alongside each grid. All four quadrants of the grid were counted for viable cells under 200X magnification and the total number from all four quadrants was added and multiplied by 2.5 x 10^3 to get the approximate number of cells/ml.

2.11 Heat stress treatments

For induced synthesis of HSP70, PErTA70 cells at a density of ~ 4 x 10^5 cells/ml were incubated at 37°C with 1 μg/ml Doxycycline for 24 h prior to heat shock. Both OFF and the induced ON PErTA70 cells were heat-shocked the following day in log-phase growth of ~ 8 x 10^5 cells/ml in a 15 ml centrifuge tube with 1 ml fresh media and 10 μl/ml of 1 M Hepes Buffer (Appendix A). The tubes were capped securely using Parafilm (Pechiney Plastic packaging) and immersed horizontally in a circulating water bath maintained at 43°C for 60 min. After hyperthermic treatment, cells were either placed directly on ice, pelleted and washed with cold dPBS for collection of protein/RNA (0 h post-heat shock), or transferred to a new flask at ~ 1 x 10^6 cells/ml in fresh 37°C RPMI media, and returned to the 37°C incubator until collection (3 h, 6 h or 9 h post-heat shock). A control sample of both ON and OFF cells maintained at the optimal growth temperature of 37°C was also collected at time 0 h (Figure 11).

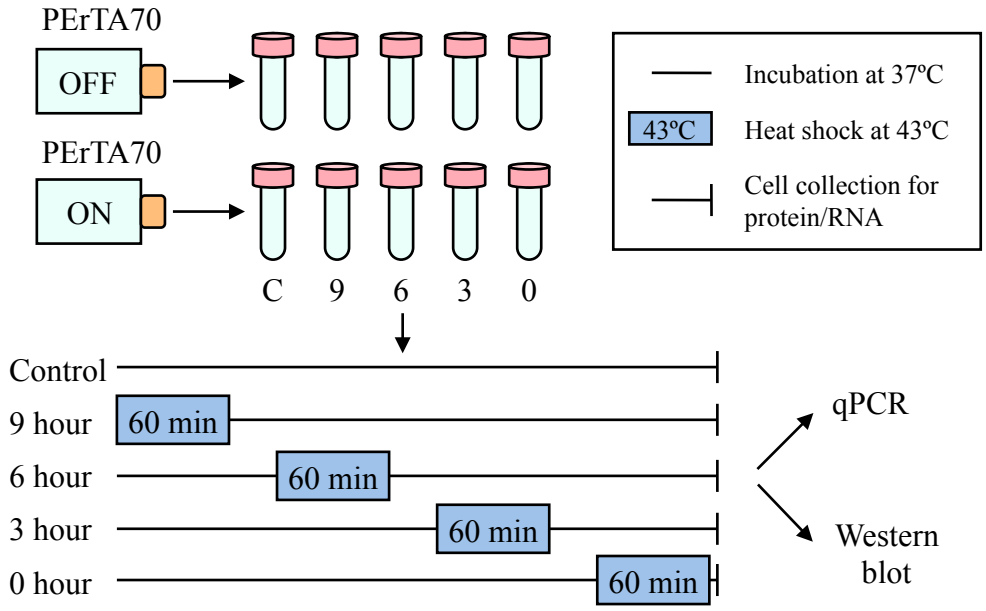

Figure 11: PErTA70 heat shock. The expression of PUMA protein and mRNA levels were examined in non-induced (OFF) and doxycycline-induced (ON) PErTA70 cells under control (37°C) and hyperthermic conditions (43°C for 60 min). Heat-shocked ON and OFF cells were collected immediately after hyperthermia (0 h) and following incubation at 37°C for 3 h, 6 h and 9 h. A sample of both ON and OFF cells maintained at the optimal growth temperature of 37°C was also collected as a control (C). Both western blots and qPCR experiments were used to analyze PUMA protein and mRNA levels respectively.

2.12 Western blotting

Western blots were used to analyze protein from samples collected from heat shock experiments of transient transfections.

2.12.1 Cell collection for protein

Heat-shocked ON and OFF PErTA70 cells were collected immediately after hyperthermia (0 h) and following incubation at 37°C for 3 h, 6 h and 9 h. Aliquots of 5 x 10^6 cells were transferred to 15 ml centrifuge tubes and centrifuged at 3,000 x g for 6 min at 4°C to pellet the cells. Samples remained on ice throughout the remainder of the collection. The supernatant was removed by aspiration in the flow hood and pellets were then resuspended in 1 ml of cold dPBS and transferred to labeled 1.5 ml microcentrifuge tubes. Samples were centrifuged at 3,000 x g for 5 min at 4°C and the supernatant was removed once again. A final centrifugation at 3,000 x g for 1 min was performed to ensure all dPBS was removed before storing the samples at -20°C.

2.12.2 BCA protein assay

Protein pellets were lysed in 1X Laemmli lysis buffer without β-mercaptoethanol and bromophenol blue containing protease and phosphatase inhibitors (Appendix A). Cell pellets containing 5 x 10^6 cells were lysed in 75 µl of lysis Buffer on ice. Cell lysates were sonicated for 10 sec to shear DNA and boiled at 95°C for 5 min to denature proteins. Samples were then centrifuged at 4,500 x g for 5 min to gather the cell lysate. The protein concentration of the lysates was measured by mixing 3 µl of the lysate with 200 µl of BCA (Bicinchoninic Acid, Protein Assay Reagent Kit, Peirce) and incubation at 37°C for 30 min. Protein concentration of cell lysates was determined by comparison of optical density measurements with a BSA standard curve (0 – 50 micrograms of BSA dissolved in 1X Laemmli lysis Buffer). Optical density (OD) at 595 nm was measured using a ThermoMax microplate reader (Molecular Devices). Data was exported from the Softmax plate reader software to Excel to construct a standard curve and calculate the protein concentration of each sample. Twenty µl of each lysate was then mixed with 5 µl of 5X Laemmli lysis Buffer (containing β-mercaptoethanol and bromophenol blue) and an appropriate volume of 1X Laemmli lysis Buffer (Appendix A) to bring each sample to the same protein concentration (generally 2.5 µg/µl).

2.12.3 Antibodies

The following primary antibodies were used for western blotting: actin: pan Ab-5 mouse monoclonal #ACTN05 (NeoMarkers, Fremont, CA) diluted 1:5000 in antibody binding solution (Appendix A); HSP70: clone C92f3A-5 mouse monoclonal (Stressgen) diluted 1/10,000; and PUMA: rabbit polyclonal antibody (ProSci Inc.) diluted 1:1000 in Antibody binding solution (ABS). Mouse horseradish peroxidase (HRP) secondary antibody was used for actin and HSP70 diluted 1: 20,000 with 5% milk in 1X TBS + Tween. Rabbit HRP conjugated secondary antibody was used for the detection of PUMA also diluted 1: 20,000 with 5% milk in 1X TBS + Tween.

2.12.4 Western blot

A 13% acrylamide separating gel was prepared for the detection of PUMA protein (23 kDa) and set to polymerize for 30 min. The stacking gel was then added to the top of the separating gel and left to polymerize for another 30 min. At this point the protein samples were re-heated at 65°C for 5 min to ensure all Sodium Dodecyl Sulfate (SDS) was dissolved before being briefly centrifuged. 50 μg of protein from each sample was loaded in the appropriate well of the stacking gel along with a PageRuler™Prestained Protein Ladder (Thermo Scientific). The molecular weight marker was used to size the protein bands on the membrane. 1X Laemmli with 1X β-mercaptoethanol Buffer (Appendix A) was added to any empty wells for even sample migration. The gel was run at 200 Volts for ~ 45 min in Tris-Glycine Electrophoresis Buffer (Appendix A). The proteins in the gel were then transferred onto an Immobilon-P: 0.45 μm pore PVDF membrane (Millipore). The transfer was performed at 300 mA for 1.5 h in CAPS Transfer Buffer (Appendix A). Once the transfer was complete, the gel was stained in Coomassie Blue gel stain for 1 h to visualize the protein run in each well. This was used to check that the lanes ran properly and the protein quantities appeared consistent before continuing with the blotting of the membrane. Meanwhile, the membrane was rocked in 5% milk with 1X TBS + Tween Buffer for 1 h to block any non-specific antibody binding sites on the membrane. The membrane was then rinsed in 1X TBS + Tween Buffer on a rocker for 3 x 20 min and transferred to a cylinder with 1: 1000 α-PUMA primary antibody in Antibody Binding Solution (Appendix A). The membrane was left to incubate overnight in primary antibody at room temperature on a rotating mixing apparatus. After 16 h in primary antibody, the membrane was washed once again on a rocker for 3 x 20 min in 1X TBS + Tween Buffer and transferred to a cylinder with 1: 20,000 anti-Rabbit

HRP secondary antibody in 5% milk made with 1X TBS + Tween Buffer. The membrane was incubated in secondary antibody at room temperature for 1 h. The membrane went through one last wash of 3 x 20 min in 1X TBS + Tween before being exposed in the dark room using ECL™ Western Blotting Substrate (Peirce) and Amersham Hyperfilm™ ECL X-ray film (GE Healthcare). Following exposure to the membrane, the film was processed using Kodak Developer for 20 s, rinsed in water for 1 min and rocked in Kodak Fixer for 30 s. The same membrane was then rinsed in 1X TBS + Tween Buffer and the process repeated for the detection of actin and HSP70.

2.13 Cell lysis and extraction for RNA

Heat-shocked OFF and ON PErTA70 cells were collected immediately after hyperthermia (0 h) and following incubation at 37°C for 3 h and 6 h. Aliquots of 5 x 10^6 cells were then transferred to a 15 ml centrifuge tube and centrifuged at 3,000 x g for 6 min at 4°C. Samples were kept on ice throughout the cell lysis process. The supernatant was removed by aspiration in the flow hood and the cell pellets were resuspended in 200 µl of dPBS. Cell suspensions were then transferred to labeled 1.5 ml microcentrifuge tubes along with 800 µl of TRIzol® Reagent (Invitrogen) and vortexed before being stored at -80°C.

2.13.1 TRIzol® RNA extraction

Total cellular RNA was isolated using the Ambion TRIzol RNA extraction solution following the manufacturer's protocol. The samples were removed from -80°C and left to incubate at room temperature for 5 min before the addition of 200 µl of chloroform to each tube. Samples were then vortexed for 15 s and left at room temperature for another 2 min. Samples were then centrifuged at 12,000 x g for 15 min at 4°C. The upper aqueous phase of each sample was removed carefully by pipetting out the solution to a new, labeled microcentrifuge tube. To isolate the RNA, 500 µl of 100% isopropanol was added to the aqueous phase of each sample and left to incubate at room temperature for 5 min. Samples were then centrifuged at 12,000 x g for 10 min at 4°C and the supernatant was removed by pouring. To wash the RNA, 1 ml of 75% ethanol was added to each sample, vortexed for 15 s and centrifuged at 7,500 x g for 5 min at 4°C. The supernatant was removed by pipetting and air dried for 15 min. Finally, the RNA was

resuspended in 50 μl 1/10 TE Buffer and heated at 55°C for 5 min to solubilize the RNA. Each sample was then aliquoted to four labeled microcentrifuge tubes and stored at -80°C until use. Each tube of RNA was used once to avoid potential RNA degradation following repeated freeze-thaw cycles.

2.13.2 Semi-quantitative reverse transcriptase-mediated PCR (RT-PCR)

RT-PCR was first used to assess PUMA mRNA levels after heat-shock. This method proved useful originally to visualize the increase in PUMA mRNA expression after heat-shock but was hard to quantify and replicate successfully. All primers for this protocol were designed based on published studies.

2.13.3 First-Strand cDNA synthesis

The DNA template was created by reverse transcribing mRNA into cDNA with the use of a viral reverse transcriptase enzyme that synthesized cDNA from single-stranded RNA initiated from an oligo-dT DNA primer followed by PCR using gene specific primers. The following components were added to a 200 μl microcentrifuge tube: 20-200 ng DDM175 oligo-dT_{18} oligonucleotide primer, up to 5 μg of total RNA, 10 mN dNTP mix and ddH_2O up to 12 μl. The mixture was then heated to 65°C for 5 min and quickly chilled on ice for 2 min. The contents of the tube were collected by brief centrifugation and 4 μl of 5X First-Strand Synthesis Buffer as well as 2 μl of 0.1 M DTT were added before mixing the tube gently and incubating the tube at 42°C for 2 min in a circulating water bath. After incubation, 1 μl (200 U) of SuperScript™ II RT enzyme was added and mixed gently by pipetting before heating the reaction to 42°C for 50 min in the water bath. The enzyme was then inactivated by heating the contents at 70°C on a heat block for 15 min and the newly synthesized complementary DNA (cDNA) was stored at -20°C until use.

2.13.4 RT-PCR

The semi-quantitative method of PCR was used to visualize and measure target the newly synthesized cDNA on an agarose gel. The following reaction components were added to a 200 μl PCR microcentrifuge tube: 10 μl 5X PCR Buffer, 50 mM $MgCl_2$, 10 mM dNTP mix, 10 μM

both forward and reverse primers (Table 2), 5 U/μl Taq DNA Polymerase, 2 μl cDNA from first-strand reaction and ddH_2O up to 50 μl. The reaction was mixed gently by pipetting and brief centrifugation before loading the tubes into the automatic thermocycler (BioRad). The PCR conditions were as follows: 94°C for 2 min to denature dsDNA followed by 29 cycles of 94°C for 30 s, 60°C for 30 s, 72°C for 45 s and a final extension cycle of 72°C for 5 min. Note that the optimal concentration of Mg2+ varies depending on the template and primer pair. Once the PCR reaction was complete, the products were run on an analytical agarose gel to quantify and compare mRNA expression of the target gene.

Table 2: Primers for RT-PCR

Gene	Primers	Tm (°C)
PUMA #1	Forward: 5'- GACCTCAACGCACAGTA -3' Reverse: 5'- CTAATTGGGCTCCATCT -3'	52.4 49.9
PUMA #2	Forward: 5'- GCCCACCACCATCTCAGGA -3' Reverse: 5'- GCTGGAGCAACCGGCAAAC -3'	61.6 61.6
GAPDH	Forward: 5'- CCCCTGGCCAAGGTCATCCATGACAACTTT -3' Reverse: 5'- GGCCATGAGGTCCACCACCCTGTTGCTGTA -3'	73.3 76.2

2.14 Quantitative real-time PCR (qPCR)

qPCR was done due to the difficulty in quantifying and replicating the RT-PCR experiments. Quantitative RT-PCR provides a more accurate measurement of relative RNA levels since it measuring changes in florescence signals at each cycle and is not subject to quantification errors that can arise from PCR amplification saturation. This provided a more quantitative and accurate measurement of mRNA transcript levels than RT-PCR. Comparative CT values (ΔCT) were used to assess changes in gene expression of treated samples. All genes of interest were normalized to the expression of the housekeeping gene RPL4.

2.14.1 Primer design

Primers were designed to be between 18 – 25 nucleotides in length, which provides sufficient base pairing for stable duplex formation and low probability of off-target binding. The overall G/C content of the primers created was between 45 – 55 % with a melting temperature (Tm) between 55 – 65°C to allow for optimal annealing. When designing the primers,

dimerization and self-complementarity were avoided by checking the sequences with the Oligo Calc software: Oligonucleotide properties calculator through the Northwestern University Medical School website (www.basic.northwestern.edu/biotools/OligoCalc). Once designed and ordered through Invitrogen, the primers arrived as a lyophilized powder that required dilution to 100 pmol/μl working stock solutions (100 μM) with ddH_2O. Primer efficiency was run for each set of primers to quantitate the optimal input of cDNA and to ensure the proper function of the primers before running experimental samples.

2.14.2 High capacity cDNA reverse transcription

The Applied Biosystems Kit was used to synthesize single-stranded cDNA from total RNA. One set of RNA samples were removed from -80°C and thawed on ice for 10 min. Samples were then quantitated and assessed for RNA purity using the Nano-Drop. RNA samples were then diluted according to the optimal input amount of 750 ng in 10 μl while the kit components were thawed on ice to prepare the 2X Reverse Transcription (RT) Master Mix (Applied Biosystems). 10 μl of 2X RT Master Mix was pipetted to each labeled microcentrifuge tube and the tubes were placed on ice. 10 μl of the diluted RNA samples (750 ng total RNA) were transferred to each respective tube. Tubes were briefly centrifuged to mix the contents and loaded into the automatic thermocycler (BioRad) at 25°C for 10 min followed by 37°C for 120 min and 85°C for 5 min. The cDNA was stored at -20°C until further use.

2.14.3 qPCR

qPCR primers (Table 3) were diluted to 10 μM working stocks and placed on ice. The cDNA was also diluted (18 μl in 72 μl ddH_2O) and placed on ice. A master mix for each target gene was made based on the number of reactions to be run and 10 μl of each master mix sample was added to the appropriate wells of a MicroAmp® Fast 96-well Reaction Plate (Applied Biosystems). 10 μl of the appropriate cDNA was then added to the respective wells of the plate. The plate was sealed with a film cover and run in a StepOne™ Real-Time PCR Instrument in the Genomics Facility at the University of Guelph. This system utilizes a sensitive 3-color optical LED recording system that records fluorescence from the SYBR® Green dye used in the master mix. Fluorescence emitted from each sample was quenched, quantified and exported to StepOne

software for analysis. A housekeeping gene was used for each sample to normalize any variances in sample preparation of the target genes.

Table 3: Primers for qPCR

Gene	Primers	Tm (°C)
GAPDH	Forward: 5'- GACAGTCAGCCGCATCTTCT- 3' Reverse: 5'- GCGCCCAATACGACCAAATC- 3'	60.1 59.9
RPL4	Forward: 5'- GCTCTGGCCAGGGTGCTTTG- 3' Reverse: 5'- ATGGCGTATCGTTTTTGGTGT- 3'	64.6 57.5
PUMA	Forward: 5'- ACCTCAACGCACAGTACGAG- 3' Reverse: 5'- TAAGGGCAGGAGTCCCATGA- 3'	60.0 59.9
miR-27a endogenous	Forward: 5'- GCTCTGCCACCGAGGATG… GTTCACAGTGGCTAAGTTCCG- 3' Reverse: 5'- CGGAACTTAGCCACTGTGAAC… CAAGTGTCACCGATTCAAGGC- 3'	60.8 61.2
miR-27a expression plasmid	Forward: 5'- AAGCCTGTGCCTGGCCTG- 3' Reverse: 5'- AGGCCAGAGGAGGTGAGG- 3'	65.0 60.0
miR-24-2 endogenous/expression plasmid	Forward: 5'- CCTGTCTGAACTGAGCCAG… CTGGCTCAGTTCAGCAGGAA- 3' Reverse: 5'- TTCCTGCTGAACTGAGCCAG… GACCGAGTCAAGTCGTCCTT- 3'	60.8 60.5
miR-29a endogenous/expression plasmid	Forward: 5'- CAACCCTCACGACCTTCTG… GCTGACTGCTGAGAGGAAATG- 3' Reverse: 5'- GATTTCCTCTCAGCAGTCAGC… CGACTGACGACTCTCCTTTAG- 3'	59.5 61.2

2.15 Site-directed mutagenesis

The psiCHECK-2 plasmid with the PUMA 3'UTR underwent site-directed mutagenesis to alter each target miRNA binding site within the 3'UTR.

2.15.1 Mutagenesis of miRNA binding sites in the PUMA 3'UTR

psiCHECK-2 plasmid was created with the PUMA 3'UTR cloned downstream of the luciferase stop codon. The miR-24-2, miR-27a and miR-29a miRNA binding sites in the psiCHECK-2 + PUMA 3'UTR luciferase reporter plasmid were then mutated using site specific mutagenesis modified from the QuickChange™ (Stratagene) protocol. In the process, primers were designed to alter a 6 base region of the mature miRNA binding site in the PUMA 3'UTR. Each binding region was changed to a restriction cut site (PacI or NheI) inhibiting binding and therefore activity of the respective miRNA. Site-directed mutagenesis on the individual miRNA

binding sites in the PUMA3'UTR were performed with the proofreading Phusion® polymerase. The primers were diluted to 100 μM master stocks and further diluted to 10 μM working stocks (Table 4). The PCR reactions was prepared as follows: 1 μl of each forward and reverse primer (10 μM), 10 – 50 ng DNA (psiCHECK-2 + PUMA 3'UTR), 1 μl 10 mM dNTPs, 10 μl 5X Phusion® HF reaction Buffer (New England BioLabs), 1 μl 2 U/μl Phusion® high fidelity DNA polymerase (New England BioLabs) and 32.5 μl ddH_2O. The contents of the tube were mixed gently and centrifuged before transferring the tubes to an automatic thermocycler (BioRad) preheated to the denaturing temperature of 95°C. The thermocycling conditions were as follows: 95.0°C for 1 min; followed by 20 cycles of 95.0°C for 50 s, 55.0°C for 50 s and 68.0°C for 5 min 30 s; and a final extension time of 10 min at 68.0°C. Following the PCR reaction, 2 μl Dpn1 restriction enzyme (New England BioLabs) was added to each reaction and left to incubate at 37°C for 1.5 h. Dpn1 enzyme was added to the reaction to cleave methylated DNA, therefore eliminating any residual parental DNA and leaving only the mutated, non-methylated DNA. The final PCR products were transformed into competent *E. coli*, mini-prep plasmid DNA was produced and screened by restriction enzyme digestion for the inserted site and then sequence verified in the Genomics Facility (University of Guelph) before use. It is important to note that miR-24-2 is the only target miRNA that has two binding sites within the PUMA 3'UTR, therefore this plasmid underwent a site-specific mutagenesis of the first site and second binding site separately as well as a double mutation of both sites.

Table 4: Primers for Site-Directed Mutagenesis of miRNA binding sites in PUMA 3'UTR

Gene	Primers	Tm (°C)
miR-24-2 #1	Forward: 5'- TGGCCAGGAGGGGCCCAG**TTAATTAA**ATC CTGTGCTCTGCCCGT -3'	83.6
	Reverse: 5'- ACGGGCAGAGCACAGGAT**TTAATTAA**CTG GGCCCCTCCTGGCCA -3'	83.6
miR-24-2 #2	Forward: 5'- GGGCCCGTGAAGAGCAAA**GCTAGC**ACG TGACCACTAGCCTCC -3'	84.8
	Reverse: 5'- GGAGGCTAGTGGTCACGT**GCTAGC**TTT GCTCTTCACGGGCCC -3'	84.8
miR-27a	Forward: 5'- GGCGCCCAGCCATCTTCC**TTAATTAA**GCC GGCGGGTGGTGGGCA -3'	86.5
	Reverse: 5'- TGCCCACCACCCGCCGGC**TTAATTAA**GGA AGATGGCTGGGCGCC -3'	86.5
miR-29a	Forward: 5'- CGCCTGGCCTCAGGCCCC**TTAATTAA**TCC CCCCCTCCTCCTCCC -3'	87.3
	Reverse: 5'- GGGAGGAGGAGGGGGGGA**TTAATTAA**GGG GCCTGAGGCCAGGCG -3'	87.3

* Note: Pac1 substitution = **TTAATTAA** and NheI substitution = **GCTAGC** *

2.16 Transient plasmid DNA transfection

Transient transfections were used to test the effects of microRNA overexpression on PUMA expression as well as luciferase activity from a PUMA 3'UTR reporter plasmid.

2.16.1 $CaPO_4$ transfection

This mode of chemical transfection was used to transfect HeLa cells for the dual-luciferase assay and western blot. Cells were plated in 3 ml of fresh DMEM at 3 x 10^5 cells/well in a 6-well plate 24 h prior to transfection. For each transfection, the following three solutions were prepared for each sample and aliquoted to 1.5 ml microcentrifuge tubes: (1) 5 μg of effector miRNA overexpression plasmid (Genecopoeia) and 20 ng of the appropriate reporter psiCHECK-2 plasmid brought up to 50 μl with 1/10 TE Buffer, (2) 5 μl of 2 M $CaCl_2$ diluted in 169 μl of ddH_2O and (3) 250 μl of 2X Hepes Buffered Saline (HBS). To start the chemical transfection, the DNA solution (1) was added drop-wise to the diluted $CaCl_2$ solution (2) along with an additional 26 μl of 2 M $CaCl_2$ and gently pipetted to mix. A 1 ml pipette was then used to slowly start bubbling the 2X HBS solution (3). In the meantime, the DNA/$CaCl_2$ mix (2) was added drop-wise to the HBS solution while continuing to bubble the solution until the entire

DNA solution was added. The final transfection cocktail was then left to incubate at room temperature for 5 – 10 min before being transferred drop-wise to a 6-well plate with 3 ml fresh DMEM media. The plates were swirled to mix, and placed in the 37°C incubator overnight. The media was changed the following morning (16 h post-transfection) with 4 ml of fresh DMEM media and collected 20 h after transfection and pellets were frozen at -20°C until use.

2.16.2 Transfection by electroporation

This transfection method was used for PEER and PErTA70 cells, as it was the only method suitable to transfect these cells. A cell suspension of 10 x 10^6 cells with 10 μg of total DNA was transferred to a 0.4 cm electroporation cuvette. The cuvette was placed in the electroporation dock of an ECM830 wave electroporator and pulsed at 200 Volts for one interval with a pulse length of 75 ms. The electroporated cells were then transferred to a 10 cm^2 culture flask with 10 ml fresh media and placed at 37°C. Cells were collected 24 h post-transfection and pellets were frozen at -20°C until analysis.

2.17 Flow cytometry

Flow cytometry was used to test both viability and transfection efficiency of certain transfection reagents. 100 – 200 μl of transfected cells in suspension were transferred to a 96-well plate and passed through the Flow Cytometer (Beckman and Coulter). A laser measured the size and florescence of the cells as they passed through a chamber in single file. The size of a cell was a good indication of viability and the amount of florescence produced was an indication of the transfection efficiency. $CaPO_4$ transfection efficiency was measured by the amount of green fluorescent protein (GFP) emitted from cells containing the transfected miRNA expression plasmid (PEXZ-MR04) shown in Figure 12.

2.18 Dual-luciferase

Dual-luciferase assays (Promega) were conducted using transiently transfected HeLa or PEER cells with the psiCHECK-2 plasmid + PUMA 3'UTR cloned downstream of the luciferase stop codon. Cell pellets were lysed in 60 μl 1X Passive Lysis Buffer and sonicated for 10 s before being centrifuged at 5,000 x g for 5 min. 20 μl of the lysate was transferred to a thin-walled tube along with 25 μl of the LarII reagent. The tube was immediately vortexed for 3 s and

inserted into the Turner TD-20e luminometer dock for the first reading, then 25 μl of the Stop and Glow reagent was added to the tube, vortexed for 3 s and inserted into the luminometer dock for the second reading. Relative luciferase activity was calculated by dividing the renilla luciferase readings by the firefly luciferase readings for each sample.

2.19 Sucrose gradient separation of ribosomes

PErTA70 cells were used to examine the fraction of PUMA mRNA and target miRNA expression present in the mono-ribosomes, di-ribosomes and poly-ribosomes in control and heat-shocked cells. OFF and ON PErTA70 cells were exposed to hyperthermia as outlined above and collected by centrifugation at 0 h and 6 h post-heat shock along with control cells maintained at 37°C. Cell were resuspended in 200 μl of Polysomal Lysis Buffer (Appendix A) and centrifuged at 12,000 x g for 10 min to remove nuclei and cell debris. Cells were treated with cycloheximide, an inhibitor of protein synthesis, in the lysis buffer and in the sucrose gradient to prevent run off of ribosomes during centrifugation, allowing the measurement of PUMA mRNA distribution among mono-ribosomes, di-ribosomes and poly-ribosomes. Each sample contained a lysate of 7 x 10^7 cells that was separated by size through a 10 – 50% sucrose gradient (Appendix A). The gradient was fractionated using a Buckler Auto-Densi Flow II apparatus. The lysates were added to the top of the gradient and centrifuged at 40,000 rpm in a Beckman SW41Ti rotor for 2.5 h at 4°C. Once the RNA bound to ribosomes were sorted by size through the gradient, fractions were collected and pooled based on the location of the mono/di/poly-ribosomes. RNA was purified from the fractions by TRIzol® (Ambion) extraction and assessed by qPCR for PUMA and target miRNA expression along with a reference housekeeping gene.

2.20 miRNA over-expression in stably transfected PEER cells

miR-24-2, miR-27a and miR-29a expression plasmids (Genecopoeia) were cut by restriction enzyme digestion with ScaI at 37°C for 5 h and run on an analytical gel to ensure the plasmids were linearized (Figure 12). A control scrambled miRNA plasmid (C-miR) with no homology to human transcripts, and therefore no predicted ability to interact with the binding sites in the PUMA 3'UTR, was also linearized for stable transfection into PEER cells. The cut plasmids were purified through a spin column and 20 μg of each plasmid was transfected into 10 x 10^6 PEER cells by electroporation. The electroporated cells were transferred to a sterile tissue

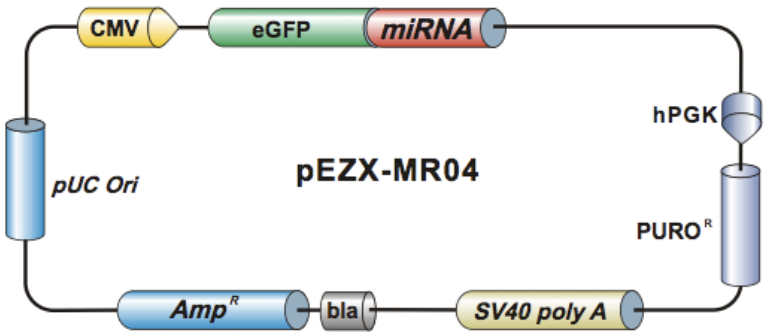

Figure 13: pEZX-MR04 miRNA expression plasmid. miR-24-2, miR-27a and miR-29a expression plasmids were purchased from Genecopoeia. Synthetic target miRNA expression sequences are cloned in the pEZX-MR04 vector backbone and encoded within the 3'UTR of the GFP gene. Once transfected into cells, this plasmid allows the overexpression of the synthetic miRNA sequence, which is processed by the cellular miRNA processing machinery. This plasmid contains both the ampicillin resistance gene (Amp^r) and the puromycin resistance gene ($PURO^r$) for selection.

culture flask and grown in fresh 20 ml RPMI media with 10% FBS for 48 h. Drug selection commenced 48 h after electroporation with 800 μg/ml puromycin. Cells underwent drug selection for 7 days before being seeded by limiting dilution in 96-well plates. Clones were grown in 96-well plates for 3 weeks with 800 μg/ml puromycin selection. When clones reached 80% confluency, they were expanded by transferring them first to a 24-well plate in 1 ml of media and then to a small flask in 5 ml of media. The stable clones were then screened by flow cytometry to identify those clones that uniformly expressed high levels of GFP. Clones that were greater than 95% GFP positive and had a high x-mean value (GFP fluorescence intensity) were selected for further analysis as these cells should also express high levels of the miRNA encoded within the 3'UTR of the GFP gene. Samples that had more than one GFP positive peak were excluded since these likely were derived from wells seeded with more than one cell. One clone negative for GFP and two clones positive for GFP with x-mean values greater than 50, were chosen for further screening by qPCR and western blot to study PUMA mRNA and protein levels with the overexpression of the respective synthetic miRNA expression sequences.

2.21 Statistical analysis of experimental results

All results were analyzed using Prism software. Student's ttest were performed when analyzing differences between samples with only one variable. Analysis of variances (ANOVA) was used when multiple factors were being assessed between treatment samples.

CHAPTER 3: RESULTS

3.1 Effect of hyperthermia on PUMA protein expression in PErTA70 cells

PUMA protein levels were examined under control and heat shock conditions by immunoblotting. Non-induced (- HSP70) and HSP70-expressing (+ HSP70) PErTA70 cells were exposed to 43°C for 1 h and then either collected immediately (recovery time at 37°C = 0 h) or returned to 37°C for 3 h, 6 h or 9 h before collection along with a control sample (C) that remained at the optimal growth temperature of 37°C (Figure 13A). A rapid loss of PUMA protein was observed in the heat-treated cells. Quantification of the results of three independent experiments showed that the rate of PUMA protein depletion in the heat shocked cells was not affected by the presence of HSP70 (Figure 13B).

3.2 Effect of hyperthermia on PUMA mRNA expression in PErTA70 cells

Initially, PUMA mRNA expression in control and heat-shocked cells was measured via RT-PCR. Due to the low endogenous expression of this gene, there was difficulty visualizing and quantifying differences between treatment samples and this method was not reproducible. Consequently, qPCR was performed in order to more accurately measure PUMA mRNA expression. RNA was collected from induced (+ HSP70) and non-induced (- HSP70) PErTA70 cells that were exposed to 43°C for 1 h and then returned to 37°C for 0 h, 3 h, 6 h or 9 h as well as control non-stressed cells. The purified RNA was reverse transcribed into cDNA, which was then measured by qPCR to determine the relative levels of PUMA mRNA expression (Figure 14). Quantification of the results from three replicates reveals the induction of PUMA mRNA in the heat-shocked cells. The kinetics of PUMA mRNA expression differed between the non-induced and induced cells with levels peaking at 3 hours in the HSP70-expressing cells whereas the non-induced cells reached maximal levels by 6 hours and attained a level of expression that was nearly 3-fold higher than that of the non-induced cells at this time. The levels of PUMA mRNA were significantly different between the non-induced and induced cells at all time points post-heat shock (1-tailed student's ttest, $P = <0.05$, $n = 3$). These results present an interesting observation that although hyperthermia causes an increase in PUMA mRNA levels, the abundance of PUMA protein in contrast drastically diminishes in heat shocked cells. This led us

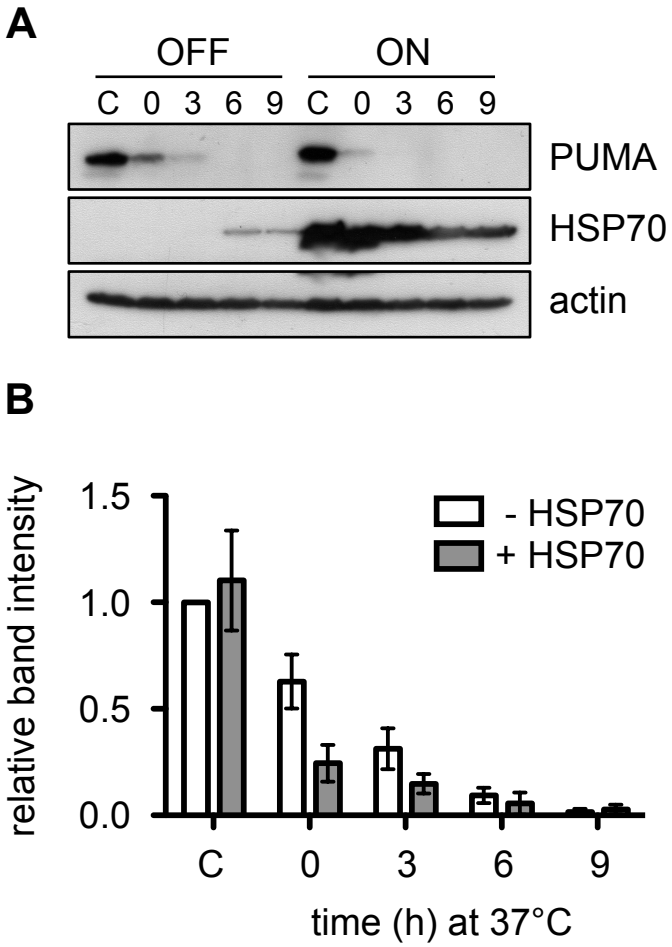

Figure 13: Effect of hyperthermia on PUMA protein expression in PErTA70 cells. Non-induced (- HSP70) and induced (+ HSP70) PErTA70 cells were exposed to 43°C for 1 h and then collected at 0 h, 3 h, 6 h and 9 h post-heat shock incubation at 37°C along with a control sample (C). **(A)** A representative immunoblot of PUMA, HSP70 and actin protein expression under control and heat shock conditions. **(B)** Quantitation of PUMA protein levels from three independent experiments. The relative band intensity corresponding to PUMA and actin was quantified using Image J software and PUMA protein was normalized to that of actin (shown are the means ± SEM, n = 3). All values were then plotted relative to the value for the control non-induced cells (set at 1.0). PUMA protein levels decreased significantly during incubation at 37°C following exposure to hyperthermia in both the non-induced and the induced cells (ANOVA, $p < 0.0001$). HSP70 did not influence the rate of decay of PUMA protein expression in heat-shocked cells (ANOVA, $p = 0.1408$).

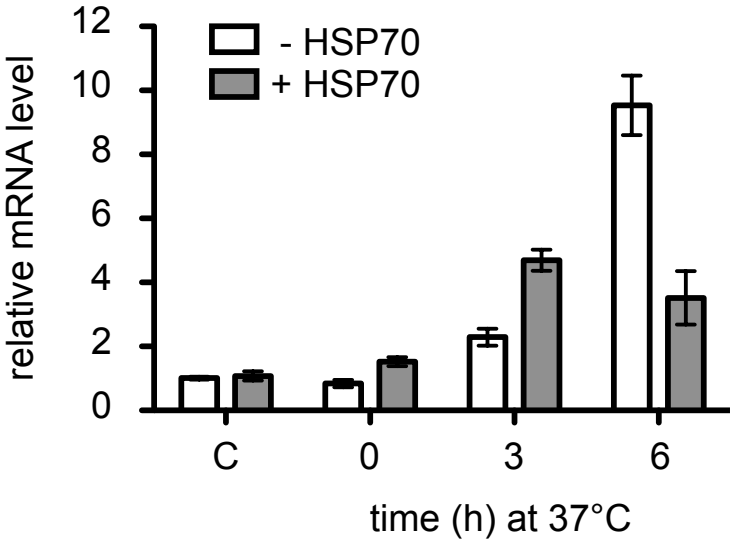

Figure 14: Characterization of PUMA mRNA expression in control and heat-shocked PErTA70 cells. Non-induced and induced PErTA70 cells exposed to 43°C for 1 h, were collected at 0 h, 3 h and 6 h post-heat shock along with a control sample (C). PUMA mRNA expression was analyzed by qPCR. Comparative CT values (ΔCT) were assessed in duplicate for each sample and standardized to the reference housekeeping gene RPL4. PUMA expression was then quantified as relative expression compared to the control OFF sample, set to 1 (mean ± SEM, n = 3). PUMA mRNA levels increased significantly by 6 h post heat shock from the control cells in both the non-induced and HSP70 expressing cells (ANOVA, $p < 0.0001$). However, HSP70 did not influence the rate of increase in PUMA mRNA levels in heat shocked cells compared to the non-induced cells (ANOVA, $p = 0.086$).

to consider the possibility that PUMA translation is regulated by miRNA-mediated translational repression in heat-stressed cells.

3.3 Predicted miRNA binding sites in the PUMA mRNA 3'UTR

Analysis of potential miRNA binding sites within the PUMA mRNA 3'UTR sequence was done with the use of miRNA-interaction prediction programs (MiRWalk, MiRBase and TargetScan). TargetScan predicts biological targets of miRNAs by searching for contributions to the context score including the presence of conserved 8-mer and 7-mer sites that match the binding region of each miRNA (Figure 15). TargetScan takes in account both the preferential conservation sites of the Aggregate P_{CT} as well as the context scores, which have the advantage of being predictive for all types of miRNA interactions, including those of miRNAs that are not highly conserved. In mammals, predictions are ranked based on the predicted efficacy of targeting as calculated using all the contributions of the sites within the UTR. This prediction software identified miR-24-2, miR-27a and miR-29a as top candidates among other miRNAs for binding to the PUMA 3'UTR. miR-29a has been previously demonstrated to regulate PUMA expression confirming the efficiency of the TargetScan software (Ouyang et al., 2013).

3.4 Effect of hyperthermia on miR24-2, miR-27a and miR-29a expression in PErTA70 cells

Endogenous miR-24-2, miR-27a and miR-29a expression was examined in non-induced (- HSP70) and induced (+ HSP70) PErTA70 cells under control and heat shock conditions by qPCR. Cells were collected immediately after heat shock (0 h) and after incubation at 37°C for 3 h and 6 h along with a control sample (C) that remained at 37°C. miR-24-2, miR-27a and miR-29a were normalized to RPL4 and control (C) and heat-shocked cells (6 h) were plotted relative to their OFF control samples (Figure 16A-C; n = 3). Hyperthermia caused a greater than 10-fold increase in the expression level of each of the three miRNAs. As well, HSP70 expression largely prevented the increased expression of each of the miRNAs examined. Figure 16D shows the results plotted relative to the control miR-24-2 value to show any differences in expression between the individual miRNAs. Relative to miR-24-2, the expression of miR29a was approximately 2-fold higher in non-stressed cells while miR-27a levels were approximately 500-fold lower.

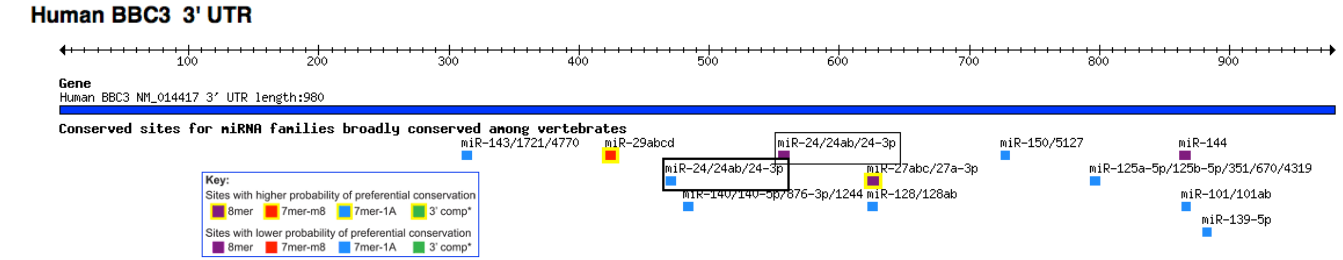

	predicted consequential pairing of target region (top) and miRNA (bottom)	seed match	site-type contribution	3' pairing contribution	local AU contribution	position contribution	TA contribution	SPS contribution	context+ score	context+ score percentile	conserved branch length	P_{CT}
Position 467-473 of BBC3 3' UTR	5' ...CCCGUGAAGAGCAAAUGAGCCAA...	7mer-1A	-0.074	0.001	0.020	0.001	0.028	-0.069	-0.09	54	2.199	0.38
hsa-miR-24	3' GACAAGGACGACUUGACUCGGU											
Position 553-560 of BBC3 3' UTR	5' ...GCCCAGCCAUCUUCCCUGAGCCA...	8mer	-0.247	0.013	0.158	-0.008	0.047	-0.121	-0.16	78	1.320	0.53
hsa-miR-24	3' GACAAGGACGACUUGACUCGGU											

	predicted consequential pairing of target region (top) and miRNA (bottom)	seed match	site-type contribution	3' pairing contribution	local AU contribution	position contribution	TA contribution	SPS contribution	context+ score	context+ score percentile	conserved branch length	P_{CT}
Position 421-427 of BBC3 3' UTR	5' ...CUGGCCUCAGGCCCCUGGUGCUU...	7mer-m8	-0.120	0.012	0.147	-0.002	-0.003	-0.048	> -0.02	9	2.199	0.82
hsa-miR-29a	3' AUUGGCUAAAGUCUACCACGAU											

	predicted consequential pairing of target region (top) and miRNA (bottom)	seed match	site-type contribution	3' pairing contribution	local AU contribution	position contribution	TA contribution	SPS contribution	context+ score	context+ score percentile	conserved branch length	P_{CT}
Position 622-629 of BBC3 3' UTR	5' ...CCAGGAGGGGCCCAGACUGUGAA...	8mer	-0.247	0.013	0.126	-0.025	0.035	-0.009	-0.11	64	1.848	0.77
hsa-miR-27a	3' CGCCUUGAAUCGGUGACACUU											

Figure 15: Predicted miRNA binding sites in the PUMA mRNA 3'UTR. Potential miRNA binding sites in the PUMA 3'UTR as predicted using TargetScan are shown. Note that miR-29a and miR-27a only have one binding site within the PUMA 3'UTR, while miR-24-2 has two. The top three miRNAs predicted to bind to the PUMA 3'UTR are miR-24-2, miR-29a and miR-27a based on their highly favorable context scores

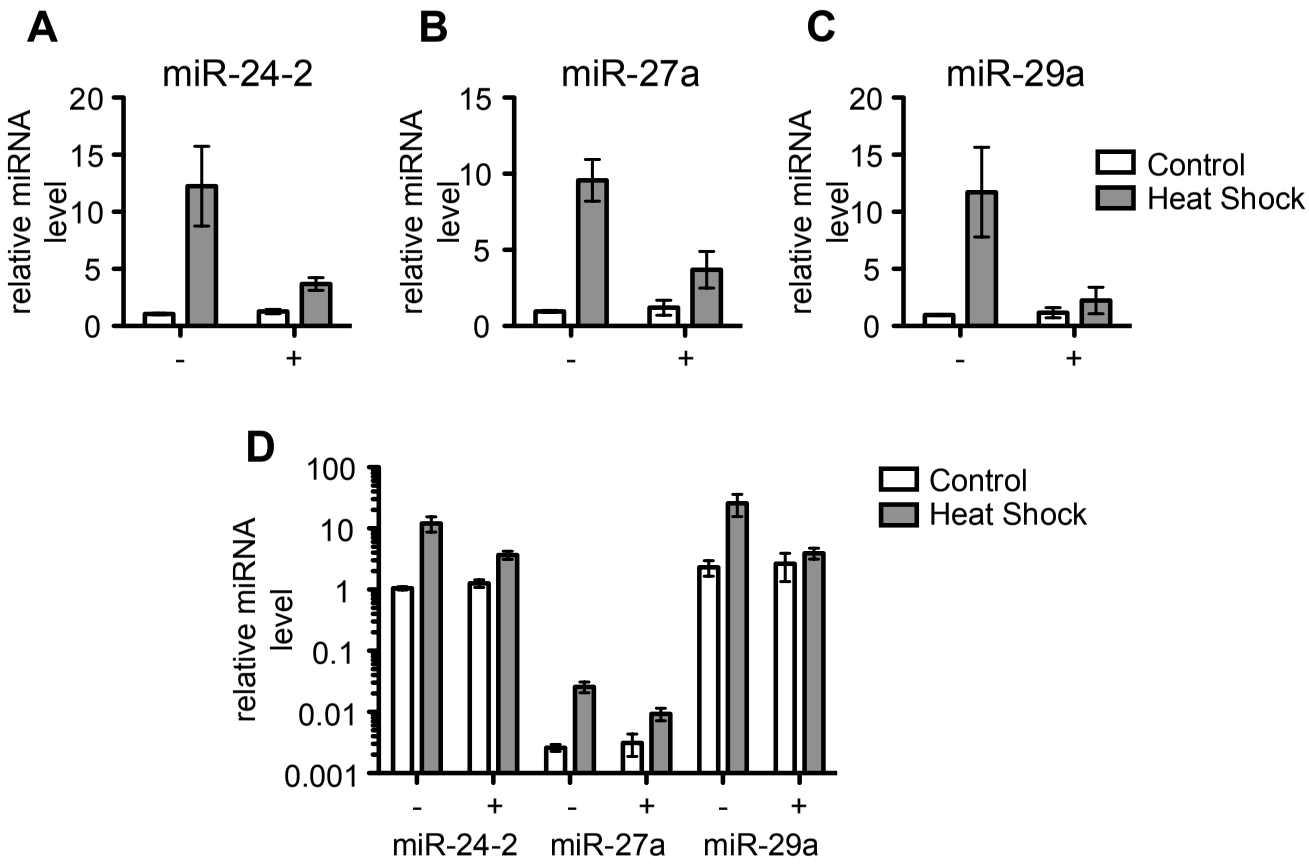

Figure 16: Effect of hyperthermia on miR24-2, miR-27a and miR-29a expression in PErTA70 cells. miRNA expression was assessed in induced and non-induced PErTA70 cells under control and heat shock conditions. Results were standardized to the housekeeping gene, RPL4, and plotted relative to the OFF control values for **A)** miR-24-2, **B)** miR-27a and **C)** miR-29a (mean ±SEM, n = 3). miR-24-2, miR27a and miR-29a expression increased by 6 h post-heat shock in non-induced cells and to a lesser degree in induced cells **(**significant differences between the control and heat shock samples are indicated with an asterisk $p < 0.05$, t-test). **D)** The relative miRNA expression of miR-24-2, miR-27a and miR-29a from parts A – C is plotted relative to the miR-24-2 non-induced control cells set to a value of one. This shows that the endogenous levels of miR-27a are far lower than that of miR-24-2 and miR-29a (mean ± SEM, n = 3).

To investigate whether the lower miRNA levels in the HSP70-expressing cells following exposure to hyperthermia was simply due to a transient increase in expression that peaked before 6 hours we next examined the relative expression of miR-24-2, miR-27a and miR-29a in control and in cells incubated for 0 h, 3 h and 6 h following exposure to heat shock (Figure 17). This analysis demonstrated that miRNA levels gradually increased in both the non-induced and HSP70-expressing cells after exposure to hyperthermia with higher levels being attained in the non-induced cells. However, unlike the results of the previous experiment, miR-29a showed only a 2-fold increase by 6 hours after exposure to hyperthermia and levels were not significantly different between the non-induced and HSP70-expressing cells (Figure 17C).

3.5 Effect of hyperthermia on PUMA mRNA/ribosome association in non-induced and induced PErTA70 cells

Non-induced (- HSP70) and induced (+ HSP70) PErTA70 cells were exposed to 43°C for 1 h and collected immediately after heat shock (0 h) or returned to 37°C for 6 h before collection. A sample of cells that remained at 37°C was also collected as a control (C). Cells were lysed and the lysate was centrifuged through a sucrose gradient to separate the mono-ribosomes, di-ribosomes and poly-ribosomes. Fractionation of the sucrose gradient was separated into three pools based on ribosome size: actively translated fractions (8 – 10) associated with the poly-ribosomes, poorly translated fractions (4 – 7) associated with the di-ribosomes and the untranslated fractions (1 – 3) associated with the mono-ribosomes. RPL4 translation fluctuated typically of what would be expected under control and heat shock conditions with the majority of RPL4 associated with poly-ribosomes in control cells (Figure 18A for the non-induced cells and Figure 18A for the HSP70-expressing cells). A dramatic switch in RPL4 association from poly-ribosomes to mono-ribosomes is seen immediately after heat shock (0 h) and partial restoration of RPL4 mRNA to di-ribosomes and poly-ribosomes occurred by 6 h after heat shock. Interestingly, this recovery was more pronounced in cells expressing HSP70 with the majority of RPL4 mRNA being associated with poly-ribosomes at 6 hours after heat shock treatment (Figure 19A). PUMA followed a similar trend differing only by a less dramatic switch to the untranslated fractions at time 0 h (Figure 18B and Figure 19B). Of interest is the finding that although PUMA

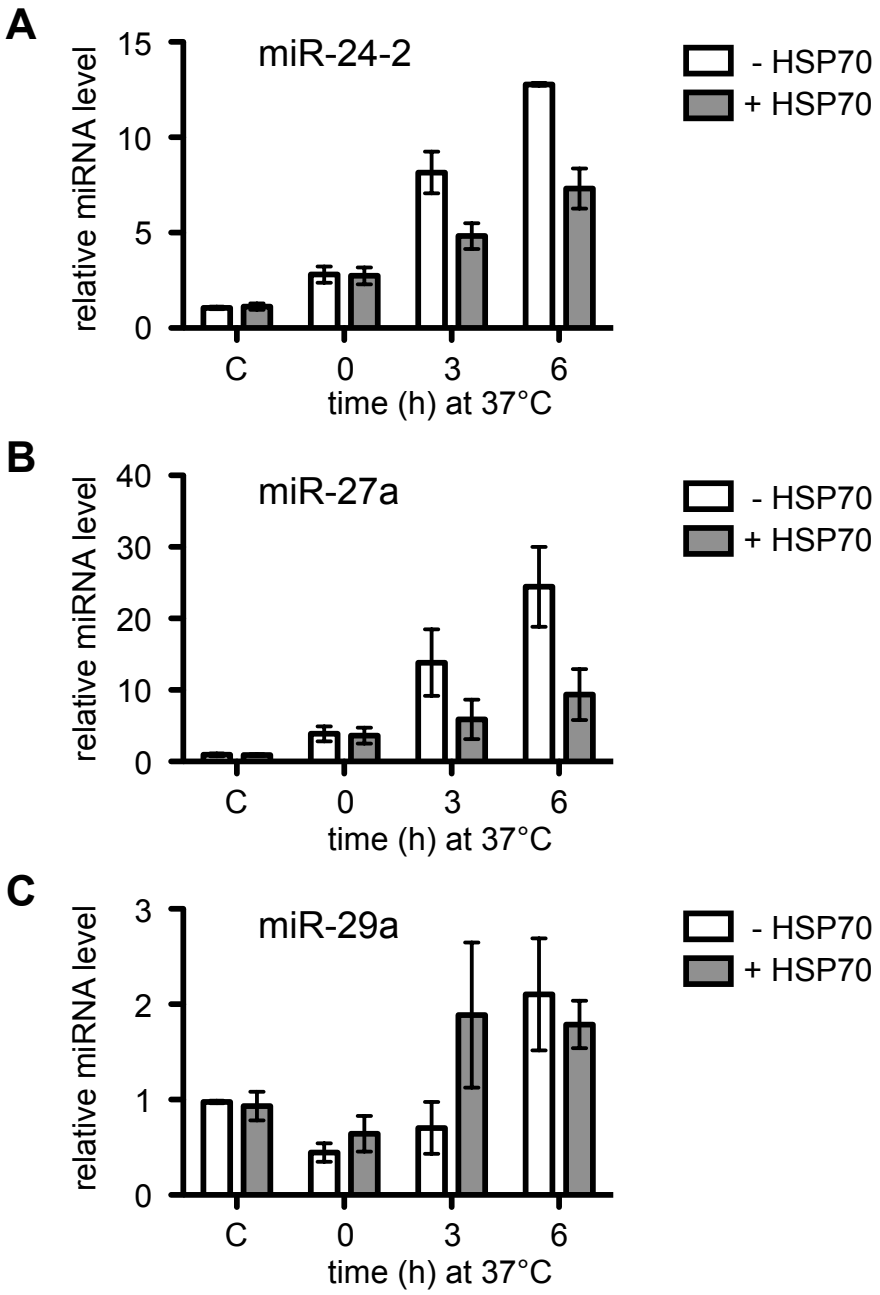

Figure 17: Temporal profile of miR24-2, miR27a and miR-29a expression in heat-shocked PErTA70 cells. Non-induced and induced PErTA70 cells were exposed to 43°C for 1 h and then collected at 0 h, 3 h and 6 h post-heat shock along with a control sample (C). Relative miRNA expression was analyzed by qPCR. Each sample was standardized to the housekeeping gene, RPL4, and plotted relative to the OFF control values for **A)** miR-24-2, **B)** miR-27a and **C)** miR-29a (mean ± SEM, n=3). Heat treatment caused a significant increase in expression of each of the miRNAs (ANOVA p values: miR-24-2 <0.0001, miR-27a <0.0001, miR-29a =0.0086). HSP70 influenced the change in miR24-2 values (p=0.0059) but not miR27a (p=0.1420) or miR29a (p=0.4873).

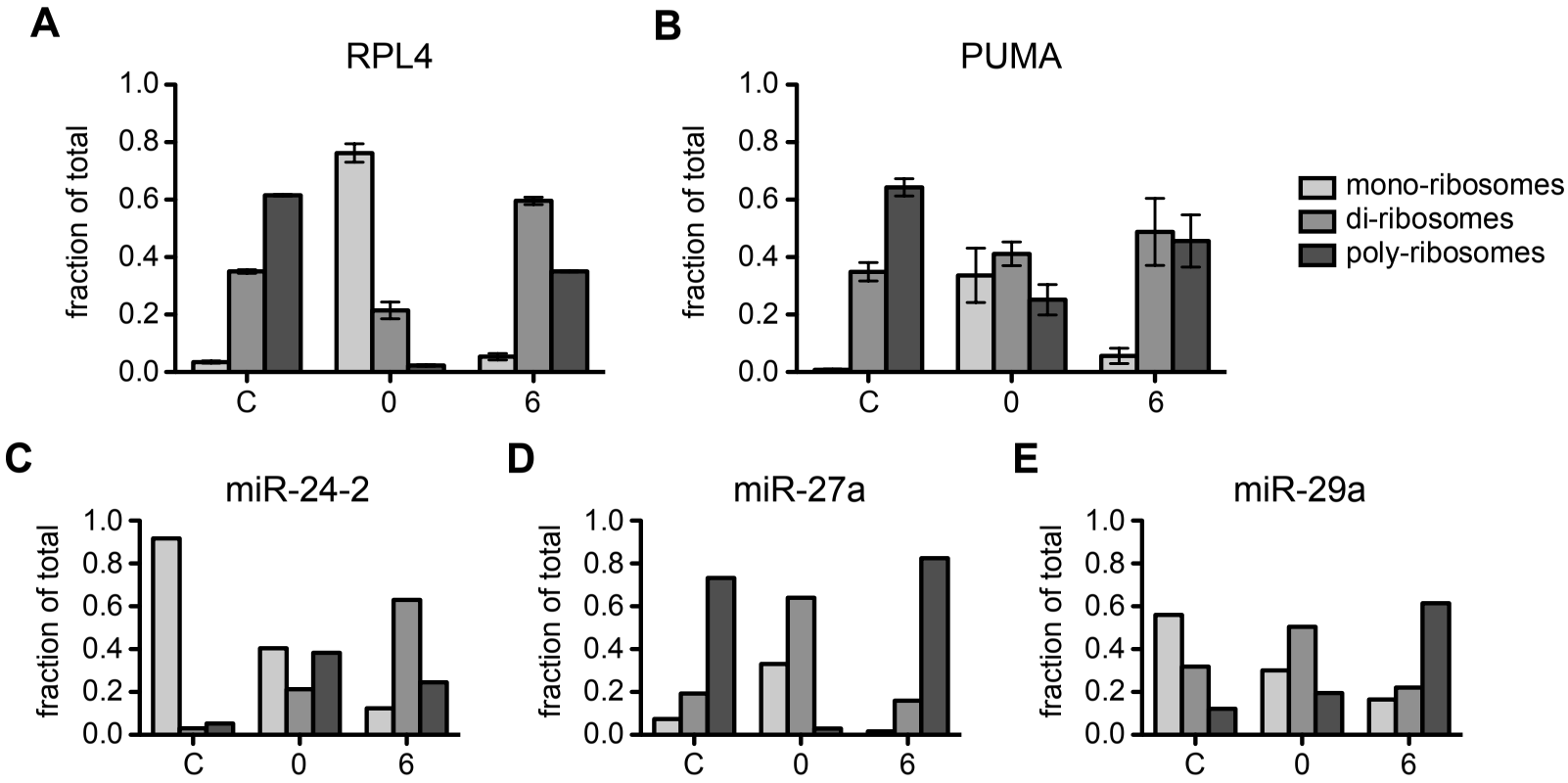

Figure 18: Effect of hyperthermia on PUMA mRNA and miRNA/ribosome association in non-induced PErTA70 cells. Non-induced PErTA70 cells were exposed to 43°C for 1 h and collected at 0 h and 6 h post-heat shock along with a control sample (C). PUMA mRNA and miRNA expression was analyzed by qPCR from fractions of polysomal sucrose gradients. **(A)** RPL4 and **(B)** PUMA results are shown as mean ±SEM from two independent experiments. **(C)** miR-24-2, **(D)** miR-27a and **(E)** miR29a measurements were only performed once.

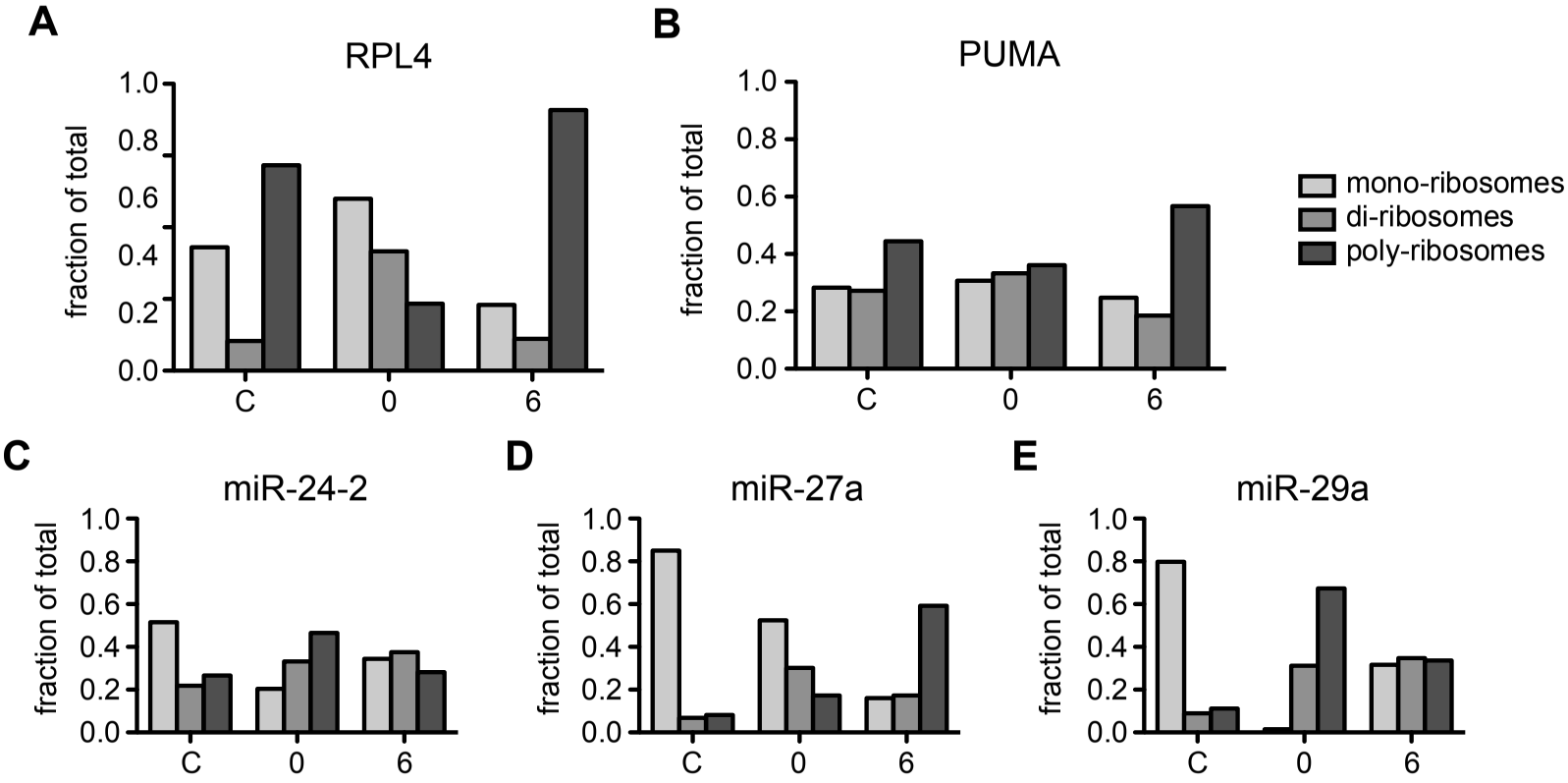

Figure 19: Effect of hyperthermia on PUMA mRNA and miRNA/ribosome association in induced PErTA70 cells. Induced PErTA70 cells were exposed to 43°C for 1 h and collected at 0 h and 6 h post-heat shock along with a control sample (C). PUMA mRNA and miRNA expression was analyzed by qPCR from fractions of polysomal sucrose gradients. **(A)** RPL4, **(B)** PUMA, **(C)** miR-24-2, **(D)** miR-27a and **(E)** miR29a measurements were only performed once.

protein is rapidly lost from cells exposed to hyperthermia (Figure 13), PUMA mRNA is found associated with poly-ribosomes in these cells.

The association of each miRNA with ribosomes and the effect of hyperthermia on their distribution varied with each miRNA (Figure 18 for non-induced cells and Figure 19 for HSP70-expressing cells). miR-24-2 (Figure 18C and Figure 19C) was largely associated with mono-ribosomes in control cells but shifted towards the di- and poly-ribosomes in heat shocked cells. miR-29a (Figure 18E and Figure 19E) followed a pattern similar to that of miR-24-2. However miR-27a appeared predominantly in the poly-ribosome fraction in control cells, shifting to mono-ribosomes immediately after heat shock and then returning to the poly-ribosome fraction 6 hours after recovery from heat shock (Figure 18D) with a seemingly opposite effect in Figure 19D. In general, miR-27a distribution followed a pattern of ribosome association most similar to that of PUMA mRNA in heat-shocked cells.

3.6 Effect of PUMA 3'UTR miRNA binding site deletion on reporter protein expression in transiently transfected PEER cells

The PUMA 3'UTR sequence was amplified by PCR from human genomic DNA and cloned downstream of the *renilla* luciferase gene in the psiCHECK-2 plasmid, which also contains a firefly luciferase gene that can be used to control for differences in transfection efficiency. The miR-24-2, miR-27a and miR-29a binding sites in the psiCHECK-2 + PUMA 3'UTR were then mutated by site-directed mutagenesis. These plasmids with the mutated miRNA binding sites were used for transient transfections in PEER cells by electroporation. Cells were collected after 20 h recovery from transfection and lysates were analyzed using the dual-luciferase assay (Promega). Luciferase activity was quenched by the appropriate buffers and measured with the use of a luminometer. The renilla luciferase measurements were divided by the firefly luciferase activity for each sample and relative luciferase activities were calculated by setting the value for psiCHECK-2 plasmid without the PUMA 3'UTR (vector) being equal to one (Figure 20). Inclusion of the PUMA 3'UTR sequence reduced the relative luciferase activity in the transiently transfected PEER cells indicating that this sequence potentially contains miRNA binding sites that actively repress mRNA translation. Similar levels of repression were

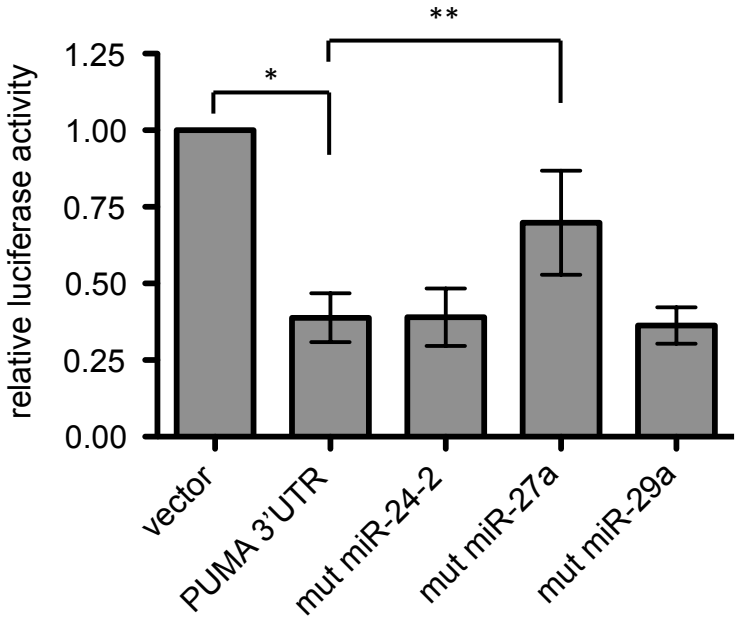

Figure 20: Effect of PUMA 3'UTR miRNA binding site deletion on reporter protein expression in transiently transfected PEER cells. PEER cells were transiently transfected by electroporation with the psiCHECK-2 empty vector, psiCHECK-2 containing the PUMA 3'UTR cloned downstream of the renilla luciferase gene or with mutant versions of this construct in which either the miR-24-2, miR-27a or miR-29a binding sites were altered by site-directed mutagenesis. Relative activity is the renilla luciferase activity normalized to firefly luciferase activity (mean ±SEM, n = 3). The presence of the PUMA 3'UTR in the psiCHECK-2 plasmid significantly reduced reporter expression (ttest: $p = 0.0082$ *). Mutation of the miR-27a binding site in the PUMA 3'UTR significantly increased the relative luciferase activity (ttest: $p = 0.038$ **). However, mutation of the miR-24-2 or miR-29a binding sites did not affect the relative luciferase activity (ttest: $p > 0.05$).

observed in the constructs containing mutations in the miR-24-2 and miR-29a binding sites, however mutation of the miR-27a binding site partially restored the luciferase activity. This result suggests that miR-27a negatively regulates PUMA mRNA translation in PEER cells. Importantly, these results only include data for the mutation of one of the miR-24-2 binding sites in the PUMA 3'UTR.

3.7 Effect of miRNA overexpression on reporter protein expression in transiently transfected HeLa cells

A luciferase reporter plasmid (psiCHECK-2) containing the PUMA mRNA 3'UTR cloned downstream of the *renilla* luciferase gene as well as mutant versions in which either the putative miR-24-2, miR-27a or miR-29a binding sites had been mutated by site-directed mutagenesis were used in transient transfection experiments in HeLa cells. A total of 5 μg of DNA was used to transfect HeLa cells at 60% confluency in 60 mm cell culture plates. Cells were collected after 20 h incubation at 37°C post-transfection and luciferase activity in the lysates was measured using the dual-luciferase assay (Promega). The relative luciferase activity values (renillia/firefly) are shown in Figure 21 (n = 3). As was observed in transiently transfected PEER cells (Figure 20) mutation of the putative miR-27a binding site resulted in an increased level of luciferase activity relative to the full length PUMA 3'UTR luciferase plasmid (Figure 21). Relative luciferase levels were not altered by mutation of the putative miR-24-2 or miR-29a binding sites relative the unaltered 3'UTR containing plasmid. These results are consistent with the idea that miR-27a is regulating the translation of PUMA mRNA in HeLa cells.

3.8 The effect of miRNA overexpression on PUMA protein expression in transiently transfected HeLa cells

The preceding results suggest that if these miRNAs are regulating PUMA expression they are doing so not at the level of PUMA mRNA levels but instead by inhibiting PUMA mRNA translation. This was examined by western blotting in transiently transfected cells. HeLa cells were transiently transfected with the control expression plasmid (C-miR), miR-24-2, miR-27a, miR-29a or all three miRNA expression plasmids. Cells were transfected with a total of 10 μg of miRNA expression or control plasmid. A negative control for the transfection used the

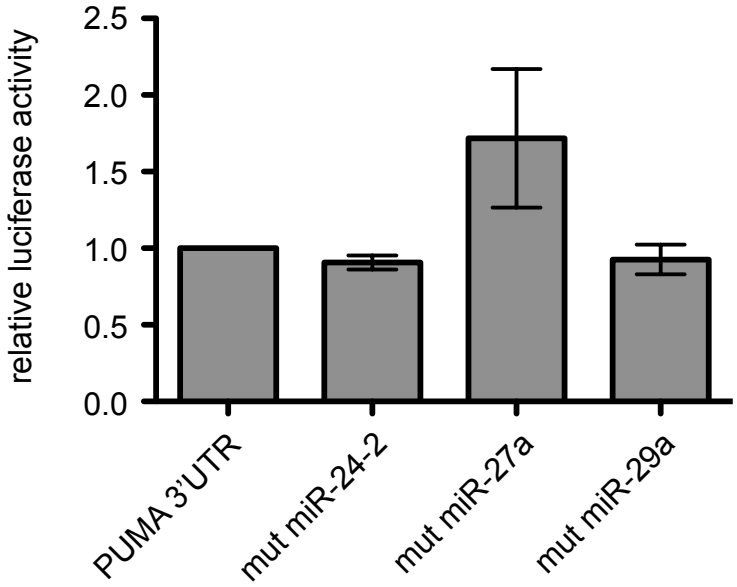

Figure 21: Effect of PUMA 3'UTR miRNA binding site deletion on reporter protein expression in transiently transfected HeLa cells. HeLa cells were transiently transfected by calcium phosphate co-precipitation with the psiCHECK-2 plasmid containing the PUMA 3'UTR cloned downstream of the renilla luciferase gene or with mutant versions of this construct in which either the miR-24-2, miR-27a or miR-29a binding sites were altered by site-directed mutagenesis. Relative activity is the renilla luciferase activity normalized to firefly luciferase activity (mean ±SEM, n = 3). Although the relative luciferase activity in cells transfected with the construct containing a mutation in the miR-27a binding site is elevated relative to the full length construct, the differences are not significantly different (ttest: $p > 0.05$).

transfection reagents without plasmid DNA (NO). After 20 h incubation at 37°C post-transfection, the cells were collected and lysates were examined by western blotting. In a representative blot, PUMA expression appears to decrease slightly in samples transfected with the miR-24-2, miR-27a and miR-29a expression plasmids as well as with a combination of all three (Figure 22A). The quantification of relative band intensity of PUMA normalized to that of actin in triplicate is shown (Figure 22B).

3.9 Effect of miRNA overexpression on PUMA mRNA expression in transiently transfected HeLa cells

The miRNA expression plasmids (miR-24-2, miR-27a and miR-29a) along with a control plasmid (C-miR) were purchased from Genecopoeia. In these plasmids (pEZX-MR04) the pre-miRNA sequences are cloned in the 3'UTR following the eGFP coding sequence. The control plasmid (C-miR) contains a sequence of similar length to the miRNAs, but which has no homology to any human transcript. These miRNA expression plasmids were used to transiently transfect PEER and HeLa cells along with the luciferase reporter plasmids.

HeLa cells were transiently transfected with the control plasmid (C-miR), miR-24-2, miR-27a, miR-29a or with all three of the miRNA expression plasmids by $CaPO_4$. Transfected cells were collected after 24 h and used to examine the effects of overexpressing these miRNAs on PUMA mRNA levels by qPCR. qPCR was run with the respective miRNA primers (Table 3) and all target genes were normalized to the housekeeping gene, RPL4 and quantified in duplicate. Puma mRNA expression appears to remain relatively unaltered by the overexpression of the each of the individual miRNAs as well as by the combination of all three miRNAs compared to the that of the control sample (Figure 23A). miR-24-2 shows an increase in expression of almost 2000-fold (Figure 23B), miR-27a shows an increase in expression just below 2000-fold (Figure 23C) and miR-29a showed the smallest increase in expression of just below 30-fold (Figure 23D) (n = 3) when transiently transfected with their respective expression plasmid. When used in combination the total amount of DNA was kept constant at 10 µg, however the concentration of each miRNA expression plasmid was now reduced by one third.

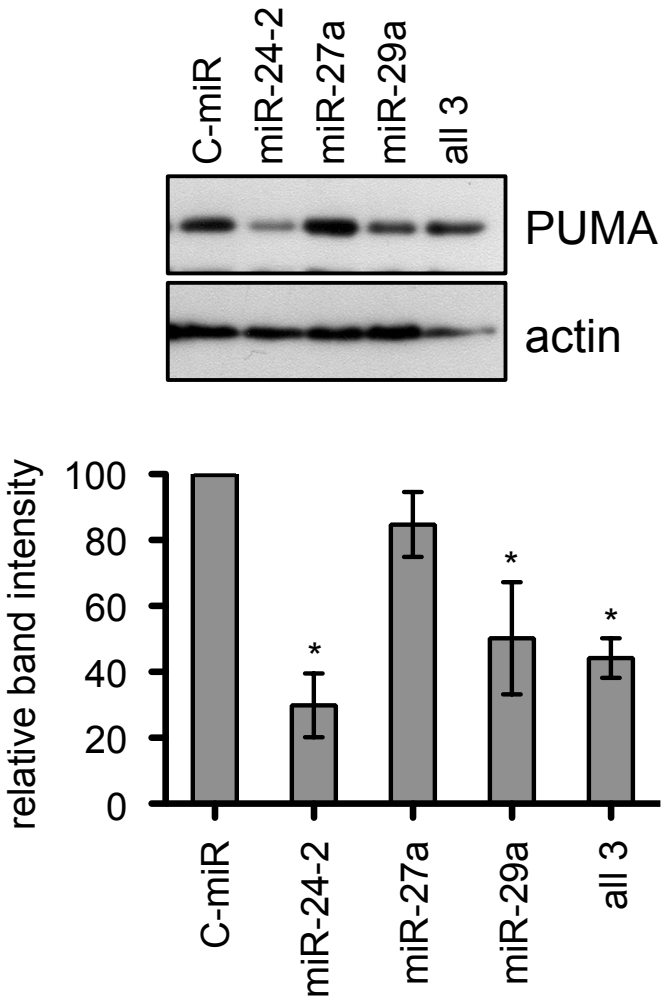

Figure 22: Effect of miRNA overexpression on PUMA protein levels in transiently transfected HeLa cells. HeLa cells were transiently transfected with pEZX-MR04 plasmids encoding miR24-2, miR-27a and miR-29a individually or all combined. The non-targeting miRNA plasmid (C-miR) was used as a control. **(A)** A representative western blot showing PUMA and actin expression. **(B)** Quantitation of the relative band intensities using Image J software (mean ±SEM, n=3). The PUMA band intensity was divided by that of actin for each sample and then the adjusted values were expressed relative to the C-miR control transfection result (set to 100%). Overexpression of miR-24-2, miR-29a or all three miRNAs together significantly reduced the level of PUMA protein (ttest: $p < 0.05$, *).

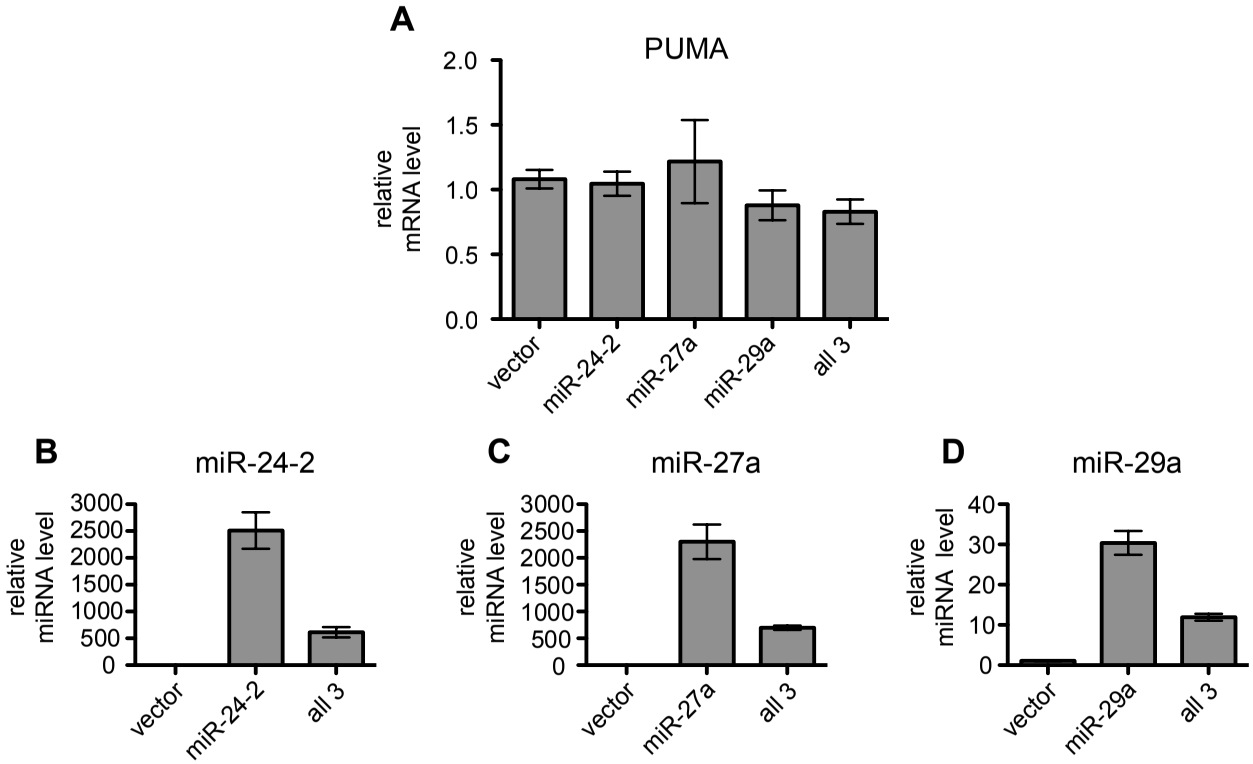

Figure 23: Effect of miRNA overexpression on PUMA mRNA expression in transiently transfected HeLa cells. HeLa cells were transiently transfected with expression plasmids for the miR24-2, miR-27a and miR-29a individually and combined. The expression of PUMA mRNA and each miRNA were assessed by qPCR and normalized to the housekeeping gene RPL4 (mean ±SEM, n = 3). **(A)** PUMA expression was not significantly altered by the expression of the miRNAs either individually or in combination (ttest: $p > 0.05$). Each miRNA was effectively overexpressed in the transiently transfected cells with higher levels being achieved for miR-24-2 **(B)** and miR-27a **(C)** than for miR-29a **(D)**. Co-transfection of all three plasmids reduced the level of expression by about one third, which corresponds to the reduction in micrograms of transfected DNA.

Consequently, the relative level of expression of each miRNA was reduced from about 3-fold (miR-29a) to 5-fold (miR-24-2 and miR-27a).

3.10 Effect of miRNA overexpression reporter protein expression in transiently transfected HeLa cells

We next examined the effect of miRNA overexpression on luciferase expression in transiently transfected HeLa cells. Cells were transfected with the control plasmid (C-miR), miR-24-2, miR-27a or miR-29a together with either the control luciferase expression vector (psiCHECK-2), the expression vector containing the PUMA 3'UTR or the plasmid containing a mutation within the corresponding putative miRNA binding site. The total amount of transfected DNA was kept at 5 μg for each transfection and contained 20 ng of the reporter plasmid plus 5 μg of either the control miRNA (C-miR) expression plasmid or the particular miRNA overexpression plasmid (miR-24-2, miR-27a or miR-29a). Cells were collected 20 h after transfection and dual luciferase assays were performed with the lysates. Figure 24 shows the results of these experiments in which renilla luciferase activity was standardized to the firefly activity of each sample. All results are set relative to the transfection of the control miRNA together with the control vector (n = 3). If the miRNA regulates the expression of the PUMA 3'UTR it would be expected that its overexpression would reduce the relative luciferase activity compared to overexpression of the control miRNA and that this effect would not be seen when overexpressed together with the plasmid contain a mutation within the miRNA binding site. This was not observed for any of the miRNAs examined.

3.11 Effect of miRNA overexpression on PUMA mRNA expression in stably transfected PEER cells

The expression plasmids containing the synthetic sequences of miR-24-2, miR-27a and miR-29a were linearized and stably transfected into PEER cells by electroporation. Stably transfected cells were selected with puromycin and clones arising in individual wells of 96-well dishes were expanded for characterization. Each clone was first analyzed by flow cytometry to assess the level of GFP expression. Two independent clones with high levels of GFP expression (x-mean values greater than 50) and a single clone with no GFP expression (to be used as a

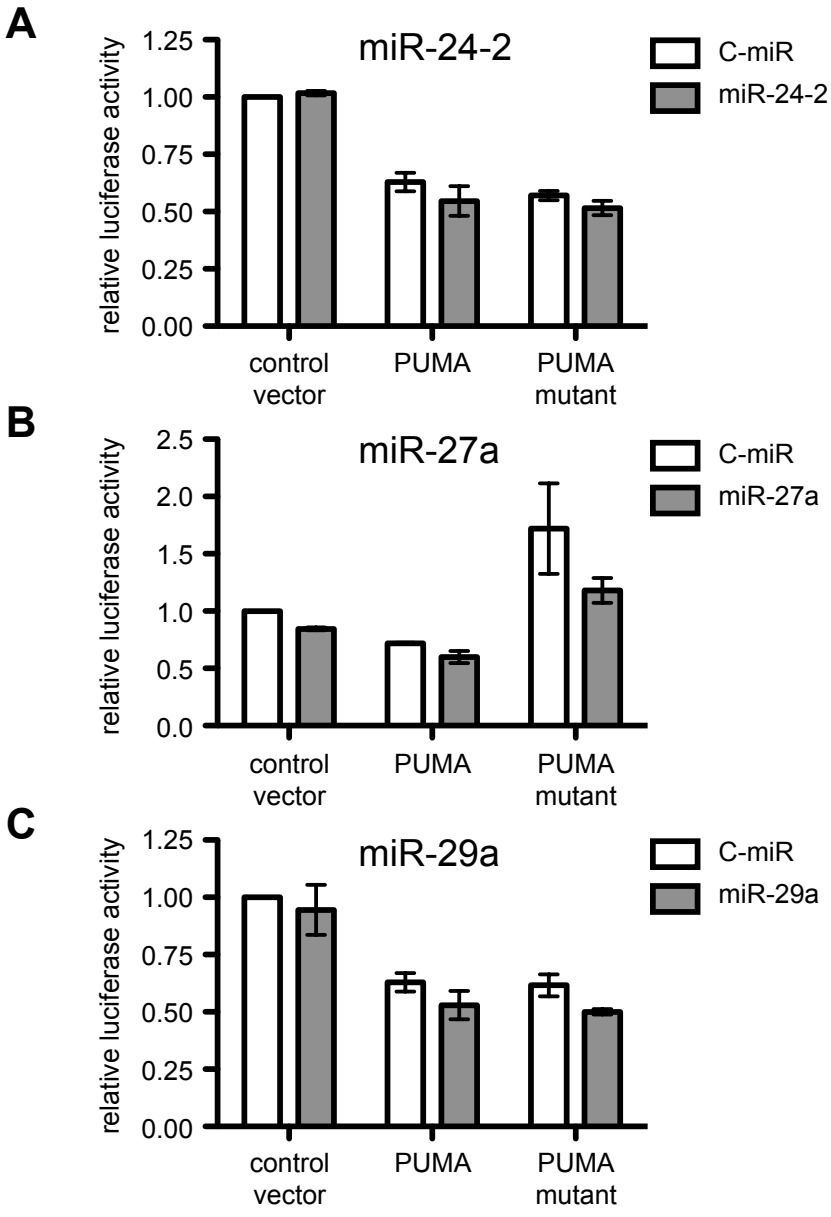

Figure 24: Effect of miRNA overexpression on reporter protein expression in transiently transfected HeLa cells. Co-transfection of HeLa cells were co-transfected with a combination of a PUMA 3'UTR luciferase reporter plasmid and a miRNA overexpression plasmid. The control plasmid is the empty psiCHECK-2 vector. PUMA refers to the psiCHECK-2 plasmid containing the PUMA 3' UTR cloned downstream of the renilla luciferase gene and the mutant plasmids contain mutations in each of the three miRNA binding sites. Reporter plasmids were co-transfected with the pEZX-MR04 miRNA expression plasmids encoding either the control miRNA (C-miR) or **(A)** miR-24-2, **(B)** miR-27a or **(C)** miR-29a. Relative activity is the renilla luciferase activity normalized to firefly luciferase activity (mean ±SEM, n = 3). There was no significant difference in relative luciferase activity levels when comparing the control miRNA and the overexpressed miRNA for each reporter plasmid (ttest: $p>0.05$).

control) were selected for further analysis of miRNA and PUMA expression level by qPCR (Figure 25).

3.12 Effect of miRNA overexpression on PUMA protein expression in stably transfected PEER cells

The stably transfected PEER cell clones expressing miR-24-2, miR-27a or miR-29a were used to examine the effect of miRNA overexpression on PUMA protein levels. As a control, a clone of stably transfected PEER cells that showed no GFP expression when screened by flow cytometry was used for each miRNA-expressing set of clones. Western blotting was performed and the levels of PUMA protein was compared for each clone relative to that of the parental PEER cell line (Figure 26). Quantification of the relative band intensity for each clone shows that miR24-2 and miR-29a appeared to significantly decrease PUMA protein expression whereas overexpression of miR-27a had a somewhat lesser effect (n = 3).

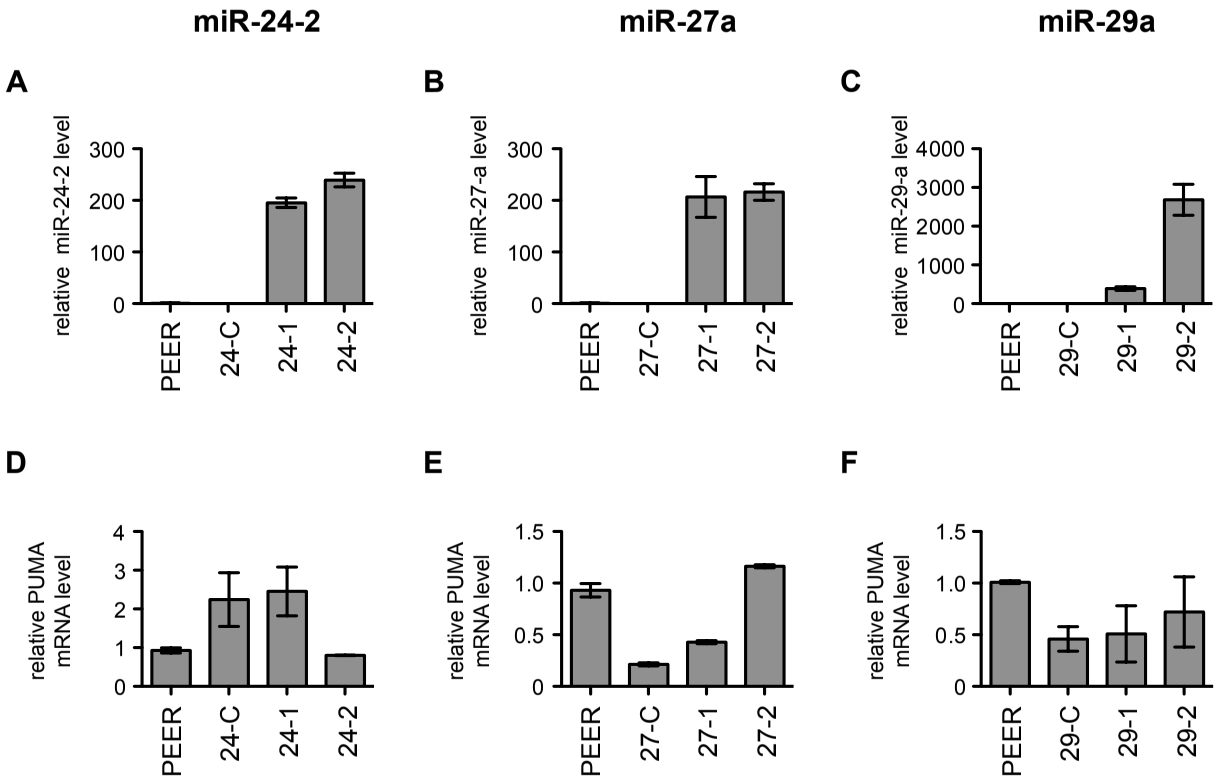

Figure 25: Assessment of miRNA expression in stably transfected PEER cells. PEER cells were stably transfected with the pEZX-MR04 plasmids encoding miR24-2, miR-27a or miR-29a and screened for GFP expression by flow cytometry. For each transfection, one clone was selected that was negative for GFP expression (indicated as C) and two clones were selected that uniformly expressed high levels of GFP (indicated as 1 and 2). PUMA mRNA and miRNA levels were assessed by qPCR. All measurements were normalized to the housekeeping gene RPL4 and then expressed relative to the value for the PEER cell line being set as equal to one. **(A)** miR-24-2 levels in PEER, control clone 24-C (clone 2E11) and overexpressing clones 24-1 (5D4) and 24-2 (4C10). **(B)** miR-27a levels in PEER, control clone 27-C (clone 1D10) and overexpressing clones 27-1 (1E10) and 27-2 (1B7). **(C)** miR-29a levels in PEER, control clone 29-C (clone 2C9) and overexpressing clones 29-1 (2E7) and 29-2 (2B9). PUMA mRNA levels are shown in **(D)** for the miR-24-2 clones, **(E)** for the miR-27a clones and **(F)** for the miR-29a clones.

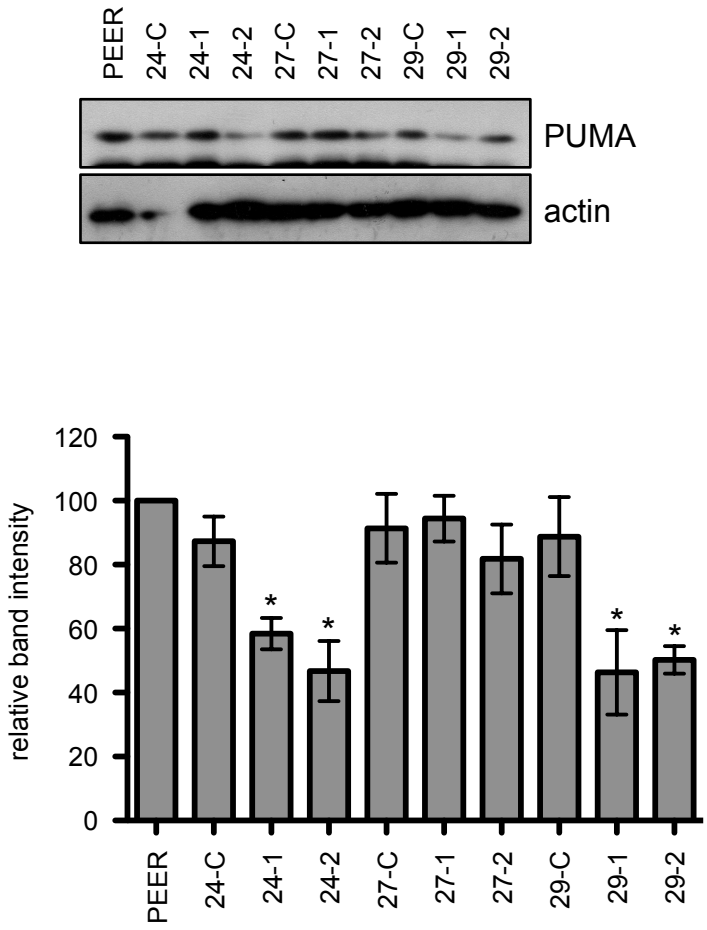

Figure 26: Effect of miRNA overexpression on PUMA protein expression in stably transfected PEER cells. PEER clones were stably transfected with the pEZY-024 plasmids encoding miR24-2, miR-27a and miR-29a and screened for GFP expression by flow cytometry. For each transfection, one clone was selected that was negative for GFP expression (indicated as C) and two clones were selected that uniformly expressed high levels of GFP (indicated as 1 and 2). **(A)** A representative western blot for PUMA and actin protein expression from the parental PEER cell line and each of the selected clones. **(B)** Quantitation of the relative band intensities using Image J software (mean ±SEM, n=4). The PUMA band intensity was divided by that of actin for each sample and then the adjusted values were expressed relative to the value for the PEER cell line (set to 100%). Overexpression of miR-24-2 or miR-29a significantly reduced the level of PUMA protein (ttest: $p < 0.05$, *).

CHAPTER 4: DISCUSSION

4.1 Heat shock decreases PUMA protein expression *in vitro*

PUMA expression is a strong inducer of apoptosis in stressed cells and therefore it is important to examine how stressful conditions such as heat-induced stress may affect PUMA expression. With the expression of this vital regulator of apoptosis characterized, we can then go on to investigate what mechanisms are responsible for the altered expression of PUMA seen in many disorders and diseases.

These studies made use of a human acute lymphoblastic T cell line, PEER, that had been engineered to inducibly overexpress HSP70 (PErTA70) using the tetracycline-regulated expression system (Mosser et al., 2000). Heat shock treatment of non-induced (- HSP70) and induced (+ HSP70) PErTA70 cells resulted in a rapid depletion of PUMA protein levels that was not affected by HSP70 overexpression (Figure 13). Previous studies have shown that this heat shock treatment leads to apoptotic cell death in over 50% of the non-induced cells, whereas the induced HSP70-expressing cells are highly resistant (Mosser et al., 2000). HSP70 expression normally decreases the apoptotic response allowing resistance to the stress signal through its chaperone capabilities of refolding misfolded proteins and sending irreversibly damaged proteins to the proteasome for degradation (Hartl, 2011). The molecular mechanism preventing the expression of PUMA protein following heat shock remains elusive and could be the result of a number of regulatory processes including inhibition of transcription, mRNA degradation or inhibition of translation. In order to assess the cause of this loss of PUMA protein, PUMA mRNA was also examined under control and heat shock conditions.

4.2 Heat shock increases PUMA mRNA expression *in vitro*

Surprisingly while heat shock treatment caused a loss of PUMA protein levels, mRNA levels increased in cells during the period of incubation at 37°C (Figure 14). Although more rapid in the ON cells, the overall induction of PUMA was found to be somewhat lower in HSP70-expressing cells. The reasoning behind the differences in the level of PUMA induction between the induced and non-induced cells remains unclear but might possibly be related to a

dampening of the stress signal leading to increased miRNA expression by HSP70 (Iwasaki et al., 2010).

Previous studies in the lab have only assessed PUMA mRNA levels by semi-quantitative RT-PCR (Stankiewicz, unpublished; Stephanie Hallows, 2005 unpublished). Although this technique was not successfully replicated, qPCR revealed a similar trend, further validating their results. Through the complete characterization of PUMA protein and mRNA under control and heat shock conditions a negative correlation between protein expression, which decreased, and mRNA expression, which increased, was observed. The molecular mechanism leading to increased PUMA mRNA expression in heat shocked cells is not known, but includes increased transcription or a reduced rate of turnover, however it is clear that this mRNA is being actively transcribed and therefore suggests a level of post-transcriptional control of PUMA expression that is preventing the translation of PUMA mRNA into protein in cells exposed to hyperthermia.

Transcription factors that have been implicated in the regulation of PUMA gene expression include p53, p73, Sp1 or Fox03a (Michalak et al., 2008; Hikisz and Kilianska, 2012). There is even evidence of increased expression of these transcription factors under cell stress conditions including hypoxia, infection or growth factor depletion which could explain the increase in PUMA transcription following hyperthermic conditions as a means to eliminate damaged cells (Wei et al., 2008; Fischer et al., 2008). Another explanation for the induction of PUMA mRNA following hyperthermia could be the result of altered mRNA stability. PUMA mRNA stability can be achieved through the fluctuation of its half-life in response to environmental stimuli such as temperature shifts (Guhaniyogi and Brewer, 2001). Deregulated mRNA stability can lead to the aberrant accumulation and expression of that mRNA and in some cases, the proteins it encodes. Not only would an increase in PUMA mRNA stability or transcription factors targeting PUMA cause the increase in mRNA expression but also regulation of these processes at the translational level could simultaneously cause a decrease in PUMA protein after heat shock.

4.3 Heat shock increases levels of miRNAs predicted to bind to the PUMA 3'UTR

The potential role of miRNA-mediated translational repression was evaluated as the mechanism responsible for the inhibition of PUMA protein synthesis in heat-shocked cells. miRNAs are important regulators of stress-induced apoptotic pathways. However, there are only a few reports on the effects of hyperthermia on heat-induced miRNA expression (Wilmink et al., 2010). Heat-induced altered expression of a miRNA that targets the PUMA 3'UTR may explain the translational regulation of PUMA mRNA resulting in the eventual turnover of the existing pools of PUMA protein.

TargetScan prediction software identified miR-24-2, miR-29a and miR-27a as the top 3 candidates for interaction with the PUMA 3'UTR (Grimson et al., 2007) (Figure 15). It should be noted that miRNA control of apoptotic regulators is well documented including that of the BH3-only protein PUMA. For example, miR-122 (Zhang et al., 2010), miR-296 (Cazanave et al., 2011), miR-149 (Ding et al., 2013) and miR-29a (Ouyang et al., 2013) have already been shown to target PUMA expression *in vitro*. For example, Zhang and colleagues have found that miRNA (miR)-221 and miR-222 directly target PUMA mRNA translation in various types of cancer cells (Zhang et al., 2010). Although not in the top 5 candidates, miR-221 and miR-222 directly interact with binding sites in the PUMA 3'UTR mRNA causing translational inhibition and ultimately repression of PUMA protein synthesis, thus allowing cell survival and tumor progression (Zhang et al., 2010). miR-29, miR-221 and miR-222 are only a few of the miRNAs shown to target and alter the expression of PUMA and many more miRNAs are expected to have an effect on PUMA expression.

Although these miRNAs are shown to affect PUMA expression in cancer cell lines, the effect of hyperthermia was not yet assessed. The predicted binding sites for miR-24-2, miR27a and miR-29a among other miRNAs that potentially target PUMA are shown along the length of the 981 bp PUMA 3'UTR (Figure 15). miRNAs elicit their function by binding to their respective sites on mRNA, targeting it for degradation or inhibiting the translation of the mRNA into proteins (Hammond, 2006). Because PUMA mRNA expression is increased following hyperthermia, it is hypothesized that the miRNAs may be acting by inhibiting PUMA mRNA translation into proteins. This would explain the suppression of PUMA translation with the

simultaneous increase in mRNA transciption. To assess the potential role of miR-24-2, miR-27a and miR-29a in miRNA-mediated suppression of PUMA translation we first assessed their expression under control and heat shock conditions.

Hyperthermia was found to increase levels of miR-24-2, miR-27a and miR-29a in both the non-induced and HSP70-expressing cells exposed to hyperthermia, although the response was higher in cells that were not over-expressing HSP70 (Figure 16A-C). Even though each individual miRNA showed a similar level of induction following heat treatment (approximately 10-fold), the absolute levels of each miRNA differed (Figure 16D). The observation that HSP70 overexpression dampened the increased expression of these miRNAs compared to that of the non-induced cells yet PUMA translation was inhibited to the same degree in both the non-induced and induced cells raises the possibility that none of these miRNAs play a significant role in translational repression in heat shocked cells. Alternatively, the single time point measurement might not capture the temporal pattern of miRNA expression in these cells. For this reason a time course experiment was undertaken in order to assess the miRNA levels at earlier time points post-heat shock treatment.

miR-24-2, miR-27a and miR-29a expression was measured at the same time points in which PUMA mRNA expression was assessed following heat treatment (0 h, 3 h and 6 h). Expression of each miRNA increased after exposure to hyperthermic conditions (Figure 17A-C). miR-24-2 and miR-27a show the highest fold change after heat shock. This dramatic increase after hyperthermic treatment indicates their potential role in the stress-induced translational suppression of their target genes. Overexpression of HSP70 suppressed the increased expression of miR-24-2 and miR-27a but did not affect expression of miR-29a, which proved to be more variable. The influence of HSP70 on miRNA expression after hyperthermia remains unclear. Interactions between HSP70 and Drosha have been identified but these interactions are limited to the cytoplasm after the majority of miRNA processing has been completed (Han et al., 2004). Specifically, HSP70, and HSP90 have been shown to play a role in the loading of miRNAs into the RISC complex by regulating conformational changes in the Argonaut protein (Iwasaki et al., 2010). HSP70 could potentially play a role in regulating the transcription of these miRNAs or inhibit their turnover in heat-stressed cells. Nevertheless, the increase in miR-24-2, miR-27a and

miR-29a expression coincides with the decreased expression of PUMA protein following heat shock. The induction of these miRNAs supports their potential role in miRNA-mediated suppression of PUMA translation under hyperthermic conditions.

4.4 miR-24-2, miR-27a and miR-29a regulate PUMA expression

With evidence that the increased expression of miR-24-2, miR-27a and miR-29a coincides with the decrease in PUMA protein expression after heat shock, further investigation was necessary to validate the role of these miRNAs in the translational regulation of PUMA expression.

4.4.1 Hyperthermia alters PUMA mRNA and miRNA-association with ribosomes

Sucrose gradient density centrifugation was used to identify a possible link between the location of miR-24-2, miR-27a and miR-29a and the translational suppression of PUMA expression after heat shock. The fractionation of ribosomes on sucrose gradients revealed that association of the mRNA for the housekeeping gene RPL4 with ribosomes behaved as would be expected for the translation of a gene under control and heat shock conditions (Figure 18A/Figure 19A). RPL4 mRNA was predominantly found associated with the poly-ribosomes in control cells. Immediately after heat shock, RPL4 mRNA shifted to the translationally repressed mono-ribosome fractions and after 6 h recovery from heat shock, it partially returned to the di-ribosomes and poly-ribosome fractions. The association of PUMA mRNA followed a similar trend, differing only in a less dramatic shift to the mono-ribosome fraction immediately after exposure to heat shock (Figure 18B/Figure 19B). This data indicates that PUMA mRNA is actively associated with poly-ribosomes by 6 h recovery from heat shock and yet is not translated, and therefore further validates the potential role of miRNA-mediated suppression of PUMA translation in heat-stressed cells. Biochemical analysis has shown that the repressed mRNAs often remain associated with the poly-ribosomes, suggesting that the inhibition of translation occurs after translation initiation (Seggerson et al., 2002; Doench and Sharp, 2004).

The locations of the target miRNAs were also examined by polysomal sucrose gradient fractionation. miR-24-2 and miR-29a appeared predominantly in the mono-ribosome fractions in non-induced and induced control cells, however post-heat shock they moved to the di-ribosome

and poly-ribosome fractions (Figure 18C/Figure 19C). miR-27a on the other hand behaves much like PUMA mRNA in that it was associated with poly-ribosomes in control cells, shifted to the mono-ribosome fraction immediately after exposure to hyperthermia and then returned to the poly-ribosome fraction during incubation at 37°C after heat shock exposure. The location of PUMA together with miR-24-2, miR-27a and miR-29a in each of the fractions does not provide definitive evidence for any one of them in the regulation of PUMA translation, although the distribution of miR-27a most closely resembled that of PUMA mRNA suggesting that it might be active in repressing its translation. On the other hand an argument could be made for the involvement of miR-24-2 or miR-29a since they are not associated with the same fraction as PUMA mRNA in non-stressed cells when PUMA is actively being translated but become associated with the same fraction after heat shock when PUMA mRNA translation is repressed. These results should be considered preliminary since they were only performed twice for RPL4 and PUMA in the non-induced cells and all other data was derived from a single experiment. As well, since miR-27a is not very abundant its detection was at the lower limit of the qPCR range after fractionation.

4.4.2 PUMA 3'UTR miRNA binding site deletion affects reporter protein expression in transiently transfected PEER and HeLa cells

In order to assess the potential role of miRNA-mediated suppression of PUMA translation, miR-24-2, miR-27a and miR-29a binding sites were mutated in the PUMA 3'UTR of the psiCHECK-2 luciferase construct and transfected into PEER and HeLa cells. Typically, if a miRNA regulates a particular mRNA and this miRNA is present in the cells being studied the addition of the 3'UTR from this mRNA downstream from a reporter construct should repress reporter gene activity from the construct. As well, if the miRNA binding site has been eliminated from the 3'UTR an increase in luciferase activity would be expected. Elevated relative luciferase activity from the PUMA 3'UTR luciferase reporter construct containing a mutation in the putative miR-27a binding site in both cell lines suggests a potential role of this miRNA in regulating PUMA translation (Figure 20/Figure 21). The mutation of miR-29a and the miR-24-2 binding sites did not show any significant change in luciferase activity relative to the wt psiCHECK-2 + PUMA 3'UTR plasmid. Furthermore, there is a repression of luciferase activity between the psiCHECK-2 empty luciferase reporter plasmid and the wt psiCHECK-2 + PUMA

3'UTR construct in PEER cells. This decrease in luciferase activity provides evidence that the PUMA 3'UTR, which contains multiple miRNA binding sites has repressed luciferase activity and that activity can only be restored when the corresponding miRNAs or their binding sites have been abolished. This is seen with the partial restoration of PUMA activity with the mutated miR-27a binding site, bringing luciferase levels back up towards those of the empty psiCHECK-2 plasmid and providing further evidence for the role of miR-27a in PUMA translational regulation across multiple cancer cell lines. Since the altered miR-27a binding site increases the relative luciferase activity from the reporter luciferase construct, it would be expected that the overexpression of this miRNA on the wt psiCHECK-2 + PUMA 3'UTR would elicit the opposite effect and decrease the relative luciferase activity by binding to the PUMA 3'UTR and prevent renilla luciferase expression but this did not occur.

Another important consideration is the fact that miR-24-2 has two binding sites in the PUMA 3'UTR and these experiments have only yet been carried out with one of the sites mutated by site-directed mutagenesis. It is important to assess a double deletion of both miR-24-2 binding sites as miRNAs with multiple binding sites in the 3'UTR often show synergistic effects resulting in more efficient inhibition of translation than that expected from the sum of the effects of each binding site acting individually (Doench et al., 2003). The lack of increased relative luciferase activity for the miR-24-2 deletion construct can therefore possibly be accounted for by its ability to bind to the second site and repress luciferase expression on the PUMA 3'UTR.

Even so, the luciferase assay results proved to be variable in expression between technical and biological replicates. The variability in these experiments reduce its efficiency and validity in assessing the effect of the PUMA 3'UTR on relative luciferase expression. That being said, this method may not provide concrete evidence for or against any of the three miRNAs tested and should be verified using stably transfected cells.

4.4.3 miRNA overexpression does not regulate PUMA mRNA expression in HeLa cells

miR-24-2, miR-27a, mir-29a and the C-miR expression plasmid with no homology to any human transcript (Genecopoeia) were then used in transient transfection experiments in HeLa

cells to assess the overexpression of these miRNAs on PUMA mRNA expression. PUMA mRNA expression appears to remain unaltered by the overexpression of the each of the individual miRNAs as well as by the combination of all three miRNAs compared to the that of the control sample (Figure 22A). These results rule out the possibility that these miRNAs are acting by binding to the PUMA mRNA 3'UTR and targeting it for destruction and support the possibility of miRNA-mediated suppression of PUMA is by binding to the PUMA 3'UTR and inhibiting translation (Fabian et al., 2010). This interpretation fits with the observations of simultaneous depletion of PUMA protein and increase in PUMA mRNA, along with the positive correlation seen in PUMA mRNA and the target miRNAs induction after heat shock. These results also illustrate that the miRNA expression plasmids are in fact being overexpressed indicating the effectiveness in inducing the individual miRNAs (Figure 22B-D). Although transient transfections show some variation in overexpression of miR-24-2, miR-27a or miR-29a, this experiment is key to evaluate the role of miRNAs in PUMA translational suppression after heat shock.

4.4.4 miRNA overexpression affects PUMA protein levels in transiently transfected HeLa cells

To better understand the role of miR-24-2, miR-27a and miR-29a on PUMA protein suppression, these miRNAs were overexpressed in HeLa cells and PUMA protein expression was assessed. The individual overexpression of miR-24-2, miR-27a and miR-29a in HeLa cells appeared to slightly decrease PUMA protein levels to a similar degree (Figure 23A-B). The combination of all three miRNAs also appeared to decrease PUMA protein expression to a similar degree (Figure 23A). However, because the overexpression of the miRNAs did not suppress PUMA protein levels to the extent seen after hyperthermic treatment, we could speculate that the increased expression of the miRNAs that target the PUMA 3'UTR may be only partially responsible for the suppression of translation of PUMA in heat-shocked cells. Interestingly, the control samples without DNA and with the control C-miR plasmid also showed a difference in PUMA protein expression. This implies that the transfections reagents alone may be causing a partial reduction of PUMA expression. Still, these results provide substantial proof that these miRNAs act by regulating PUMA translation without having any effect on PUMA mRNA expression.

4.4.5 miRNA overexpression shows no affect on reporter protein expression in transiently transfected HeLa cells

Because PUMA protein and mRNA expression was characterized in PErTA70 cells, PEER cells were initially used to assess the transcriptional control of the miRNA expression plasmids on the PUMA 3'UTR. Unfortunately PEER cells can only be transfected by electroporation (Chu et al., 1987), which generally kills 50% of the cells and transfection efficiency only reaches 40%. This limited the use of these cells for co-transfection experiments in which the miRNA overexpression plasmids needed to be present at a 160-fold excess over the reporter plasmid, making it difficult to obtain measurable luciferase activity. Luciferase activity measurements were possible with the PUMA 3'UTR reporter plasmid and the plasmids containing mutations in the individual miRNA binding sites. However, although attempted it was not possible to carry out these experiments in heat-shocked cells due to the very low levels of luciferase activity in the stressed cells. Regrettably, this problem was never fully resolved in PEER cells and therefore co-transfections were carried out in HeLa cells, which had higher transfection efficiency. Co-transfections of the miRNA expression plasmids with the empty psiCHECK-2 luciferase reporter plasmid and the psiCHECK-2 + PUMA 3'UTR wt and mutated miRNA binding site luciferase reporter plasmids were carried in HeLa cells. Although co-transfections were successful in these cells, the affect of hyperthermia on luciferase expression from the PUMA 3'UTR did not indicate that any of the miRNAs had an effect on luciferase activity. We speculate that this may be the result of HeLa cell resistance to the optimized heat shock treatment for PEER cells.

As seen previously, the repression of luciferase activity seen between the empty psiCHECK-2 plasmid and the psiCHECK-2 + PUMA 3'UTR, this time co-transfected with the control miRNA expression plasmid (C-miR) indicates the potential for miRNAs to target and act on the PUMA 3'UTR, altering its expression. Furthermore, even with the increased luciferase activity seen with the miR-27a mutated binding site, co-transfections in HeLa cells reveal no significant repression of relative luciferase expression from the miRNAs, individually or combined, on the reporter luciferase plasmid with the PUMA 3'UTR (Figure 24 A-C). Decreased luciferase activity in the miR-24-2, miR-27a or miR-29a expression transfection samples would indicate binding and possible translational repression by the miRNAs. This does

not provide any further evidence supporting the influnce of miR-24-2, miR-27a, miR-29a or a combined effect of all three miRNAs on the PUMA 3'UTR in HeLa cells. Stable overexpression of miRNA expression in PEER cells would be a beneficial tool for studying the effect of these miRNAs on PUMA protein and mRNA expression without the obstacles associated with electroporation transfection.

4.4.6 miRNA overexpression shows no affect on PUMA mRNA levels in stably transfected PEER cells

In order to better study and understand the effect of altered miRNA expression on the regulation of PUMA translation, stably transfected cell lines were created to overexpress miR-24-2, miR-27a and miR-29a along with a control clone for each. The benefit of using stable cell lines is that they will constantly express these individual miRNAs and therefore the variability associated with transient transfection is eliminated.

Two positive clones and a negative clone for GFP for each miRNA were selected through screening and were used to assess the effects of stable miRNA expression on PUMA mRNA by qPCR. In agreement with previous experiments in HeLa cells (Figure 23), the expression of the miRNAs did not have any significant effect on PUMA mRNA expression (Figure 25 data not shown). The expression of miR-24-2, miR-27a, and miR-29a in the individual clones varied from 200-fold to almost 1000-fold higher than that of the GFP negative control clone. This level of expression is far higher than that obtained by exposing cells to hyperthermia, however it demonstrates that even at these very high levels of expression there is no effect on the level of PUMA mRNA ruling out PUMA mRNA degradation as mechanism for suppressing PUMA expression.

4.4.7 miRNA overexpression affects PUMA protein levels in stably transfected PEER cells

The stably transfected miR-24-2, miR-27a and miR-29a PEER clones provided clear evidence that these miRNAs act to suppress PUMA expression. miR-24-2 clones 4C10 and 5D4 showed the largest decrease in PUMA protein expression, followed by the miR-29a clones (2B10 and 2B9) and to a lesser extent the miR-27a clones (1E10 and 1B7) show the smallest reduction in PUMA protein expression compared to the control clone and the non-transfected PEER cells

(Figure 26). The ability of miR-24-2 to have the strongest repression of PUMA protein may be attributed to the fact that this miRNA has an extra binding site in the PUMA 3'UTR allowing for increased binding potential and therefore repression of PUMA mRNA translation (Doench et al., 2003). These results demonstrate that miR-24-2, miR-27a and miR-29a each play a role in miRNA-mediated suppression of PUMA translation.

4.4.8 Transient and stable miRNA shRNA knockdown transfection to restore PUMA expression in HeLa and PEER cells

Oligonucleotides were designed to target both miR-24-2 and miR-27a along with mutant oligonucleotides for each miRNA (Table 5). The oligonucleotides were annealed as described previously. The pSuper plasmid, in which an shRNA expression cassette can be expressed from a mouse U9 promoter (Haraguchi et al., 2009), was linearized by restriction enzyme digestion with BsmBI at 37°C for 5 h. The digested plasmid was run on an analytical gel to verify the cut before running the remainder of the digest for gel extraction and purification. Once linearized, the annealed oligonucleotides will be ligated into the pSuper-shRNA plasmid and transformed into *E. coli* for DNA amplification. Colonies of *E. coli* will be selected for mini-prep and digested with EcoRI and HindIII. Once confirmed by restrictions enzyme digestion, the miRNA shRNA knockdown plasmids will be sequenced in the Advanced Analysis Centre (University of Guelph). These plasmids will then be used in transient and stable transfections in hopes to restore PUMA protein expression and hopefully sensitize cells to heat-induced apoptosis.

Table 5: Oligonucleotides for target miRNA shRNA knockdown

Gene	Primers
miR-24-2	Forward: 5'- CATCAACCTGTTCCTGCTGAACTGAGCCACAAGTATTC TGGTCACAGAATACAACTGGCTCAGTTCAGCAGGAACAGCAAG -3' Reverse: 5'- TCATCTTGCTGTTCCTGCTGAACTGAGCCAGTTGTAT TCTGTGACCAGAATACTTGTGGCTCAGTTCAGCAGGAACAGGTT -3'
miR-24-2 mutant	Forward: 5'- CATCAACCTGGTCCTGCCAAACTGAAACACAAGTATT CTGGTCACAGAATACAACTGTTTCAGTTTGGCAGGACCAGCAAG -3' Reverse: 5'- TCATCTTGCTGGTCCTGCCAAACTGAAACAGTTGTATT CTGTGACCAGAATACTTGTGTTTCAGTTTGGCAGGACCAGGTT-3'
miR-27a	Forward: 5'- CATCAACGCGGAACTTAGCCACTGTGAACAAGTATTC TGGTCACAGAATACAACTTCACAGTGGCTAAGTTCCGCCAAG -3' Reverse: 5'- TCATCTTGGCGGAACTTAGCCACTGTGAAGTTGTATT CTGTGACCAGAATACTTGTTCACAGTGGCTAAGTTCCGCGTT -3'
miR-27a mutant	Forward: 5'- CATCAACGCGTAACTTAAACACTGGAAACAAGTATTCT GGTCACAGAATACAACTTTCCAGTGTTTAAGTTACGCCAAG -3' Reverse: 5'- TCATCTTGGCGTAACTTAAACACTGGAAAGTTGTATTCT GTGACCAGAATACTTGTTTCCAGTGTTTAAGTTACGCGTT -3'

CHAPTER 5: CONCLUSIONS AND FUTURE DIRECTIONS

The expression of PUMA is often altered under conditions of cellular stress leading to aberrant apoptosis in many disorders and diseases along with poor prognosis. In this thesis, a characterization of PUMA expression in heat-stressed cells revealed an increase in PUMA mRNA coinciding with a decrease in PUMA protein. The exact mechanisms that control the decreased expression of PUMA protein in heat-shocked PEER cells, previously unknown, suggested some form of translational control. This inspired the study of miRNA-mediated regulation of PUMA translation in heat-shocked cells. miR-24-2, miR-27a and miR-29a were investigated based on the conserved presence of binding sites for these miRNAs in the PUMA 3'UTR. Although miR-24-2, miR-27a and miR-29a expression plasmids did not seem to alter PUMA mRNA expression, the expression of each of these miRNAs did appear to have an effect in decreasing PUMA protein levels to some degree. This, along with the induced expression of PUMA mRNA after heat shock, ruled out the possibility that the miRNAs were targeting PUMA mRNA for degradation. Instead, it is hypothesized that the miRNAs bind to the PUMA 3'UTR to prevent the translation of the PUMA mRNA into protein. Further investigation will be conducted with the use of stable cell lines that over-express or knockdown the target miRNAs to verify their role in suppressing PUMA translation in heat-stressed cells.

It seems counterintuitive that cells would increase the abundance of a particular mRNA, in this case coding for PUMA, only to also increase the expression of a miRNA that inhibits its translation. This might reflect an attempt to maintain homeostasis in a hostile environment, however this loss of PUMA protein occurs under conditions that lead to the apoptotic elimination of a majority of the PEER cells. Its possible that exposure to more extreme heat stress could alter the ratio of PUMA mRNA relative to the miRNAs that regulate it such that under these conditions a higher proportion of cells ultimately succumb to apoptosis. Nevertheless, the role of PUMA in heat-induced apoptosis is uncertain but could simply reflect particular cell line used in this study. The effect of hyperthermia on PUMA expression in other cell lines should be examined. The increased expression of miRNAs targeting PUMA observed in the PEER cell line studied here might not be universal, but could suggest a strategy to decrease the apoptotic

threshold of cells. For example, down-regulation of these miRNAs might be expected to lead to higher levels of PUMA protein expression and increase the extent of cell killing in stressed cells.

An important consideration is that miRNAs cannot fully account for the 100% loss of PUMA protein in the heat-stressed cells. Another explanation for this loss could be due to proteasomal/lysosomal degradation of PUMA, which might be increased in cells exposed to hyperthermia. Consequently, despite the increased mRNA expression, which could be the result of increased transcription or altered mRNA stability, PUMA protein levels do not increase as the rate of its degradation is also enhanced.

By understanding and developing new *in vitro* tools to regulate the expression of the Bcl-2 proteins in stressed cells, we could potentially augment their function to stimulate the apoptotic response in tumor cells. We expect that a method to alter PUMA expression will lead to a novel pathway for treating aberrant apoptosis, which contributes to carcinogenesis and altered sensitivity to chemotherapeutic agents, in which expression of PUMA protein plays an essential role. Studies in our lab indicate that directly targeting the apoptotic machinery through the manipulation of miRNA expression may offer new hope for improved therapy for cancer and other autoimmune and infectious diseases. Cell lines that stably express the miRNAs under study here will allow the examination of their role in the heat induced regulation of PUMA expression and also other regulators of apoptosis that they have been implicated in controlling. More importantly, stably transfected shRNA knockdown cells will be created to abolish miR-24-2, miR-27a and miR-29a expression in hopes of restoring PUMA protein expression under conditions of cellular stress.

REFERENCES

1. Adams, J. M. & Cory, S. Life-or-death decisions by the Bcl-2 protein family. Trends in Biochemical Sciences, 26: 61–66 (2001).
2. Adams, J. M. & Cory, S. The Bcl-2 apoptotic switch in cancer development and therapy. Oncogene, 26: 1324–1337 (2007).
3. Antignani, A. & Youle, R. J. How do Bax and Bak lead to permeabilization of the outer mitochondrial membrane? Cell Biology, 18: 685–689 (2006).
4. Antonsson, B. Bax and other pro-apoptotic Bcl-2 family "killer-proteins" and their victim the mitochondrion. Cell and Tissue Research, 306: 347–361 (2001).
5. Beere, H. M., Wolf, B. B., Cain, K., Mosser, D. D. et al. Heat-shock protein 70 inhibits apoptosis by preventing recruitment of procaspase-9 to the Apaf-1 apoptosome. Cell Biology, 2: 469–475 (2000).
6. Borchert, G. M., Lanier, W., & Davidson, B. L. RNA polymerase III transcribes human microRNAs. Nature Structural & Molecular Biology: 13(12), 1097–1101 (2006).
7. Borner, C. The Bcl-2 protein family: sensors and checkpoints for life-or-death decisions. Molecular Immunology, 39: 615–647 (2003).
8. Buchberger, A., Bukau, B. & Sommer, T. Protein quality control in the cytosol and the endoplasmic reticulum: brothers in arms. Molecular Cell Biology, 40(2): 238–252 (2010).
9. Cain, K., Bratton, S. B. & Cohen, G. M. The Apaf-1 apoptosome: a large caspase-activating complex. Biochimica et Biophysica Acta, 84: 203–214 (2002).
10. Cazanave, S. C., Mott, J. L., Elmi, N. A., Bronk, S. F., et al. A role for miR-296 in the regulation of lipoapoptosis by targeting PUMA. Journal of Lipid Research, 52(8): 1517–1525 (2011).
11. Charvet, C, Wissler, M., Brauns-Schubert, P., Wang, S-J., Tang, Y., Sigloch, F. C., Mellert, H. et al. Phosphorylation of Tip60 by GSK-3 determines the induction of PUMA and apoptosis by p53. Molecular Cell Biology, 42: 584–596 (2011).
12. Chen, L., Willis, S. N., Wei, A. et al. Differential targeting of pro-survival Bcl-2 proteins by their BH3-only ligands allows complementary apoptotic function. Molecular Cell Biology, 17: 393–403 (2005).
13. Chhabra, R., Adlakha, Y. K., Hariharan, M., Scaria, V. & Saini, N. Up-regulation of miR-23a-27a-24-2 cluster induces caspase-dependent and -independent apoptosis in human embryonic kidney cells. PloS one, 4: e5848 (2009).
14. Chirico, W. J., M. Gerard W., & Guenter B. 70K heat shock related proteins stimulate protein translocation into microsomes. Nature, 332: 6167 (1988).
15. Chipuk, J. E. & Green, D. R. How do BCL-2 proteins induce mitochondrial outer membrane permeabilization? Cell Biology, 18: 157–164 (2008).

16. Chipuk, J. E., Moldoveanu, T., Llambi, F., Parsons, M. J. et al. The BCL-2 family reunion. Molecular Cell Biology, 37: 299–310 (2010).

17. Choi, W. Y., Giraldez, A. J., & Schier, A. F. Target protectors reveal dampening and balancing of Nodal agonist and antagonist by miR-430. Science, 318(5848): 271–274 (2007).

18. Choy, E. Y. W., Siu, K. L., Kok, K. H., Lung, R. W. M., et al. An Epstein-Barr virus-encoded microRNA targets PUMA to promote host cell survival. The Journal of Experimental Medicine, 205(11): 2551–2560 (2008).

19. Chu, G., Hayakawa, H. & Berg, P. Electroporation for the efficient transfection of mammalian cells with DNA. Nucleic Acids Research, 15: 1311–1326 (1987).

20. Cimmino, A., Calin G. A., Fabbri, M, et al. miR-15 and miR-16 induce apoptosis by targeting BCL2. Proceedings of the National Academy of Sciences, 102: 13944–13949 (2005).

21. Clavería, C., Giovinazzo, G., Sierra, R., & Torres, M. Myc-driven endogenous cell competition in the early mammalian embryo. Nature, 500 (7460): 39–44 (2013).

22. Cory, S. & Adams, J. M. The Bcl2 family: regulators of the cellular life-or-death switch. Nature Reviews Cancer, 2: 647–656 (2002).

23. Cory, S., Huang, D. C. S. & Adams, J. M. The Bcl-2 family: roles in cell survival and oncogenesis. Oncogene, 22: 8590–8607 (2003).

24. Cotter, T. G. Apoptosis and cancer: the genesis of a research field. Nature Reviews Cancer, 9: 501–507 (2009).

25. Czabotar, P. E., Lessene, G., Strasser, A., & Adams, J. M. Control of apoptosis by the BCL-2 protein family: implications for physiology and therapy. Nature Reviews Molecular Cell Biology, 15(1): 49–63 (2014).

26. Desagher, S. & Martinou, J. C. Mitochondria as the central control point of apoptosis. Cell Biology, 10: 369–377 (2000).

27. Ding, S. L., Wang, J. X., Jiao, J. Q., Tu, X., et al. A pre-microRNA-149 (miR-149) genetic variation affects miR-149 maturation and its ability to regulate the Puma protein in apoptosis. Journal of Biological Chemistry, 288(37): 26865–26877 (2013).

28. Doench, J. G., Petersen, C. P., & Sharp, P.A. siRNAs can function as miRNAs. Genes & Development, 17: 438–442 (2003).

29. Doench, J. G., & Sharp, P. A. Specificity of microRNA target selection in translational repression. Genes & development, 18(5): 504–511 (2004).

30. Du, C., Fang, M., Li, Y., Li, L., & Wang, X. Smac, a mitochondrial protein that promotes cytochrome c-dependent caspase activation by eliminating IAP inhibition. Cell Biology, 102: 33–42 (2000).

31. Earnshaw, W. C., Martins, L. M. & Kaufmann, S. H. Mammalian caspases: Structure, Activation, and Substrates. Annual Review of Biochemistry, 77: 383–424 (1999).

32. Ebert, M. S., & Sharp, P. A. MicroRNA sponges: progress and possibilities. RNA, 16(11): 2043–2050 (2010).

33. Er, E., Oliver, L., Cartron, P. F., et al. Mitochondria as the target of the pro-apoptotic protein Bax. Biochimica et Biophysica Acta, 1757: 1301–1311 (2006).

34. Evan, G. I. & Vousden, K. H. Proliferation, cell cycle and apoptosis. Nature, 411: 342 (2001).

35. Fabian, M. R., Sonenberg, N. & Filipowicz, W. Regulation of mRNA translation and stability by microRNAs. Annual Review of Biochemistry, 79: 351–379 (2010).

36. Fadeel, B., Orrenius, S. & Zhivotovsky, B. Apoptosis in human disease: a new skin for the old ceremony. Biochemical and Biophysical Research Communications, 266: 699–717 (1999).

37. Fischer, S. F., Belz, G. T. & Strasser, A. BH3-only protein PUMA contributes to death of antigen-specific T cells during shutdown of an immune response to acute viral infection. Proceedings of the National Academy of Sciences, 105: 3035–3040 (2008).

38. Flynt, A. S., & Lai, E. C. Biological principles of microRNA-mediated regulation: shared themes amid diversity. Nature Reviews Genetics, 9(11): 831–842 (2008).

39. Fricker, M., O'Prey, J., Tolkovsky, A. M. & Ryan, K. M. Phosphorylation of PUMA modulates its apoptotic function by regulating protein stability. Cell Death & Disease, 1: e59 (2010).

40. Friedman, R. C., Farh, K. K. H., Burge, C. B., & Bartel, D. P. Most mammalian mRNAs are conserved targets of microRNAs. Genome Research: 19(1), 92–105 (2009).

41. Gabai, V. L., Meriin, A. B., Yaglom, J. A, Volloch, V. Z. et al. Role of HSP70 in regulation of stress-kinase JNK: implications in apoptosis and aging. FEBS letters, 438: 1–4 (1998).

42. Garzon, R., Calin, G. A., & Croce, C. M. MicroRNAs in cancer. Annual Review of Medicine: 60, 167–179 (2009).

43. Garzon, R., Marcucci, G., & Croce, C. M. Targeting microRNAs in cancer: rationale, strategies and challenges. Nature Reviews Drug Discovery, 9(10): 775–789 (2010).

44. Gavathiotis, E., Suzuki, M., Davis, M. L., Pitter, et al. BAX activation is initiated at a novel interaction site. Nature, 455(7216): 1076–1081 (2008).

45. Gerner, E. W. & Schneider, M. J. Induced thermal resistance in HeLa cells. Nature, 256: 500–502 (1975).

46. Golstein, P. Cell death in us and others. Science, 281: 1283–1283 (1998).

47. Green, D. R. & Evan, G. I. A matter of life and death. Cancer Cell, 1: 19–30 (2002).

48. Grimson, A., Farth, K. K-H., Johnston, W. K., Garrett-Engele, et al. MicroRNA targeting specificity in mammals: determinants beyond seed pairing. Molecular Cell Biology, 27: 91–105 (2007).

49. Guhaniyogi, J., & Brewer, G. Regulation of mRNA stability in mammalian cells. Gene, 265(1): 11–23 (2001).

50. Hammond, S. M. MicroRNA therapeutics: a new niche for antisense nucleic acids. Trends in Molecular Medicine, 12: 99–101 (2006).

51. Han, J., Flemmington, C., Houghton, A. B., Gu, Z., et al. Expression of bbc3, a pro-apoptotic BH3-only gene, is regulated by diverse cell death and survival signals. Proceedings of the National Academy of Sciences, 98: 11318–11323 (2001).

52. Happo, L., Cragg, M. S., Phipson, B., Haga, J. M., et al. Maximal killing of lymphoma cells by DNA damage-inducing therapy requires not only the p53 targets PUMA and Noxa, but also Bim. Blood, 116: 5256–5267 (2010).

53. Happo, L., Strasser, A. & Cory, S. BH3-only proteins in apoptosis at a glance. Journal of Cell Science, 125: 1081–1987 (2012).

54. Haraguchi, T., Ozaki, Y., & Iba, H. Vectors expressing efficient RNA decoys achieve the long-term suppression of specific microRNA activity in mammalian cells. Nucleic Acids Research, 37(6): 1–13 (2009).

55. Hartl, F. U., Bracher, A. & Hayer-Hartl, M. Molecular chaperones in protein folding and proteostasis. Nature, 475: 324–332 (2011).

56. Hermeking, H., Lengauer, C., Polyak, K., He, T. C., et al. < i> 14-3-3σ</i> Is a p53-Regulated Inhibitor of G2/M Progression. Molecular Cell Biology, 1(1): 3–11 (1997).

57. Hikisz, P. & Kiliańska, Z. M. PUMA, a critical mediator of cell death–one decade on from its discovery. Molecular Cell Biology, 17: 646–669 (2012).

58. Hotchkiss, R. S., Strasser, A., McDunn, J. E. & Swanson, P. E. Cell death. The New England Journal of Medicine, 361: 1570–1583 (2009).

59. Huang, D. C., Hahne, M., Schroeter, M., Frei, K., et al. Activation of Fas by FasL induces apoptosis by a mechanism that cannot be blocked by Bcl-2 or Bcl-xL. Proceedings of the National Academy of Sciences, 96(26): 14871–14876 (1999).

60. Huang, D. C. & Strasser, A. BH3-Only proteins-essential initiators of apoptotic cell death. Cell, 103: 839–842 (2000).

61. Isomoto, H., Oka, M., Yano, Y. et al. Expression of heat shock protein (Hsp) 70 and Hsp 40 in gastric cancer. Cancer Letters, 198: 219–228 (2003).

62. Iwasaki, S., Kobayashi, M., Yoda, M., Sakaguchi, Y. et al. Hsc70/Hsp90 chaperone machinery mediates ATP-dependent RISC loading of small RNA duplexes. Molecular Cell Biology, 39: 292–299 (2010).

63. Jaattela, M., Wissing, D., Kokholm, K., Kallunki, T. & Egeblad, M. HSP70 exerts its anti-apoptotic function downstream of caspase-3-like proteases. The EMBO Journal, 17: 6124–6134 (1998).

64. Jeffers, J. R., Parganas, E., Lee, Y., et al. PUMA is an essential mediator of p53-dependent and -independent apoptotic pathways. Cancer Cell, 4: 321–328 (2003).

65. Johnstone, R. W., Ruefli, A. A., & Lowe, S. W. Apoptosis: a link between cancer genetics and chemotherapy. Cell, 108: 153–164 (2002).

66. Kanduc, D., Mittelman, A., Serpico, R., Sinigaglia, E., et al. Cell death: Apoptosis versus necrosis (Review). International Journal of Oncology, 21(1): 165–170 (2002).

67. Kerr, J. F. R., Wyllie, A. H., & Currie. A. R. Apoptosis: a basic biological phenomenon with wide-ranging implications in tissue kinetics. Cancer, 26: 239 (1972).

68. Kim, H., Rafiuddin-Shah, M., Tu, H-C. et al. Hierarchical regulation of mitochondrion-dependent apoptosis by BCL-2 subfamilies. Nature: Cell Biology, 8: 1348–1358 (2006).

69. Kim, H., Tu, H. C., Ren, D., Takeuchi, et al. Stepwise activation of BAX and BAK by tBID, BIM, and PUMA initiates mitochondrial apoptosis. Molecular Cell Biology, 36(3): 487–499 (2009).

70. Krammer, P. H. CD95's deadly mission in the immune cells. Nature, 407: 789–795 (2000).

71. Krek, A., Grün, D., Poy, M. N., Wolf, R., et al. Combinatorial microRNA target predictions. Nature Genetics: 37(5), 495–500 (2005).

72. Kumar, S. & Colussi, P. A. Prodomains, adaptors, oligomerization: the pursuit of caspase activation in apoptosis. Trends in Biochemical Sciences, 24: 1–4 (1999).

73. Kumar, M. S., Lu, J., Mercer, K. L., Golub, T. R., & Jacks, T. Impaired microRNA processing enhances cellular transformation and tumorigenesis. Nature Genetics, 39(5): 673–677 (2007).

74. Kuwana, T., Bouchier-Hayes, L., Chipuk, J. E., Bonzon, et al. BH3 domains of BH3-only proteins differentially regulate Bax-mediated mitochondrial membrane permeabilization both directly and indirectly. Molecular Cell Biology, 17: 525–535 (2005).

75. Kvansakul, M., Yang, H., Fairlie, W. D., Czabotar, P. E., et al. Vaccinia virus anti-apoptotic F1L is a novel Bcl-2-like domain-swapped dimer that binds a highly selective subset of BH3-containing death ligands. Cell Death & Differentiation, 15(10): 1564–1571 (2008).

76. Lagos-Quintana, M., Rauhut, R., Lendeckel, W., & Tuschl, T. Identification of novel genes coding for small expressed RNAs. Science, 294(5543), 853–858 (2001).

77. Lai, E. C., Burks, C., & Posakony, J. W. The K box, a conserved 3′ UTR sequence motif, negatively regulates accumulation of enhancer of split complex transcripts. Development, 125(20): 4077–4088 (1998).

78. Lee, Y., Kim, M., Han, J., Yeom, K. H., et al. MicroRNA genes are transcribed by RNA polymerase II. The EMBO Journal: 23(20), 4051–4060 (2004).

79. Li, G. C., Mivechi, N. F. & Weitzel, G. Heat shock proteins, thermotolerance, and their relevance to clinical hyperthermia. International Journal of Hyperthermia, 4: 459–488 (1995).

80. Li, H., Zhu, H., Xu, C. J. & Yuan, J. Cleavage of BID by caspase 8 mediates the mitochondrial damage in the Fas pathway of apoptosis. Cell, 94: 491–501 (1998).

81. Lima, R. T., Busacca, S., Almeida, G. M., Gaudino, G., et al. H. MicroRNA regulation of core apoptosis pathways in cancer. European Journal of Cancer, 47(2): 163–174 (2011).

82. Lithgow, T., Strasser, A., Driel, V. & Bertram, J. F. The Protein Product of the Oncogene bcl-2 is a Component of the Nuclear Envelope, the Endoplasmic Reticulum, and the Outer Mitochondrial Membrane. Cell Growth & Differentiation, 5: 411–417 (1994).

83. Locksley, R. M., Killeen, N. & Lenardo, M. J. The TNF and TNF receptor superfamilies: integrating mammalian biology. Cell, 104: 487–501 (2001).

84. Lomonosova, E. & Chinnadurai, G. BH3-only proteins in apoptosis and beyond: an overview. Oncogene, 27: 1–19 (2008).

85. Lynch, T. J., Bell, D. W., Sordella, R., Gurubhagavatula, S., et al. Activating mutations in the epidermal growth factor receptor underlying responsiveness of non–small-cell lung cancer to gefitinib. New England Journal of Medicine, 350(21): 2129–2139 (2004).

86. MacRae, I. J., Ma, E., Zhou, M., Robinson, C, V., et al. *In vitro* reconstitution of the human RISC-loading complex. Proceedings of the National Academy of Sciences, 105.2: 512–517 (2008).

87. Mattson, M. P. Apoptosis in neurodegenerative disorders. Nature reviews. Molecular Cell Biology, 1: 120–129 (2000).

88. Meier, P., Finch, A & Evan, G. Apoptosis in development. Nature, 407: 796–801 (2000).

89. Meier, P. & Vousden, K. H. Lucifer's labyrinth: ten years of path finding in cell death. Molecular Cell Biology, 28: 746–754 (2007).

90. Michalak, E. M., Villunger, A, Adams, J. M. & Strasser, A. In several cell types tumor suppressor p53 induces apoptosis largely via PUMA but Noxa can contribute. Cell Death & Differentiation, 15: 1019–1029 (2008).

91. Mirault, M. E., Goldschmidt-Clermont, M., Moran, L., Arrigo, A. P., et al. The effect of heat shock on gene expression in Drosophila melanogaster. Cold Spring Harbor Symposia on Quantitative Biology, 42: 819–827 (1978).

92. Morimoto, R. I. Regulation of the heat shock transcriptional response: cross talk between a family of heat shock factors, molecular chaperones, and negative regulators. Genes & Development, 12: 3788–3796 (1998).

93. Mosser, D. D., Caron, A. W., Bourget, L., Denis-Larose, et al. Role of the human heat shock protein HSP70 in protection against stress-induced apoptosis. Molecular Cell Biology, 17(9): 5317 (1997).

94. Mosser, D. D., Caron, A. W., Bourget, L., Meriin, et al. The Chaperone Function of HSP70 Is Required for Protection against Stress-Induced Apoptosis. Molecular Cell Biology, 20: 7146–7159 (2000).

95. Mosser, D. D. & Martin, L. H. Induced Thermotolerance to Apoptosis in a Human T Lymphocyte Cell Line. Journal of Cellular Physiology, 151: 561–570 (1992).

96. Mosser, D. D. & Morimoto, R. I. Molecular chaperones and the stress of oncogenesis. Oncogene, 23: 2907–2918 (2004).

97. Muchmore, S. W., Sattler, M., Liang, H., Meadows, R. P., et al. X-ray and NMR structure of human Bcl-xL, an inhibitor of programmed cell death. Nature, 38: 335–341 (1996).

98. Muller, P. A. J. & Vousden, K. H. p53 mutations in cancer. Nature, 15: 2–8 (2013).

99. Nagata, S., Hanayama, R. & Kawane, K. Autoimmunity and the clearance of dead cells. Cell, 140: 619–630 (2010).

100. Nakano, K. & Vousden, K. H. PUMA, A Novel Pro-apoptotic Gene, Is Induced by p53 National Cancer Institute at Frederick, 7: 683–694 (2001).

101. Nicholson, D. W. Caspase structure, proteolytic substrates, and function during apoptotic cell death. Cell Death & Differentiation, 6: 1028–1042 (1999).

102. Ouyang, Y. B., Xu, L., Lu, Y., Sun, X., et al. Astrocyte-enriched miR-29a targets PUMA and reduces neuronal vulnerability to forebrain ischemia. Glia, 61(11): 1784–1794 (2013).

103. Pear, W. S., Nolan, G. P., Scott, M. L., & Baltimore, D. Production of high-titer helper-free retroviruses by transient transfection. Proceedings of the National Academy of Sciences, 90(18): 8392–8396 (1993).

104. Pelham H. R. Speculations on the functions of the major heat shock and glucose-regulated proteins. Cell, 46: 959–961 (1986).

105. Plati, J., Bucur, O. & Khosravi-Far, R. Apoptotic cell signaling in cancer progression and therapy. Integrative Biology, 3: 279–96 (2011).

106. Powers, M. V. & Workman, P. Inhibitors of the heat shock response: biology and pharmacology. FEBS Letters, 581: 3758–3769 (2007).

107. Rathmell, J. C. & Thompson, C. B. Pathways of apoptosis in lymphocyte development, homeostasis, and disease. Cell, 109: 97–107 (2002).

108. Ravid, Z., Goldblum, N., Zaizov, R., Schlesinger, M., et al. Establishment and characterization of a new leukaemic T-cell line (Peer) with an unusual phenotype. International Journal of Cancer, 25: 705–710 (1980).

109. Reinhart, B. J., Slack, F. J., Basson, M., Pasquinelliet al. The 21-nucleotide let-7 RNA regulates developmental timing in Caenorhabditis elegans. Nature, 403(6772): 901–906 (2000).

110. Riedl, S. J. & Salvesen, G. S. The apoptosome: signaling platform of cell death. Molecular Cell Biology, 8: 405–413 (2007).

111. Richter, K., Haslbeck, M., & Buchner, J. (2010). The heat shock response: life on the verge of death. Molecular cell Biology, 40(2), 253–266.

112. Ritossa, F. A new puffing pattern induced by temperature shock and DNP in Drosophila. Cellular and Molecular Life Sciences, 18: 571–573 (1962).

113. Rohde, M., Daugaard, M., Jensen, M. H. et al. Members of the heat-shock protein 70 family promote cancer cell growth by distinct mechanisms. Genes & Development, 19: 570–582 (2005).

114. Rosman, G. J. & Miller, A. D. Improved method for plasmid shipment. Journal of Biotechnology, 8: 509 (1990).

115. Sattler, M. Structure of Bcl-xL-Bak Peptide Complex: Recognition Between Regulators of Apoptosis. Science, 275: 983–986 (1997).

116. Screaton, G. & Xu, X. N. T cell life and death signaling via TNF-receptor family members. Current Opinion in Immunology, 12: 316–322 (2000).

117. Seggerson, K., Tang, L., & Moss, E. G. Two genetic circuits repress the Caenorhabditis elegans heterochronic gene lin-28 after translation initiation. Developmental biology, 243(2): 215 (2002).

118. Shi, Y. Mechanisms of Caspase Activation and Inhibition during Apoptosis. Molecular Cell Biology, 9: 459–470 (2002).

119. Stankiewicz, A. R., Lachapelle, G., Foo, C. P. Z., Radicioni, S. M. et al. HSP70 Inhibits Heat-induced Apoptosis Upstream of Mitochondria by Preventing Bax Translocation. Journal of Biological Chemistry, 280: 38729–38739 (2005).

120. Strasser, A., Connor, L. O. & Dixit, V. M. Apoptosis Signaling. Annual Reviews in Biochemistry, 69: 217–245 (2000).

121. Strasser, A., Jost, P. J., & Nagata, S. The many roles of FAS receptor signaling in the immune system. Immunity, 30(2): 180–192 (2009).

122. Strasser, A., Cory, S. & Adams, J. M. Deciphering the rules of programmed cell death to improve therapy of cancer and other diseases. The EMBO journal, 30: 3667–3683 (2011).

123. Suzuki, M., Youle, R. J., & Tjandra, N. Structure of Bax: coregulation of dimer formation and intracellular localization. Cell, 103(4): 645–654 (2000).

124. Suzuki, H. I., Yamagata, K., Sugimoto, K., Iwamoto, T., Kato, S., et al. Modulation of microRNA processing by p53. Nature, 460(7254), 529–533 (2009).

125. Tait, S. W. G. & Green, D. R. Mitochondria and cell death: outer membrane permeabilization and beyond. Nature reviews: Molecular Cell Biology, 11: 621–632 (2010).

126. Taylor, R. C., Cullen, S. P. & Martin, S. J. Apoptosis: controlled demolition at the cellular level. Nature reviews: Molecular Cell Biology, 9: 231–241 (2008).

127. Thompson, C. B. Review: Apoptosis in the Pathogenesis and Treatment of Disease. American Association for the Advancement of Science, 267: 1456–1462 (1995).

128. Timmer, J. C. & Salvesen, G. S. Caspase substrates. Cell Death & Differentiation, 14: 66–72 (2007).

129. Tissieres, A., Mitchell, H. K., & Tracy, U. M. Protein synthesis in salivary glands of Drosophila melanogaster: relation to chromosome puffs. Journal of Molecular Biology, 84:389–398 (1974).

130. Tsang, J. S., Ebert, M. S., & van Oudenaarden, A. Genome-wide dissection of microRNA functions and cotargeting networks using gene set signatures. Molecular cell Biology, 38(1): 140–153 (2010).

131. Tsujimoto, Y., Cossman, J., Jaffe, E., & Croce, C. M. Involvement of the bcl-2 gene in human follicular lymphoma. Science, 228(4706): 1440–1443 (1985).

132. Utz, P. J. & Anderson, P. Life and death decisions: regulation of apoptosis by proteolysis of signaling molecules. Cell Death & Differentiation, 7: 589–602 (2000).

133. Vabulas, R. M., Raychaudhuri, S., Hayer-Hartl, M. & Hartl, F. U. Protein folding in the cytoplasm and the heat shock response. Cold Spring Harbor Perspectives in Biology, 2: a004390 (2010).

134. Vaux, D. L., Cory, S. & Adams, J. M. Bcl-2 gene promotes haemopoietic cell survival and cooperates with c-myc to immortalize pre-B cells. Nature, 335: 440–442 (1988).

135. Vaux, D. L. & Strasser, A. Review: The molecular biology of apoptosis. Proceedings of the National Academy of Sciences, 93: 2239–2244 (1996).

136. Veronese, A., Lupini, L., Consiglio, J., Visone, R., et al. Oncogenic role of miR-483-3p at the IGF2/483 locus. Cancer Research, 70(8): 3140–3149 (2010).

137. Wang, G.-K., Zhu, J-Q., Zhang, J-T., Li, Q. et al. Circulating microRNA: a novel potential biomarker for early diagnosis of acute myocardial infarction in humans. European Heart Journal, 31: 659–666 (2010).

138. Wang, P., Yu, J. & Zhang, L. The nuclear function of p53 is required for PUMA-mediated apoptosis induced by DNA damage. Proceedings of the National Academy of Sciences, 104: 4054–4059 (2007).

139. Wang, X. The expanding role of mitochondria in apoptosis. Genes & Development, 15: 2922–2933 (2001).

140. Wang, Y., Li, Z., He, C. et al. MicroRNAs expression signatures are associated with lineage and survival in acute leukemia's. Blood Cells, Molecules and Diseases, 44: 191–197 (2011).

141. Wei, J., O'Brien, D., Vilgelm, A. et al. Interaction of Helicobacter pylori with gastric epithelial cells is mediated by the p53 protein family. Gastroenterology, 134: 1412–1423 (2008).

142. Willis, S. N., Fletcher, J. I., Kaufmann, T., van Delft, M. F., et al. Apoptosis initiated when BH3 ligands engage multiple Bcl-2 homologs, not Bax or Bak. Science, 315(5813): 856–859 (2007).

143. Wilmink, G. J., Roth, C. L., Ibey, B. L., Ketchum, N. et al. Identification of microRNAs associated with hyperthermia-induced cellular stress response. Cell Stress & Chaperones, 15: 1027–1038 (2010).

144. Wolf, B. B. & Green, D. R. Suicidal Tendencies: Apoptotic Cell Death by Caspase Family Proteinases. Journal of Molecular Biology, 274: 29 (1999).

145. Wu, B., Qiu, W., Wang, P. et al. p53 independent induction of PUMA mediates intestinal apoptosis in response to ischemia-reperfusion. Gut, 56: 645–654 (2007).

146. Youle, R. J. & Strasser, A. The BCL-2 protein family: opposing activities that mediate cell death. Nature reviews. Molecular Cell Biology, 9: 47–59 (2008).

147. Yu, J. & Zhang, L. PUMA, a potent killer with or without p53. Oncogene, 27: 71–83 (2008).

148. Yu, J., Zhang, L., Hwang, P. M., Kinzler, K. W. et al. PUMA induces the rapid apoptosis of colorectal cancer cells. Molecular Cell Biology, 7: 673–682 (2001).

149. Yu, J., Wang, Z., Kinzler, K. W., Vogelstein, B. et al. PUMA mediates the apoptotic response to p53 in colorectal cancer cells. Proceedings of the National Academy of Sciences, 100: 1931–1936 (2003).

150. Zamzami, N. & Kroemer, G. Review: The mitochondrion in apoptosis: how Pandora's box opens. Molecular Cell Biology, 2: 46–57 (2001).

151. Zhang, C., Zhang, J., Zhang, A. et al. PUMA is a novel target of miR-221/222 in human epithelial cancers. International Journal of Oncology, 1621–1626 (2010).

152. Zhang, L., Li, J. & Xu, W. A review of the role of PUMA, Noxa and Bim in the tumorigenesis, therapy and drug resistance of chronic lymphocytic leukemia. Nature, 1: 7 (2012).

153. Zörnig, M., Hueber, A., Baum, W. & Evan, G. Apoptosis regulators and their role in tumorigenesis. Biochimica et Biophysica Acta, 1551: 1–37 (2001).

154. Zou, H., Li, Y., Liu, X. & Wang, X. An APAF-1 Cytochrome c Multimeric Complex is a Functional Apoptosome that Activates Procaspase-9. Journal of Biochemistry, 274: 11549–11556 (1999).

APPENDIX A: BUFFERS AND SOLUTIONS

Luria broth (LB):
10 g Tryptone, 5 g Yeast, 5 g NaCl/1 Liter of ddH_2O. Autoclave sterilized.

LB agar plates with Ampicillin:
10 g Tryptone, 5 g Yeast, 5 g NaCl, 10 g Agar/1 Liter of ddH_2O. Autoclave sterilized. 1 ml (50 μg/ml) Ampicillin is added and mixed well by swirling.

Ampicillin Stock (50 mg/ml):
500 mg of Ampicillin dissolved in 10 ml of 70% ETOH. Store at -20°C.

Glycerol frozen stocks:
50% glycerol, 0.1 M $MgSO_4$, 25mM Tris-HCl (pH 8.0)

TAE Buffer:
The Tris-acetate-EDTA (TAE) buffer for agarose gels consists of 40 mM Tris, 20 mM acetic acid, 1 mM EDTA (pH 8.0), in ddH_2O

10X Tris-Glycine electrophoresis buffer:
60.4 g Tris-Base, 2.88 g glycine, 20 g SDS and ddH_2O to 2 L.

10X TBS:
48.4g Tris-Cl (Base), 160.0 NaCl, HCl to pH 7.4 using Accumet pH meter, ddH_2O to 2 L.

1X TBS + 0.2 %Tween:
100 ml of 10X TBS stock, 900 ml double distilled H_2O, 1 ml Tween.

CAPS Transfer Buffer:
The transfer buffer for Western Blotting consists of 25 mM Tris, 20% methanol, and 192 mM glycine. (4.43 g CAPS, 1.8 L ddH_2O, 10 mM NaOH to pH 11.0, 200 ml Methanol).

5% Milk:
100 ml 1X TBS + Tween, 5 g powdered skim milk (no name).

dPBS:
1 bottle of Hyclone dPBS powder into 5 L ddH_2O. Filtered through 0.22 μm pore filter (GP express) and autoclaved on a L30 cycle. phosphate buffered saline: 137 mM NaCl, 2.7 mM KCl, 10 mM Na_2HPO_4, and 1.8 mM KH_2PO_4, adjusted to pH 7.4 with HCl)

Protease inhibitors:
Mix together 200 μl Pepstatin A (1mg/ml), Leupeptin (1 mg/ml) and Aprotinin (1 mg/ml) for a final concentration of 333 μg/ml of each inhibitor. Add 30 μl/ml of lysis buffer to give 10 μg/ml of each inhibitor.

Phosphatase inhibitors:
Mix together 100 µl of sodium vanadate (1 mM), 100 µl of β-glycerolphosphate (3 mM), 200 µl of each sodium fluoride (10 mM), sodium phosphate (20 mM), and sodium pyrophosphate (5 mM) to give a volume of 800 µl. Each inhibitor is now at 25X. Add 40 µl/ml of this mixture to lysis buffer.

Agarose gel:
1% gel: 2 g Ultrapure Agarose, 200 ml 1X TAE. Microwave on high for 3 min, add 10 µl RedSafe and pour into gel tray with appropriate sized combs. Let polymerize.

GTE + RNAse:
GTE solution (50 mM Glucose, 25 mM Tris pH 8.0, 10 mM EDTA, and 1 mg/ml RNAse A) Mix 60 µl RNAse (100 mg/ml) from -20°C in 50 ml GTE solution in a 50 ml labeled conical tube and store at 4°C.

SDS/NaOH lysis buffer:
Mix 10 ml of 1% SDS in 90 ml ddH_2O. Add 2 ml 0.2 M NaOH

5 M Potassium acetate precipitation buffer (pH 4.8):
Dissolve 29.5 ml glacial acetic acid in 50 ml ddH_2O. pH mixture to 4.8 with 10 M KOH. Bring final volume up to 100 ml with ddH_2O.

dNTP (10 mM):
Mix 10 µl of each: 100 mM dTTP, 100 mM dGTP, 100 mM dATP, and 100 mM dCTP and bring too 100 µl with ddH_2O. Aliquot 20 µl in 5 x 1.5 ml centrifuge tubes and store at -20°C.

1X Laemmli Buffer (Tris-Glycine SDS Buffer):
63 mM Tris HCl, 10% Glycerol, 2% SDS, 0.0025% Bromophenol Blue, pH to 6.8

1X Laemmli with β-mercaptoethanol:
200 µl of 5X Laemmli with β-mercaptoethanol (2-Mercaptoethanol) in 800 µl of ddH_2O.

10X loading dye:
50% glycerol, 1%SDS, 0.1% EDTA, 0.25% bromophenol blue, 0.25% xylene cyanol.

2X HBS (Hepes buffered saline):
16.4g NaCl, 11.9g Hepes acid, 0.21g Na2HPO4, 800ml H2O. Titrate to pH7.05 with NaOH and add water to 1 liter. Filter sterilize through a 0.45um nitrocellulose filter, freeze in 50 ml aliquot.

Laemmli lysis buffer:
40 µl Phosphatase inhibitor, 30 µl Protease Inhibitor and 930 µl 1x Laemmli buffer.

Polyethylenimine (PEI):
Dissolve 40 mg of Polyethylenimine in 30 ml of ddH_2O. Adjust to pH 7.0 with HCl. The final volume brought up to 40 ml with ddH_2O and filter sterilized through a 0.22 µm membrane in the flow hood. Stored in 1 ml (1mg/ml) aliquots at -80°C until use.

Sucrose gradient:
25 mM Hepes, 2 mM MgAc, 50 μg/ml Cycloheximide, 15 mM 2-mercaptoethanol, 250 mM KCl and 5 – 10 g Sucrose.

Polysomal lysate:
10 mM MOPS (pH7.2), 250 mM NaCl, 2.5 mM MgCl, 0.5% NP-40, 0.1 mM PMSP, 200 μg/ml Heparin and 50 μg/ml Cycloheximide.